The role of mitochondrial reactive oxygen species in oxygen sensing in the pulmonary vasculature – use of novel genetic tools

Inaugural Dissertation
submitted to the
Faculty of Medicine
in partial fulfillment of the requirements
for the PhD-Degree
of the Faculties of Veterinary Medicine and Medicine
of the Justus Liebig University Giessen

by
Alebrahimdehkordi Nasim
of
Ahvaz, Iran

Giessen, 2021

From the Department of Internal Medicine II and the Excellence Cluster Cardio-Pulmonary System (ECCPS)
Director: Prof. Dr. Werner Seeger
of the Faculty of Medicine of the Justus Liebig University Giessen

First Supervisor and Committee Member: PD Dr. Natascha Sommer
Second Supervisor and Committee Member: Prof. Dr. Sybille Mazurek
Committee Members: Prof. Dr. Klaus-Dieter Schlüter

Date of Doctoral Defense: 31.05.2021

Declaration

I declare that I have completed this dissertation single-handedly without the unauthorized help of a second party and only with the assistance acknowledged therein. I have appropriately acknowledged and referenced all text passages that are derived literally from or are based on the content of published or unpublished work of others, and all information that relates to verbal communications. I have abided by the principles of good scientific conduct laid down in the charter of the Justus Liebig University of Giessen in carrying out the investigations described in the dissertation.

Nasim Alebrahimdehkordi
Giessen, Germany

Table of Contents

List of figures

List of tables

List of abbreviations

$[Ca^{2+}]_i$	Intracellular calcium concentration
$^{\bullet}OH$	Hydroxyl radical
Acetyl CoA	Acetyl coenzyme A
AECC	American-European Consensus Conference
AMP	Adenosine monophosphate
AOX	Alternative oxidase
ARDS	Acute respiratory distress syndrome
ATP	Adenosine triphosphate
B2M	β2 microglobulin
BAT	Brown adipose tissue
BMPC	Brain mitochondrial carrier protein,
BSA	Bovine serum albumin
BW	Body weight
CAC/TCA cycle	Citric acid cycle/Tri-carboxylic acid cycle
$CaCl_2$	Calcium chloride
CB	Carotid body
CI	Cardiac index
CI-CIV	Mitochondrial complex I-IV
CMH	1-hydroxy-3-methoxycarbonyl-2, 2, 5, 5-tetramethylpyrrolidine
CO	Cardiac output
CO_2	Carbon dioxide
COPD	Chronic obstructive pulmonary disease
COX/CIV	Cytochrome c oxidase/complex IV
COX4	Cytochrome c oxidase subunit 4
COX4i2	Cytochrome c oxidase subunit 4 isoform 2
CTEPH	Chronic thromboembolic pulmonary hypertension
DCA	Dichloroacetate
DiOC6	3,3'-Dihexyloxacarbocyanine iodide
DMSO	Dimethyl sulfoxide

dNTP	Deoxynucleotide triphosphate
Drp1	Dynamin-related protein 1
DTPA	Diethylenetriamine-pentaacetic acid
ECG	Echocardiography
ECL	Enhanced chemiluminescence
EDG	Endoglin
ESR	Electron spin resonance spectroscopy
FAD^+	Oxidized flavin adenine dinucleotide
$FADH_2$	Reduced flavin adenine dinucleotide
FBS	Fetal bovine serum
Fe_3O_4	Iron (ш) oxide
FFPE	Formalin-fixed paraffin-embedded
FI	Fulton Index
Fis1	Fission 1 protein
FOXO1	Forkhead box protein O1
GDP	Guanosine-5'-diphosphate
GP_X	Glutathione peroxidase
GSSG/GSH	Ratio of oxidized to reduced glutathione
H_2O_2	Hydrogen peroxide
H_2S	Hydrogen sulfide
HEK293T	Human kidney epithelial cell lines
HIF	Hypoxia-inducible factor
Higd1a	Hypoxia-inducible domain family, member1A
HIV	Human immunodeficiency virus
HO	Heme oxygenase
$HOO^{\bullet}$	Hydroperoxyl radical
HOSS	Homeostatic oxygen sensing system
HOX	Hypoxia
HPV	Hypoxic pulmonary vasoconstriction
HRB	HEPES-Ringer buffer
HRP	Horseradish peroxidase
IHC	Immunohistochemistry
ILD	Interstitial lung disease
IP_3	Inositol trisphosphate

KCl	Potassium chloride
KCN	Potassium cyanide
KH_2PO_4	Potassium dihydrogen phosphate
KOH	Potassium hydroxide
K_V	Voltage-gated potassium channel
LC3B	Microtubule-associated protein 1 light chain 3B
LOOH	Lipid peroxide
LPS	Lipopolysaccharide
LV + S	Left ventricle + septum
LVEF	Left ventricular ejection fraction
LVP	Left ventricular pressure
LVSP	Left ventricular systolic pressure
MAC	Mitochondrial anion carrier
METC	Mitochondrial electron transport chain
$MgCl_2$	Magnesium chloride
$MgSO_4$	Magnesium sulfate
MICU	Mitochondrial calcium uptake
mitoK_{ATP}	Mitochondria ATP-sensitive potassium channel
MLC	Myosin light chain
MMP	Mitochondrial membrane potential
MNRR1	Mitochondria nuclear retrograde regulator 1
MWT	Medial wall thickness
n-PG	n-propyl gallate
N_2	Nitrogen
NaCl	Sodium chloride
NAD^+	Oxidized nicotinamide adenine dinucleotide
NAD^+/NADH	Ratio of oxidized to reduced nicotinamide adenine dinucleotide
NADH	Reduced nicotinamide adenine dinucleotide
NADPH	Reduced nicotinamide adenine dinucleotide phosphate
NaH_2PO_4	Sodium dihydrogen phosphate
$NaHCO_3$	Sodium bicarbonate
NF-κB	Nuclear factor kappa-light-chain-enhancer of activated B cells
NFATc2	Nuclear factor of activated T-cells, cytoplasmic 2
NOS	Nitric oxide synthase

NOX	Normoxia
NSCC	Non-selective calcium cannel
O_2	Oxygen
$O_2^{\bullet}$	Superoxide anion
ORE	Oxygen responsive element
OSA	Obstructive sleep apnea
P/S	Penicillin-streptomycin
PAEC	Pulmonary arterial endothelial cell
PAH	Pulmonary arterial hypertension
PAP	Pulmonary arterial pressure
PASMC	Pulmonary arterial smooth muscle cell
PAT/PET	Ratio of pulmonary artery acceleration time to ejection time
PBGD	Porphobilinogen deaminase
PBS	Phosphate-buffered saline
PCH	Pulmonary capillary haemangiomatosis
PDK	Pyruvate dehydrogenase kinase
PEEP	Positive end-expiratory pressure
PEG-SOD	Superoxide dismutase-polyethylene glycol
PH	Pulmonary hypertension
PHD	Prolyl hydroxylase
PMSF	Phenylmethane sulfonyl fluoride
PO_2	Arterial partial pressure of oxygen
PPARγ	Peroxisome proliferator-activated receptor
PPHN	Persistent pulmonary hypertension of the newborn
pSOD	Polyethylene-glycol conjugated superoxide dismutase
PVDF	Polyvinylidene difluoride
PVOD	Pulmonary veno-occlusive disease
PVR	Pulmonary vascular resistance
Q	Ubiquinone
Q cycle	Ubiquinone cycle
$Q^{\cdot-}$	Semiquinone
QH_2	Ubiquinol
RCA	Right common carotid artery

RISP	Rieske iron-sulfur protein
RNA	Ribonucleic acid
RNS	Reactive nitrogen species
$RO_2^{\bullet}$	Peroxyl radical
ROCC	Receptor-operated calcium channel
ROS	Reactive oxygen species
RVH	Right ventricular hypertrophy
RVID	Right ventricular internal diameter
RVSP	Right ventricular systolic pressure
RVWT	Right ventricular wall thickness
RyR	Ryanodine-sensitive receptors
SAP	Systemic arterial pressure
SDH	Succinate dehydrogenase
SDS-PAGE	Sodium dodecyl sulfate–polyacrylamide gel electrophoresis
SEM	Standard error of mean
Siah2	Seven in-absentia homolog 2
SMC	Smooth muscle cell
SOCC	Store-operated calcium channel
SOD2, SOD1	Superoxide dismutase 1 and 2
STAT3	Signal transducer and activator of transcription 3
TAPSE	Tricuspid annular plane systolic excursion
TBS	Tris buffer saline
TMRE	Tetramethylrho-damineethyl ester
TMRM	Tetramethylrho-daminmethyl ester
TPP	Triphenylphosphonium chloride
UCP	Uncoupling protein
V/Q	Ratio of alveolar ventilation to blood perfusion
VDAC	Voltage-dependent anion channel
VEGF	Vascular endothelial growth factor
VOCC	Voltage-operated calcium channel
WSPH	World Symposia on Pulmonary Hypertension
WT	Wild-type
ΔpH	Proton gradient

1. Introduction

1.1. Hypoxic pulmonary vasoconstriction (HPV)

1.1.1. Physiological relevance of HPV

Alveolar ventilation carries oxygen (O_2) into the lung and eliminates carbon dioxide (CO_2) from it. Similarly, the venous blood carries CO_2 into the lung and absorbs alveolar O_2 [1]. Therefore, the relationship between alveolar ventilation and blood perfusion (V/Q) regulates the distribution of O_2 and CO_2 among alveolar gas and pulmonary capillary blood [2-4]. Amongst others, the V/Q ratio can be influenced by gravity as well as airway and vascular structures [5]. Haldane et al. proposed that a mechanism might be present to regulate blood flow of the lung and arterioles may contract or dilate to redistribute the blood [6].

In 1946, von Euler and Liljestrand found that the pulmonary arterial pressure (PAP) measured in the isolated lung of cats undergoes a large increase in response to 10.5% O_2. They suggested that hypoxic pulmonary vasoconstriction (HPV) is an intrinsic mechanism of the lung in response to alveolar hypoxia (HOX) that conveys blood flow from less-ventilated lung units to more ventilated lung units and matches local perfusion to ventilation, thereby maintaining V/Q balance and optimizing oxygenation of arterial blood (Figure 1) [2, 7, 8]. HPV has been shown to exist in several mammals [9-12], and, based on the study by Motley et al., this mechanism also plays a crucial role in humans [13]. Additional support for this finding appeared in 1947 and 1948, when Motley and Dirken et al., respectively, demonstrated that low O_2 breathing in humans (10% O_2) and intact animals (12% O_2) could induce an increase in pulmonary pressure [14, 15].

Impairment of V/Q matching and a drop in the arterial blood oxygenation due to impaired HPV can occur during several conditions, such as anesthesia [16, 17], adult respiratory distress syndrome (ARDS) [18], liver cirrhosis [19], and the hepatopulmonary syndrome [20]. Physiological factors might affect HPV, including volatile agents (e.g., carbon monoxide and carbon dioxide), metabolism (e.g., pH) [21], temperature, the nervous system [22, 23], and blood viscosity [24]. Both respiratory and metabolic acidosis causes pulmonary vasoconstriction [16], and one study on the left lower lobe of the lung in open-chested dogs demonstrated that HPV is alleviated by hypothermia and augmented by hyperthermia [25].

Furthermore, HPV can be influenced by species, gender [26], and age. However, few details are known about the impact of age on HPV in adults.

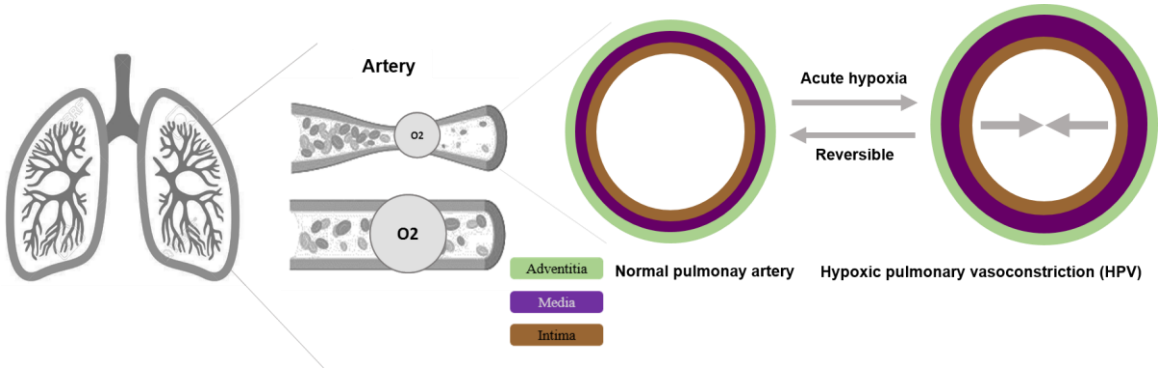

Figure 1. Acute hypoxic pulmonary vasoconstriction (HPV)

HPV optimizes gas exchange by adjusting perfusion to ventilation. In the schematic representation of a small pulmonary artery, green, purple, and brown colors indicate adventitia, media, and intima, respectively.

1.1.2. Characterization of acute HPV

1.1.2.1. The localization of the acute oxygen sensor

The level of O_2 is an important physiological determinant in several tissues. Tissues that specifically detect local O_2 pressure consist of type 1 cells in the carotid body, smooth muscle cell (SMC) in small pulmonary arteries, chromaffin cells of the fetal adrenal medulla, fetoplacental arteries in the placenta, and the ductus arteriosus [27]. The O_2-sensing mechanism in the lung seems to be located in the vascular compartments of the alveolar unit. Several studies suggested that HPV is executed on the arterial side of the pulmonary vasculature and induced by alveolar hypoxia [28, 29]. Pulmonary arteries are located in the vicinity of terminal respiratory units, so that O_2 can diffuse readily from the alveolar space through the walls of these small vessels where alveolar hypoxia can induce HPV. In contrast, changes in mixed venous O_2 tension did not provoke any vasoconstrictive response in the pulmonary artery [30]. In contrast, Staub et al. showed that ventilation of one lung lobe in cats with nitrogen (N_2) containing 10% CO_2 led to the contraction of pulmonary arteries, but no difference in lumen diameter was detected when the animals were exposed to 10% CO_2 in air [31].

A variety of techniques have shown that HPV occurs in dog small muscular pulmonary arteries with diameters ≥ 100 µm [32]. Furthermore, Murray proved the critical role of the pulmonary arterial smooth muscle cell (PASMC) in HPV in the early 1990s. The measurements of the tension (force) produced by fetal calve cells grown on a flexible growth surface illustrated the rise of cell contractility (displayed as wrinkles on the surface) when exposed to HOX (PO_2 = 25 mmHg for 5 minutes) [33]. Hence, the O_2 sensing and signal conduction machinery of HPV was considered to be located in PASMC [7]. In contrast, HOX did not change the myocyte length from systemic arteries, which was shown by Madden et al. in 1992 [34]. They provided the evidence that cat SMC isolated from pulmonary arteries with a diameter ≤ 200µm or 200–600 µm, were shortened significantly under HOX. However, the SMC from pulmonary arteries with a diameter 800 µm or cerebral arteries exhibited no increase in tension in response to HOX. Similarly, another investigation demonstrated a significant drop in the length of porcine distal PASMC upon exposure to HOX (PO_2 < 10 mmHg), but no change in the size of the SMC femoral artery [35].

According to the concept that the primary O_2 sensing mechanism of HPV has been proposed to be intrinsic to PASMC, there was no experimental evidence that humoral agents (such as adenosine, histamine, angiotensin 2, and systemic neural activity) were required for HPV, although a variety of these factors can modulate HPV [28, 36, 37]. Additionally, the concept emerged that the pulmonary endothelium only plays a modulatory role in HPV, which was supported by the following observations: first, isolated PASMC were able to contract in the absence of the endothelium when exposed to HOX (as outlined above), and second, the response of the pulmonary artery was still intact by endothelial denudation in the isolated pulmonary artery [22, 38-40]. On the contrary, there is evidence indicating the important role of pulmonary endothelium in HPV. It has been shown that connexin 40 conducted the HOX-induced endothelial membrane depolarization at the alveolar capillary to arteriole and caused a vasoconstrictive response at the arteriole [41].

1.1.2.2. Requirements for the O_2 sensor in acute HPV

To understand the O_2 sensing mechanism, one also has to keep in mind that HPV is induced at mild hypoxia (about 15% in mice and 10% in men) [42-48]. However, there are discrepancies at which O_2 levels, HPV is induced, depending on the species and experimental setup [33, 49]. Most importantly, this intrinsic response of the lung occurs in

between seconds after onset of alveolar hypoxia and has been shown to be present in lungs of different species [28]. HPV lasts few minutes to several hours and can lead to a biphasic reaction depending on the experimental setup. Thus, the O_2 sensor needs to be sensitive in a range of hypoxia which is considered to be rather mild, and sense hypoxia and mediate the signal in between seconds, at least for acute HPV.

1.1.2.3. Mitochondria as O_2 sensors in acute HPV

Several cellular O_2-sensitive components have been suggested, including the mitochondria, the nicotinamide adenine dinucleotide phosphate oxidase (NADPH oxidase), heme oxygenase (HO) [51], cytochrome P-450, nitric oxide synthase (NOS), and several other enzymes (e.g. cyclooxygenase and lipoxygenase) [52, 53]. This study focusses on mitochondria.

Mitochondria play an important role in many key features of animal physiology and are the largest consumers of O_2. They are responsible for production of adenosine triphosphate (ATP) via cellular respiration, regulation of cellular calcium homeostasis and apoptosis, reactive oxygen species (ROS) generation and a variety of other metabolic functions. Amino acids, glucose, and fatty acids are crucial metabolic fuels for mitochondrial ATP production. Pyruvate is the final product of glycolysis, which is transported into mitochondria as a principal fuel for the citric acid cycle (CAC), also known as the tricarboxylic acid cycle (TCA cycle) or Krebs cycle. Pyruvate and β-oxidation of fatty acids in the mitochondria generate acetyl CoA, which participates in the Krebs cycle to generate reduced nicotinamide adenine dinucleotide (NADH) and reduced flavin adenine dinucleotide ($FADH_2$). In the TCA cycle, substrate molecules are steadily dehydrogenated, inducing the reduction of NAD^+ and FAD to NADH and $FADH_2$, respectively, which are subsequently re-oxidized by the mitochondrial electron transport chain (METC).

The METC consists of four multi-protein complexes (CI–IV) located in the mitochondrial inner membrane. Mitochondrial complexes I and II (CI and CII) oxidize NADH and $FADH_2$ by oxidoreductases, respectively. Afterward, electrons are carried down a redox gradient through ubiquinone (Q), a mitochondrial mobile component, involving a reduction of Q to ubiquinol (QH_2). QH_2 transfers one of its electrons to cytochrome c, as a mobile carrier, via cytochrome c1 (of CIII) resulting in the formation of semiquinone ($Q^{\cdot-}$) and another electron to cytochrome b which transfers the electrons at the inner ubiquinone binding site to ubiquinone (Q cycle) [54, 55]. Subsequently, CIV (containing cytochrome aa3) oxidizes

cytochrome c, where O_2 accepts electrons and is reduced to H_2O. The delivery of electrons via the METC is accompanied by ejection of protons into the mitochondrial intermembrane space at CI (4 H^+), III (4 H^+), and IV (2 H^+), thus causing the mitochondrial membrane potential (MMP ~ 150_180 mV) and proton gradient (expressed by the symbol Δ pH). This protonmotive force drives the production of ATP in the mitochondrial matrix by translocation of protons from the intermembrane space to the matrix via the F_1F_0 ATP synthase [2]. However, some protons can get back towards the mitochondrial matrix through a proton "leak", either through the lipid membrane or possibly through uncoupling proteins (UCPs), that dissipate MMP and thus uncouple mitochondrial respiration from ATP synthesis [56]. Around 3% of the electron flux through the METC results in the generation of superoxide anions ($O_2^{\bullet}$) [57] mostly by mitochondrial CI and III. The $O_2^{\bullet}$ is one of the common ROS, which is formed by the addition of one electron to the O_2 molecule. The other most-common ROS comprises highly reactive free O_2 radicals, for instance, peroxyl ($RO_2^{\bullet}$), hydroperoxyl ($HOO^{\bullet}$), and hydroxyl ($^{\bullet}OH$) anions as well as non-radical species, such as hydrogen peroxide (H_2O_2) and lipid peroxide (LOOH) [58]. Moreover, there are other sources of ROS within mitochondria, such as Monoamine oxidase [59], dihydroorotate dehydrogenase [60], pyruvate dehydrogenase, and α-ketoglutarate dehydrogenase [61, 62], and the cell such as NADPH oxidases [63], xanthine oxidases [64], cyclooxygenases, cytochrome P450 enzymes [65], lipoxygenases [66], and NOS [67]. Nevertheless, mitochondria are broadly believed to be the crucial source of ROS [68, 69].

The balance of intracellular ROS concentration is reached by several specialized ROS-defense systems within the cell, such as superoxide dismutase 2 (SOD2, a manganese-dependent enzyme) acting in the mitochondrial matrix and superoxide dismutase 1 (SOD1, a copper or zinc-dependent enzyme) functioning in the intermembrane space and cytosol. The $O_2^{\bullet}$ is converted into H_2O_2 via mitochondrial SOD enzymes or is conveyed to the cytosol from the mitochondrial intermembrane space through voltage-dependent anion channels (VDAC; in the outer mitochondrial membrane). H_2O_2 is inactivated by glutathione peroxidase (GP_X) that catalyze the reduction of H_2O_2 by glutathione (GSH) to water in the mitochondrial matrix. The cytosol also contains antioxidant defense mechanisms, including GP_X [70], catalase [71], SOD1, and thioredoxin [72]. Although ROS were originally considered as toxic outcomes of cellular metabolism, they are now recognized as signaling molecules that play a wide range of regulatory functions in the vascular SMC. The METC may be an essential prerequisite for O_2 sensing, not only in PASMC but also in carotid body

(CB) type 1 and neonatal chromaffin cells [73, 74]. The importance of mitochondria for O_2 sensing has been shown long ago.

Cells depleted of mitochondrial deoxyribonucleic acid (DNA; p0 cells generated from wild-type [WT] rat pulmonary artery myocytes) that lack critical METC subunits encoded in the mitochondrial genome, cannot support normal oxidative phosphorylation [75]. Furthermore, the contraction response to 2 hours HOX (2% O_2) in these cells was absent compared with controls, while the unspecific vasoconstriction response to the thromboxane analog U46619 was preserved [76]. U46619 binds to the thromboxane A2 receptor, increases intracellular calcium, and consequently induces vasoconstriction of the vasculature in a HOX-independent manner-as an approach to monitor the intact pulmonary vascular apparatus [77]. Thus, the relevance of mitochondria for acute O_2 sensing is generally accepted, however, the specific sensing and mediator mechanism is still under debate. Low PO_2 can change mitochondria-dependent factors, among which ATP concentration, redox state, and ROS production could signal HPV.

Early evidence supported a role of mitochondrial ATP production as an O_2 sensor in the pulmonary circulation. This hypothesis was based on the finding that, isolated, perfused rat lungs lacked the hypoxic response, when mitochondrial respiration (and thus ATP production) was suppressed [78]. However, O_2 affinity of mitochondria was considered to be too high to sense mild hypoxia in the range, in which HPV is induced [34, 44] and not every inhibitor of the METC could suppress HPV [79]. Therefore, the idea that at least a substantial decrease in ATP or energy depletion could trigger HPV, was abandoned and other mediators favoured [80, 81]. Later it was suggested that mitochondria of PASMC may express specific cytochrome c oxidase (COX) subunits which decrease O_2 affinity. However, it was shown that O_2 affinity of mitochondria in intact PASMC was in the range comparable to other intact cells. Nevertheless the same investigations proved that respiration of PASMC was slightly decreased in an O_2 range, when also a hypoxia-induced calcium increase was detected [44]. Along these lines, it was proposed that the ATP/adenosine monophosphate (AMP) ratio may regulate HPV via the AMP-kinase [82, 83].

In the last years, ROS have attained much attention, as their release may fulfill the requirements of an acute O_2 sensor which are to be fast and sensitive in the range of hypoxia that induces HPV. ROS release is considered to be an O_2-dependent process. Mitochondrial ROS is produced at the METC during forward electron flow at CI and III and during reverse electron flow at CII [84, 85]. ROS can activate several pathways that are proposed to be participating in HPV, including Ca^{2+} signaling. ROS also affect the cellular redox state which

is altered in lung tissue, PASMC, and CB glomus cells, and characterized by a change in the ratio of oxidized to reduced proteins (e.g., oxidized to reduced glutathione [GSSG/GSH] or NAD^+/NADH) [86-88].

However, two contradictory hypotheses emerged, one favoring an increase in ROS, the other a decrease in ROS/redox state as mediator underlying HPV [44, 89, 90]. The redox hypothesis suggests that acute HOX causes reduced ROS levels and a decrease in the ratio of GSSG/GSH and NAD^+/NADH. This in turn induces inhibition of potassium currents, PASMC depolarization, increased Ca^{2+} influx, and subsequently PASMC contraction [86, 91, 92]. A central tenet of this hypothesis was formulated following the observation that ROS in lung tissue decreased during acute HOX and inhibition of CI and III mimicked the ROS decrease in HOX, leading to vasoconstriction in normoxia (NOX), and suppression of hypoxic vasoconstriction because the ROS level could not decrease further. In contrast, inhibition of CIV by cyanide caused normoxic vasoconstriction, as well as an increase in ROS release; however, it did not cause inhibition of HPV [91, 93-96]. In contrast, other investigations showed increasing ROS production originating from mitochondria during HOX [97, 98]. This interpretation was supported by a rise in mitochondrial ROS production revealed by MitoSOX™ (fluorescent dye) during exposure to acute HOX in rabbit PASMC [99]. In addition, ROS measurements in mouse lung slices via RoGFP (a redox-sensitive protein sensor) during HOX showed an enhancement in cytosolic ROS [100]. Additional support for the crucial role of an increase in mitochondrial ROS in hypoxic signaling was shown with the help of various mitochondrial ROS inhibitors. The superoxide scavenger, nitro-blue tetrazolium, inhibited HPV in isolated rabbit lungs, whereas the unspecific vasoconstriction responses to the U46619 and angiotensin II were still intact [101].

Furthermore, a study conducted by Schumacker et al. showed an increase in ROS release into the mitochondrial intermembrane space in mouse PASMC after exposure to acute HOX [102]. In line with these findings, the authors determined that deletion of the Rieske iron-sulfur protein (RISP) of CIII in mouse PASMC abolished the HOX-induced rise in ROS release into the mitochondrial intermembrane space and cytosol [103]. Together with inhibitor studies, it was concluded that the release of ROS at the outer QH_2-binding site of CIII acts as the main mediator in acute HOX.

However, the mechanism of the paradoxical increase of ROS in acute HOX is still unresolved and matter of debate. Several conditions may promote mitochondrial ROS production even when the concentration of O_2 is decreasing. It is generally accepted that mitochondrial hyperpolarization can enhance ROS production, while a decrease of MMP

could attenuate ROS release [104]. Weissmann et al. studied rabbit lungs and revealed the reduction of mitochondrial cytochrome c at a PO_2 of 38 mmHg and cytochrome aa3 at 23 mmHg, which was accompanied by the considerable increase in the HOX-induced increase of mitochondrial superoxide, MMP, and intracellular calcium release [7]. However, another investigation showed that HOX decreased production of mitochondrial ROS and MMP to a more depolarized level in the rat PASMC [93].

Downstream signaling of ROS may include direct or indirect interaction with phospholipases, protein kinases, and plasmalemmal ion channels to induce an intracellular calcium increase and contraction [7]. One study illustrated that H_2O_2 treatment elicited a bi-phasic intracellular Ca^{2+} increase in rat intra-lobar PASMC, in which the initial phase included the calcium release from the intracellular stores (inositol triphosphate [IP_3] receptor or ryanodine receptor-gated Ca^{2+} stores), and the second phase comprised the extracellular Ca^{2+} influx that is independent of the Ca^{2+} channels [105].

1.1.2.4. Downstream hypoxic signaling

It is well established that acute HOX inhibits potassium channels causing cellular membrane depolarization [106, 107] and subsequently PASMC contraction through an increase in intracellular Ca^{2+} concentration ($[Ca^{2+}]_i$). Several studies suggest that the increase in $[Ca^{2+}]_i$ is due to its release from the sarcoplasmic reticulum through ryanodine-sensitive receptors (RyR) and entry of extracellular Ca^{2+} through voltage-, receptor-, or store-operated channels (VOCC, ROCC, SOCC) in the sarcolemma. Consistently, studies on isolated rat lungs showed that HPV could be suppressed by antagonists of SOCC/NSCC [108, 109]. Importantly, inhibition of the non-selective cation channels (NSCC) completely inhibited HPV [110, 111], while inhibition of L-type calcium channels only attenuated HPV [112, 113]. However, the signaling pathways that link the O_2 sensor to the increases in $[Ca^{2+}]_i$ have not been fully characterized.

Regulation of the calcium channels in hypoxic conditions can be attained by cellular membrane depolarization via potassium channels. HOX inhibits different types of potassium channels associated with membrane depolarization, particularly the voltage-gated potassium channels (K_V) [108, 114]. Several K_V channels (e.g., K_V2.1, K_V1.1, 1.2, 1.3, 1.5, and 1.6) were studied by Archer et al., who shed light on the importance of the K_V2.1 and K_V1.5 channels and their contribution to PASMC function and vascular tone, and, consequently HPV [108, 115, 116]. As outlined above, these ion channels may be affected by ROS or cellular redox state which thereby could trigger HPV. However, the exact contribution of

ROS for hypoxic regulation of different ion channels and the net effect on intracellular calcium increase is under debate. Furthermore, localized and time-dependent difference have to be taken into account.

1.2. Pulmonary hypertension (PH)

1.2.1. Classifications and characterization of PH

Pulmonary hypertension (PH) is characterized by a mean PAP above 20 mmHg determined by right heart catheterization at rest according to new definitions and can give rise to significant morbidity and mortality [117, 118]. The first PH categorization was suggested in 1973 by the World Symposia on Pulmonary Hypertension (WSPH), where PH was categorized into two groups: primary PH, with unknown causes of PH, and secondary PH, with the existence of clear causes of PH. In the revised WSPH classification released in 2018, PH was classified into 5 groups, "by taking into account resemblances in pathophysiological mechanisms, clinical indications, and therapeutic strategies" (adapted from Simonneau et al.): 1) PAH; 2) PH due to left heart diseases, 3) PH due to lung diseases and/or HOX; 4) PH due to pulmonary artery obstructions, and 5) PH with unclear and/or multifactorial mechanisms [117] (Table 1).

Some general symptoms can affect all groups of PH, including breathlessness, fatigue, chest pain (*angina pectoris*), dizziness, peripheral edema and dry cough, all of which become more severe as the disease progresses. [119]. All precapillary types of PH (group I, III, IV, V) are characterized by a rise in pulmonary vascular resistance (PVR) as a consequence of pulmonary vascular remodeling, which gives rise to an increase in right ventricular afterload and, subsequently, right heart failure. Pulmonary vascular remodeling in PH is distinguished by the narrowing of the vascular lumen, caused by increased proliferation of different vascular cells in the vascular wall (PASMC, endothelial cell, fibroblast) [120] (Figure 2). Genetic mutations [121-123], an imbalance in vasoconstrictors and vasodilators [124-126], growth factors [127], cytokines, and chemokines [128, 129] could all be primary stimuli of pulmonary vascular remodeling in PH. On cellular level numerous molecular pathways may be affected including activation of several transcriptional factors such as HOX-inducible factors (HIF) [130], forkhead box protein O1 (FOXO1) [131], NF-κB (nuclear factor kappa-light-chain-enhancer of activated B cells) [132], peroxisome proliferator-activated receptor (PPARγ) [133] as well as $[Ca^{2+}]_i$ homeostasis [134], and alterations in mitochondrial function [130].

1. Pulmonary Arterial Hypertension (PAH)
1.1. Idiopathic PAH
1.2. Heritable PAH
1.3. Drug- and toxin-induced PAH
1.4. PAH associated with:
1.4.1. Connective tissue disease
1.4.2. HIV (human immunodeficiency virus) infection
1.4.3. Portal hypertension
1.4.4. Congenital heart disease
1.4.5. Schistosomiasis
1.5. PAH long-term responders to calcium channel blockers
1.6. PAH with overt features of venous/capillaries (PVOD/PCH) involvement
1.7. Persistent PH of the newborn syndrome
2. PH due to left heart disease
2.1. PH due to heart failure with preserved LVEF
2.2. PH due to heart failure with reduced LVEF
2.3. Valvular heart disease
2.4. Congenital/acquired cardiovascular conditions leading to post-capillary PH
3. PH due to lung diseases and/or hypoxia
3.1. Obstructive lung disease
3.2. Restrictive lung disease
3.3. Other lung diseases with mixed restrictive/obstructive pattern
3.4. Hypoxia without lung disease
3.5. Developmental lung disorders
4. PH due to pulmonary artery obstructions
4.1. Chronic thromboembolic PH
4.2. Other pulmonary artery obstructions
5. PH with unclear and/or multifactorial mechanisms
5.1 Haematological disorders
5.2 Systemic and metabolic disorders
5.3 Others
5.4 Complex congenital heart disease

Table 1. Clinical classification of pulmonary hypertension (PH) by Simonneau et al., 2018 [135]

PAH: pulmonary arterial hypertension; PVOD: pulmonary veno-occlusive disease; PCH: pulmonary capillary haemangiomatosis; LVEF: left ventricular ejection fraction.

1.2.2. Characterization and mechanism of chronic hypoxia-induced PH

Group III of PH includes patients with PH due to chronic obstructive pulmonary disease (COPD), interstitial lung disease (ILD), obstructive sleep apnea (OSA), alveolar hypoventilation disorders, and chronic exposure to high-altitude. However, the exact prevalence of PH in these conditions remains incompletely understood. Chronic alveolar HOX causes pulmonary vasoconstriction and pulmonary vascular remodeling, both contributing to the persistent increase of PVR in chronic HOX-induced PH [136-138]. The pulmonary vascular remodeling is caused by enhanced proliferation as well as a decrease in the level of apoptosis of vascular cells [139, 140].

On important factor that may trigger chronic hypoxia-induced PH are HIFs. HIFs are proteins that rapidly accumulate when HOX occurs and mediate transcriptional control of several targets involved in cell proliferation, angiogenesis, erythropoiesis, and metabolism. HIF-1 has been demonstrated to play an integral role in sensing low O_2 tension depending on different factors, including hypoxic duration, O_2 concentration, and cycles of HOX and NOX. The HIF-1 complex is a heterodimer that consists of the regulatory HIF-1α subunit [141] and the HIF-1β subunit. Under NOX, HIF-1α is hydroxylated at conserved proline residues by prolyl hydroxylase domain proteins (PHDs) [142], which gives rise to the proteasomal degradation of HIF-1α. During HOX, HIF-1α is stabilized and accumulates in the cytoplasm through decreased activity of PHDs, as O_2 acts as the substrate for PHDs [143, 144]. Then, HIF-1α translocates to the nucleus, where it binds to HIF-1β and induces translation of HOX-related genes [91, 145-149]. HIF-dependent genes mediate a large range of processes, comprising vascular endothelial growth factor (VEGF)-induced vascularization, erythropoiesis, cellular proliferation and migration, and cellular metabolism [150-152]. HIF-1α is expressed ubiquitously in most species, such as in human, rat, and mouse organs, including the lung [153-155]. HIF-1α expression was shown as early as 30 minutes after exposure to HOX in the human Hep3B and HeLa cells and reached the highest level after 4 to 8 hours of continuous HOX, although it was barely detectable in the normoxic situation [156-158]. Consistent with this, cell proliferation and upregulation of VEGF expression were abolished in *Hif-1α* knockout embryonic stem cells during exposure to HOX [150, 151]. Furthermore, cell migration of embryonic fibroblasts was significantly reduced in the absence of HIF-1α compared to WT mouse cells [159]. Another report by Shimoda et al. brought evidence that the reduction in potassium current density, cellular membrane depolarization, and PASMC hypertrophy following exposure to HOX was blunted in *Hif-1α*

heterozygous mice [146, 160, 161]. In addition, there are studies showing the decrease in hypoxia-induced PASMC hyper-proliferation as well as pulmonary arterial remodeling and subsequently PH in *Hif-1a*$^{+/-}$ and SMC-*Hif-1a* knockout mice as well as HIF-1α-deficient rats (deficiency induced by intratracheal application of HIF-1α shRNA) [162-164]. These findings indicate that HIF-1α plays an important role in the response of the pulmonary vasculature to prolonged HOX and participates in pulmonary vascular remodeling.

In addition to acute HOX, mitochondria play an important role in the vascular response to prolonged and chronic HOX and are shown to be implicated in non-hypoxic forms of PH. The metabolic hypothesis of PH was introduced by Archer et al., suggesting a metabolic switch from mitochondrial oxidative phosphorylation to glycolysis in response to hypoxia that leads to the increase in $[Ca^{2+}]i$ and cellular membrane depolarization. Furthermore, these mitochondria were characterized by hyperpolarization and decreased H_2O_2 release which can promote anti-apoptotic properties [165]. Mitochondrial alterations were also linked to K_V channel downregulation which plays an important role in resistance to apoptosis and PH development [116]. Mitochondrial dysfunction in PH is associated with increased pyruvate dehydrogenase (PDH) kinase (PDK) activity and decreased pyruvate oxidation [166] Accordingly, treatment with dichloroacetate (DCA; a compound that inhibits mitochondrial PDK and, therefore, increases PDH activity and improves mitochondrial function) prevented chronic HOX-induced PH [167]. In addition, DCA was able to reverse mitochondrial membrane hyperpolarization, enhance the release of H_2O_2, and reverse the hypoxia-induced K_V channel downregulation in PASMC of the non-hypoxic animal model of PH caused by monocrotaline-treatment in rats. As a result, DCA attenuated monocrotaline-induced PH, shown by a decrease in PVR, medial wall thickness of pulmonary arteries, and right ventricular hypertrophy [168]. In addition, a first clinical trial with DCA treatment indicated beneficial effects in specific PAH patients [169]. Similar to the role of mitochondrial ROS in HPV, there is a debate on whether ROS are increased or decreased during PH development. Above mentioned studies linked decreased ROS to mitochondrial alterations, and chronic hypoxia-induced PH. Recently, a drop in superoxide levels was observed in mouse lung homogenate and PASMC after exposure to chronic HOX [170-172]. In contrast, another study on human PASMC found a significant ROS enhancement after chronic exposure to HOX [173]. Discrepancies may be related to measurement techniques and protocol, in particular potential re-oxygenation artefacts have to be taken into account.

Several investigations showed a relationship between mitochondria and the HIF pathway. In hypoxic conditions, HIF-1 could increase PDK1 expression as well as lactate dehydrogenase

activity and lactate production. Subsequently, this process could lead to a decrease in mitochondrial activity and shift the metabolism from mitochondrial respiration to glycolysis (Warburg effect) [174, 175]. In turn, mitochondrial ROS signaling may affect HIF-1α stabilization, and it was suggested that mitochondrial ROS could suppress PHD activity, thereby decreasing HIF degradation. Hernansanz-Agustin et al. observed an increase in ROS release and PHD suppression in HOX-exposed systemic endothelial cells, resulting in HIF-1α stabilization [176]. Furthermore, studies showed that a deficiency in GRIM-19 (NDUFA13, a subunit of CI) or SDHB (Succinate dehydrogenase subunit B, the iron-sulfur cluster containing subunit of CII) provoke HIF-1α stabilization following the induction of ROS production in Hela, Hep3B hepatoma, alveolar epithelium-derived tumor human cells, as well as in rat PC12 cells [177-179]. Also, ROS release from CIII was identified as stabilizing factor of HIF-1α in Hs29-4T and HEK-293 cells [180, 181]. Suppression of the RISP expression (part of CIII) in human cell lines could decrease ROS production and HOX-induced HIF-1α stabilization [182]. Furthermore, cytochrome c null mouse embryonic cells, as well as mitochondria-deficient cells (Hep3B and HEK293cells), failed to sufficiently increase mitochondrial ROS production and HIF-1α stabilization upon exposure to 1.5% O_2. H_2O_2 treatment prevented HIF-1α degradation in these cells, even when cytochrome c of the METC is not functional [183]. On the contrary, there are studies showing that a decrease in ROS or H_2O_2 production stabilizes HIF-1α [184, 185].

The above described mitochondrial alterations may not only promote cellular proliferation via HIF-1α stabilization but also mitochondrial hyperpolarization, which in turn can attenuate mitochondria-dependent apoptosis [186]. Accordingly, pharmacological inhibition of PH was associated with inhibition of mitochondrial hyperpolarization and induction of apoptosis [187]. Another study showed that puerarin treatment, which mediates autophagy, suppressed cell growth and provoked apoptosis in human cells under HOX. The puerarin-induced apoptosis in hypoxic human PASMC was accompanied by reduced MMP, cytochrome c release from the mitochondria, and caspase-9 activation, and a decrease in the level of Bcl-2, with concurrent up-regulation of Bax [188]. Mouse embryonic cells cultured in 3% O_2 had substantially greater MMP compared with those cultured in 20% O_2 [189]. In this regard there is another study showed the mitochondrial hyperpolarization in mouse undergone hypoxia-induced PH [190]. In this regard, it was also suggested that HOX could increase the activity of the mitochondrial ATP-sensitive potassium channels (mitoKATP), and consequently, cause mitochondrial membrane depolarization [191].

Chronic HOX also affects the mitochondrial structure. It has been shown in several studies that chronic hypoxia induced fission and reduced fusion in PASMC and therefore, inhibition of fission could inhibit different forms of PH including chronic hypoxia-induced PH [192, 193]. Increased fission may not only affect metabolic alterations and ROS release but also mitochondrial calcium handling by interaction with the endoplasmic reticulum. Alterations in $[Ca^{2+}]_i$ are crucial for pulmonary vascular remodeling and the development of PH. It should be taken into account that mitochondria and the endoplasmic reticulum are important for Ca^{2+} regulation. In this regard, Sutendra et al. observed that the NOGO-B protein is activated by HOX only in lung vessels and serves to disrupt the close affiliation between the endoplasmic reticulum and the mitochondria. Accordingly, genetic deletion of *Nogo* suppressed the induction of PH development in HOX-exposed mice [194]. $[Ca^{2+}]$i can also be regulated by HIF-1α that mediated enhancement of Ca^{2+} entry by increasing the activity and expression of SOCCs in mice and rats exposed to chronic HOX as well as in mouse PASMC (4% O_2, 60 hours) [195]. $[Ca^{2+}]$i can affect calcium-dependent transcription factor and thus induction of pulmonary vascular remodeling and PH [196].

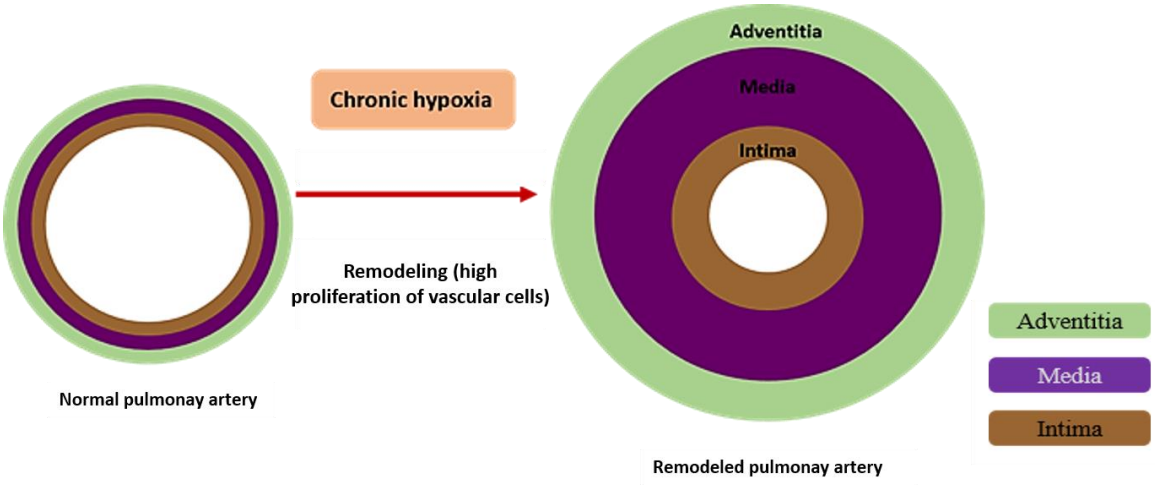

Figure 2. Pulmonary vascular remodeling in chronic hypoxia-induced pulmonary hypertension (PH)

Chronic hypoxia (HOX) causes pathological thickening of the vascular wall resulting in narrowing of the vascular lumen (pulmonary vascular remodeling) and, subsequently, PH. HOX-induced pulmonary vascular remodeling is partially reversible after re-exposure to normoxia (NOX) (197). Schematic representation of pulmonary vascular remodeling in the small pulmonary arteries in PH. Green, purple, and brown colors indicate adventitia, media, and intima, respectively.

1.3. Alternative oxidase (AOX)

1.3.1. Characteristics of the AOX

The recognition that plants had protection against METC inhibitors (such as cyanide) by Genevois et al. in 1929 [197] led to the discovery of a 32 kDa, homodimer protein, named alternative oxidase (AOX), from *Arum maculatum* mitochondria in 1978 [198, 199]. AOX, which belongs to the di-iron carboxylate protein family, is localized in the matrix site of the inner mitochondrial membrane and is expressed in plants, lower organisms, and some animals, but not in mammals [186, 200-202]. This protein is capable of coupling QH_2 oxidation to O_2 reduction for water production with the involvement of 4 electrons [203] and thus prevents the Q from being more reduced, which is a major source of superoxide release from the METC [204]. Importantly, the availability of QH_2 acts as a limiting factor for AOX activity to avoid its activation when the METC is functional. Therefore AOX has a relatively low affinity for QH_2 compared to CIII [204]. In addition, experiments determined that iron

(Fe^{2+}) in the active site of AOX plays an important role in shuttling the electrons from the Q pool to O_2 by showing inactivation and activation of AOX protein in the absence and presence of iron, respectively, on the yeast *Hansenula anomala* [205]. *Aox* expression was increased in the presence of mitochondrial METC inhibitors such as cyanide and rotenone (inhibitors of CIV and III, respectively), and resulted in maintenance of mitochondrial signaling pathways [206-210]. Because AOX has no proton pumping capacity and bypasses the proton-pumping complexes CIII and IV, MMP and ATP production is decreased when AOX is activated [211]. Although AOX cannot maintain ATP production at high levels, it allows to regulate key metabolic functions such as the NAD/NADH ratio and ROS levels. With regard to ROS, it has been demonstrated that *Aox*- overexpressing tobacco cells had lower gene expression encoding ROS-scavenging enzymes (*Sod* genes and *Gpx*), and in contrast, a higher ROS level when AOX was suppressed [212]. The same outcome was observed when the production of superoxide was enhanced in the mitochondria from the pericarp tissue of green bell pepper after treatment with disulfiram (an inhibitor of the AOX) [213]. Moreover, H_2O_2 treatment could induce *Aox* mRNA expression in tobacco cells [214].

1.3.2. Function of AOX in mammalian cells

As described above, AOX has important physiological functions in plants and specific lower organisms. Researchers succeeded in expressing chordate *Ciona intestinalis* AOX in cultured human cells with no significant impact on the normal activity of the METC components. This expression endowed special cyanide- and antimycin-insensitive and non-proton motive properties to mitochondria that were inhibited by a specific AOX inhibitor, n-propyl gallate (n-PG) [215]. Consistent with this, Dassa et al. found that *Aox* expression could counteract metabolic abnormality in *Cox15/Cox10*-deficient human cells [216]. According to a study on human kidney epithelial cells (HEK293T), AOX attenuated high mitochondrial ROS production and blocked the induction of superoxide dismutase under a hypoxic situation [216, 217]. *In vivo* expression of *Ciona intestinalis* AOX in *Drosophila* was innocuous in absence of METC inhibitors, but gave rise to resistance to deleterious effects of cyanide and antimycin [218]. Interestingly, El-Khoury et al. proved that *Ciona intestinalis* AOX could be functionally expressed in the mouse. This Aox^{tg} mice preserved METC from inhibition by cyanide and consequently, high Q reduction and superoxide production [204]. In line with this, it was shown that Aox^{tg} mice could survive against lethal dose application of cyanide and therefore, they resisted to its inhibitory effect on METC [219].

1.4. Cytochrome c oxidase subunit 4 (COX4)

1.4.1. Characteristics of COX4

The mitochondrial cytochrome c oxidase (COX), or complex IV (CIV), is a dimeric protein of the METC containing 13 subunits per monomer [220], with a molecular weight of 204 kDa, in which 3 subunits are encoded by the mitochondrial genome and the remaining 10 subunits are encoded by nuclear genes. This enzyme provides a crucial function in cellular respiration by transferring electrons from cytochrome c to O_2 to produce water. This function is accomplished by 4 redox-active metal sites of the complex, namely, heme a, heme a3, CuA, and CuB. In addition, this process is coupled to the pumping of 4 protons from the mitochondrial matrix toward the intermembrane space to generate an MMP, which, in turn, is essential for ATP production [221]. Cytochrome c oxidase subunit 4 (COX4) is the largest nuclear-encoded subunit and is located at the matrix side of the complex. This subunit possesses 2 isoforms: a ubiquitously expressed isoform, COX4i1, with 169 amino acids, and COX4i2, which is 171 amino acids long and is specifically expressed in the lung and placenta with high levels found in pulmonary SMC [222].

1.4.2. Function of COX4

COX4 is important, on the one hand, for COX assembly and function, and thereby mitochondrial respiration, and on the other hand, for adjusting cellular energy production to energy demand by inhibition of COX activity at high levels of ATP [223, 224]. In bovine heart mitochondria it was shown that COX4 could decrease the activity of COX by binding of ATP to COX4, and thereby controlling the cytosolic and matrix ATP/ADP ratio, which enables COX activity to be adjusted to energy need [225-227]. The function of COX4i2 compared to the function of COX4i1 is currently under investigation. Hüttemann et al. showed attenuated COX activity and also a drop in lung ATP levels in the *Cox4i2* knockout mouse compared to WT [228]. In addition, It has been shown that COX4i2 was upregulated under the condition of hypoxia in astrocytes which in turn decreased the COX sensitivity to ATP [229]. However, the loss of ATP sensitivity of COX4i2 is under debate, as Hüttemann et al. described that there was no difference in ATP regulation of COX activity in liver that lacks COX4i2 compared to the COX4i2-containing lung, and in WT lung compared to *Cox4i2* knockout lung [228]. COX4i2 and COX4i1 are predominantly present in the lung, specifically in SMC and respiratory epithelium cells, respectively [227]. Several studies

showed a change in *Cox4i2* expression depending on O_2 availability [230] in which COX4i1 and COX4i2 were highly expressed in normoxic and hypoxic conditions, respectively [230, 231].

According to Fukuda et al. HIF-1 could activate *Cox4i2* gene expression as well as increase COX4i1 protein degradation in human and mouse cells exposed to HOX [230]. Recently, Aras et al. found that the transcription factors RBPJ, CXXC5, and CHCHD2 bind to the proximal region of the *Cox4i2* promoter (a highly conserved 13-bp sequence), thereby regulating its expression at low O_2 levels [224, 232]. Nevertheless, the molecular function of COX4i2 still remains elusive. Hüttemann et al. showed the presence of 3 conserved cysteine residues in COX4i2 which do not exist in COX4i1 which may affect COX function [233]. Recently, the group of Pecina showed that COX4i2 expression in Hek cells decreased O_2 affinity of the METC [234]; however, the physiological role of COX4i2 still needs to be described (Figure 3).

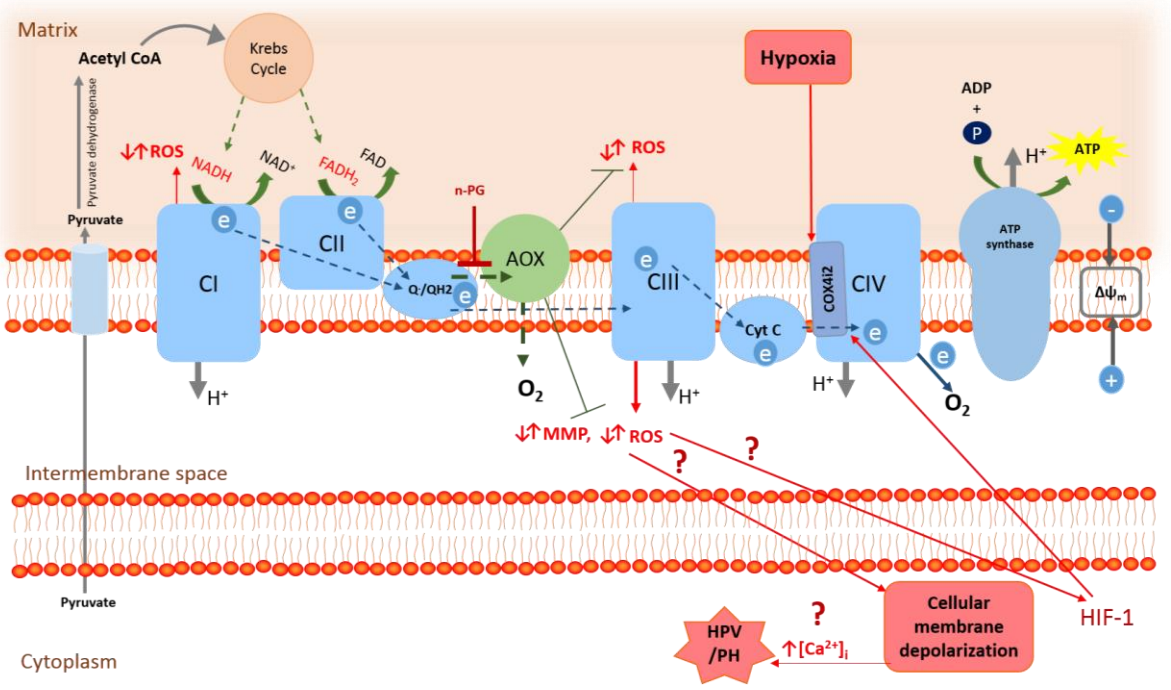

Figure 3. A simplified scheme of the METC featuring the alternative oxidase (AOX) and the cytochrome c oxidase subunit 4 isoform 2 (COX4i2)

The AOX bypasses the cytochrome segments of the mitochondrial electron transport chain (METC) to shuttle electrons directly from the ubiquinol (QH_2) to the oxygen molecule (O_2) and produce water. AOX confers resistance to respiratory blockade distally to the Q pool (e.g. by cyanide) and bypasses complexIII/IV (CIII/IV) thereby inhibiting reactive oxygen species (ROS) release from CIII. AOX is activated by a highly reduced ubiquinone (Q) pool and can be inhibited by n-propyl gallate (n-PG). COX4i2 is a isoform of cytochrome c oxidase subunit 4 (COX4) which expression is induced during hypoxia.

It is under debate whether HOX triggers an increase or decrease in MMP and ROS from CI and/or CIII [235, 236], which may lead to cellular membrane depolarization and subsequently, intracellular calcium increase and contraction of PASMC. Furthermore, it is unlear if ROS can contribute to HOX-induced HIF-1α stabilization which activates several genes, including *Cox4i2*.

Mitochondrial complexes I, II and III: CI, CII, and CIII; reactive oxygen species: ROS; coenzyme Q cycle: Q./QH_2; cytochrome c oxidase subunit 4 isoform 2: COX4i2; cytochrome c: cyt c; mitochondrial membrane potential: MMP; adenosine diphosphate: ADP; adenosine triphosphate: ATP; the oxidized form of nicotinamide adenine dinucleotide: NAD^+; the reduced form of nicotinamide adenine dinucleotide: NADH; the oxidized form of flavin adenine dinucleotide: FAD; the reduced form of flavin adenine dinucleotide: FADH2; phosphoric acid: P; Cytosolic calcium concentration: $[Ca^{2+}]i$; HOX-inducible factors (HIF-1); proton: H^+; oxygen: O_2; electron: e.

1.5. Uncoupling protein 2 (UCP2)

1.5.1. Characteristics of UCP2

UCPs are anion transporter proteins anchored within the inner mitochondrial membrane. In 1978, it was revealed that UCP1, which was initially identified in brown adipose tissue (BAT) [237], could increase the transportation of protons into the mitochondrial matrix to produce heat and catalyze thermogenesis in the BAT in infants at birth. In 1997, scientists isolated a cDNA that encodes a protein similar to UCP1 from mouse and human skeletal muscle, called UCP2, and later, they were also able to clone UCP3 from rat and human cDNA. UCP4 and UCP5 were later identified in the brain and had a lower sequence identity to UCP1 [238, 239]. UCPs contain 3 repeat domains, each connected by two α-helix loops in the lipid bilayer with the orientation towards the mitochondrial matrix, whereas the N and C-terminal of UCP are extended into the intermembrane space of mitochondria. The amino acid sequences of UCP1 and UCP2 have a 59% resemblance, and the amino acid sequences of UCP2 and UCP3 have a 73% resemblance [240].

UCP2 is almost expressed in all tissues, such as bone marrow, the lung, kidney, stomach, and endocrine tissues, as well as in the immune system (monocytes/macrophages) and was reported to have a half-life of 30 minutes [241]. In contrast, UCP3 is mostly expressed in skeletal muscles, heart tissues, and BAT [242, 243]. Unlike UCP1, UCP2 and UCP3 are not involved in thermogenesis.

1.5.2. Function of UCP2

UCP2 is known to be involved in several physiological and pathological conditions, such as the metabolism of fatty acids, regulation of obesity, development of diabetes, suppression of O_2 radicals, and the aging process. However, there is currently no consensus on the molecular mechanism of UCP2, but several functions have been proposed. It has been suggested that UCP2 is involved in proton transportation only when specific physiological conditions are present [244, 245]. In aortic endothelial cell mitochondria, high expression of *Ucp2* could enhance the MMP [246]. However, a report by Couplan et al. found no evidence for engagement of UCP2 in proton conductance: the authors found no difference between the proton conductance of mitochondria isolated from lung and spleen in UCP2 and WT mice under basal conditions [247-249]. Moreover, Echtay et al. showed that UCP2 needs Q and fatty acids to be functional as a proton transporter, and a low concentration of nucleotides

could inhibit this process [250]. In contrast, others found that proton transportation by UCP2 doesn't need Q activation, but they also confirmed the inhibitory effect of ATP on UCP2 activity [251].

The proton-leak property of UCP2 can affect MMP and ATP synthesis. One study reported a drop in the proton leak level, and, therefore, an increase in MMP and ATP production in thymocytes and β-cells from *Ucp2* deficient mice compared to those from WT mice [252-254]. It was also suggested that UCP2 might be an important regulator of intracellular ROS production and, in turn, UCP2 could also be affected by ROS. In support of this hypothesis, superoxide could affect UCP2 activity and increase proton transportation in a GDP-sensitive manner, although not in the tissues lacking UCP2 [255]. In another study, Echtay et al. showed the activation of the proton leak by exogenous superoxide. In addition, they showed increased UCP2 protein expression after experimental inflammation with LPS application [240]. *Ucp2* overexpression, in return, could prevent mitochondrial membrane hyperpolarization, excessive ROS production, and mitochondrial calcium accumulation caused by LPS treatment [256]. Further experiments revealed a higher level of ROS in *Ucp2* knockout pancreatic α and β mouse cells, which had severe hyperglycemia after streptozotocin treatment, compared to similar cells from WT mice [257]. Accordingly, elevated superoxide production under hyperglycemia- and obesity-induced β cell impairment and loss of glucose responsiveness could induce an increase of UCP2 protein expression in islet cells. [254]. Altogether, this evidence proposes that UCP2 protects cells from damage by ROS and keeps the membrane potential sufficiently low [258].

However, the uncoupling function of UCP2 was challenged by a report showing that UCP2 can regulate mitochondrial Ca^{2+} uptake in liver mitochondria by proving the absence of ruthenium red-sensitive Ca^{2+} uptake in mitochondria from *Ucp2* knockout mice [259]. In addition, Trenker et al. found that high expression of *Ucp2* led to a substantial increase in mitochondrial Ca^{2+} uptake [259]. Notably, UCP2 was found to be essential for mitochondrial Ca^{2+} uptake; a study showed that UCP2 could increase the activity of methylated mitochondrial Ca^{2+} uptake 1, a regulatory subunit of mitochondrial Ca^{2+} uniporter, and subsequently, increase the Ca^{2+} entry to mitochondria [260, 261]. In spite of that, Brookes et al. showed no Ca^{2+} uptake difference in mice lacking UCP2 compared to the WT mice [262]. Other factors that can affect UCP2 protein expression are glucose and free fatty acid concentrations, and there is a hypothesis that UCP2 eliminates pyruvate-induced redox pressure by extruding the pyruvate out of mitochondria (similar to the Warburg effect) and increasing glycolysis [263]. High expression of the *Ucp2* gene and impairment of PDH

activity was observed in the rat pancreatic islets exposed to free fatty acids and glucose. This process could, in turn, decrease glucose-stimulated mitochondrial membrane hyperpolarization and changes in the ATP/ADP ratio [264-266]. The discrepancies of data of different studies might be depend on cell type, method of UCP2 manipulation, metabolic state of the cell/isolated mitochondria, direct vs. indirect effects of UCP2.

Most importantly, studies show that UCP2 may play a role in the development of PH. It was demonstrated that *Ucp2* knockout mice exhibited right heart hypertrophy compared to WT mice, which was indicated by higher right ventricular systolic pressure (RVSP) in normoxic and intermittent hypoxic conditions and attributed to the elevation of mitophagy and apoptosis [267]. In addition, Michelakis et al. found that normoxic *Ucp2* knockout mice developed PVR and PH similar to chronic HOX via decreasing the level of Ca^{2+} within the mitochondria and increasing the levels of HIF-1α [268]. In line with these studies, our previous research also showed an increase in the level of cellular proliferation, MMP, and ROS production in *Ucp2* knockout mice compared to WT mice, which could lead to the development of PH [190] (Figure 4).

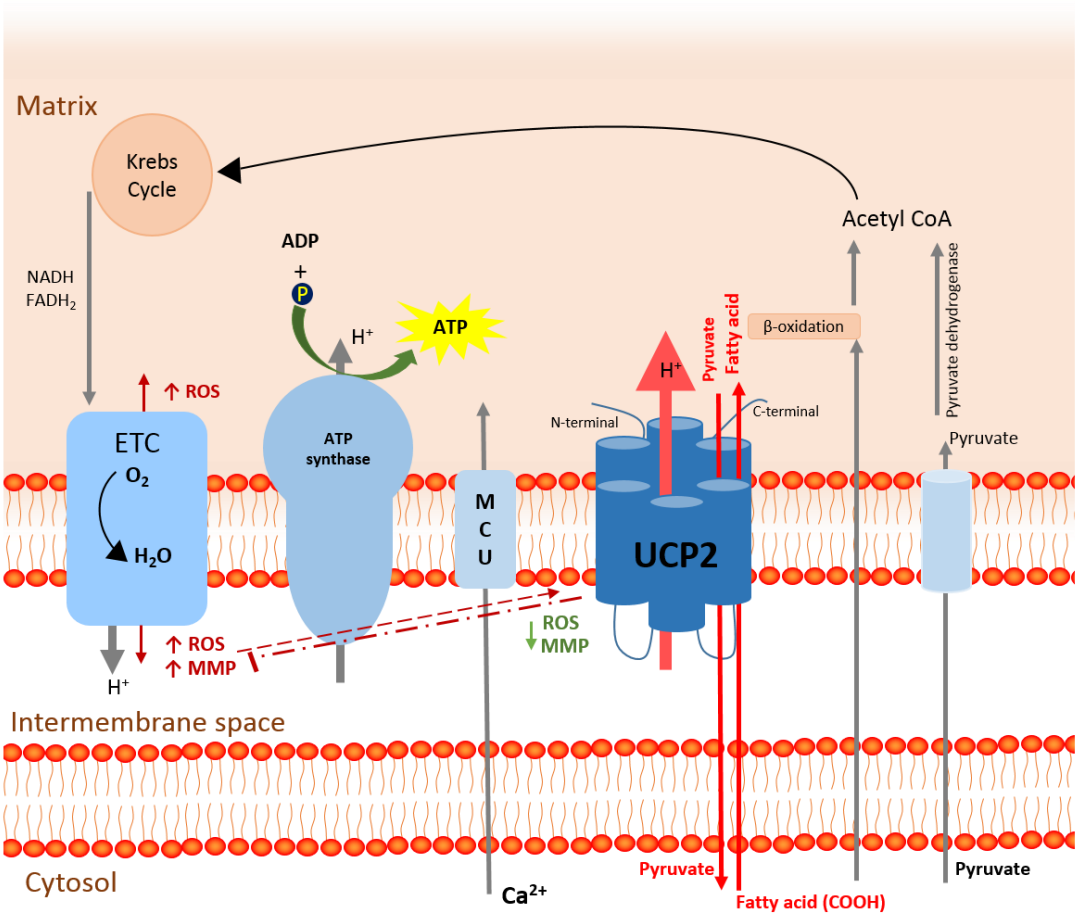

Figure 4. A simplified scheme of the METC featuring the uncoupling protein 2 (UCP2) and its proposed functions

UCP2 is ubiquitously expressed in most cell types and can be activated amongst others by a superoxide-dependent mechanism. UCP2 is suggested to lower mitochondrial membrane potential (MMP) and superoxide release. The underlying molecular mechanisms remains unclear. UCP2 may mediate proton conductance similar to UCP1, however, this function was challenged. UCP2 may also promote mitochondrial fatty acid oxidation and limit the use of pyruvate and C4 metabolites [266] to fuel oxidative phosphorylation

Mitochondrial electron transport chain: ETC; reactive oxygen species: ROS; mitochondrial membrane potential: MMP; mitochondrial calcium uniporter MCU; adenosine diphosphate: ADP; adenosine triphosphate: ATP; phosphoric; acid: P; proton: H^+; Calcium: Ca^{2+}; proton: H^+; oxygen: O_2; water: H_2O.

1.6. The aim of this study

In most cell types mitochondria are the main sources of cellular ROS which have been suggested to play a crucial role in O_2 sensing underlying HPV and regulation of PH. The MMP as an important component of the proton motive force can affect the rate of ROS production and thus may be involved in the regulation of HPV and HOX-induced PH. Although different concepts of the contribution of mitochondria and mitochondrial ROS for HPV and chronic HOX-induced PH have been developed, the exact O_2 sensing mechanism and role of mitochondrial ROS remains incompletely understood. In particular it is under debate, if mitochondrial ROS release is increased or decreased during acute and chronic HOX in the pulmonary vasculature.
This study aimed to investigate the role of mitochondrial ROS and its release mechanism in HPV and chronic HOX-induced PH by using different genetic models that affect mitochondrial ROS release. Furthermore, the cell-type specific role of UCP2 which may affect mitochondrial MMP and ROS release was further examined.

To achieve these aims the following mouse models were used:

Mice overexpressing *Aox* (*Aox*^{tg}): In plants, lower organisms, and some animals, but not in mammals, a non-proton-motive and cyanide-resistant AOX can oxidize QH_2 to produce water, when the activity of the distal segments of the METC (CIII to IV) are limited and thus prevent overproduction of ROS [207, 208]. Mice overexpressing *Aox* did not show any overt phenotype [219]. This study investigated the hypothesis that decreased ROS production in AOX may inhibit HPV and chronic HOX-induced PH.

Mice deficient of *Cox4i2*: COX4i2 has been shown to affect mitochondrial ROS production and membrane potential in astrocytes [269, 270]. Furthermore, it is highly expressed in the lung and the placenta, both organs with specialized O_2 sensing cell types. *Cox4i2* knockout mice showed no overt phenotype [271]. This study thus investigated the hypothesis that *Cox4i2* specifically regulates HOX-induced ROS release in the pulmonary vasculature and *Cox4i2* knockout mice exhibit less HPV and HOX-induced PH compared to WT mice.

Mice deficient of *Ucp2*: Although the exact molecular mechanism of UCP2 remains under debate, it has been shown that UCP2 can mitigate ROS production, therefore protecting cells from the damage of oxidative stress. Furthermore, it was previously shown that the lungs of

Ucp2 knockout mice displayed PH and remodeling of pulmonary vasculature under baseline normoxic conditions [272]. This study thus investigated the hypothesis that *Ucp2* knockout specifically in SMC can induce PH under baseline normoxic conditions and may enhance chronic hypoxia-induced PH.

This study investigated the response to acute HOX *in vitro* in PASMC and in isolated ventilated lungs, as well as the development of PH in NOX and after chronic hypoxic exposure by *in vivo* measurement of pulmonary hemodynamics and pulmonary vascular remodeling to address these specific questions:

1) To investigate if inhibition of mitochondrial ROS release by inhibitors, the presence of AOX or the absence of COX4i2 inhibits HPV or chronic HOX-induced PH and if the genetic modifications affect MMP and ROS production as a potential underlying mechanism of the hypoxic responses.
2) To investigate if SMC specific knockout of *Ucp2* affects pulmonary vascular remodeling in NOX and chronic HOX-induced PH.

2. Materials and Methods

2.1. Materials

2.1.1. The model of the isolated perfused and ventilated mouse lung

Substance	Concentration
Calcium chloride ($CaCl_2$)	2.4 mM
Glucose	13.32 mM
Hydroxyethylamylopectin (molecular weight 200,000)	5% (wt/vol)
Magnesium chloride ($MgCl_2$)	1.3 mM
Potassium chloride (KCl)	4.3 mM
Potassium dihydrogen phosphate (KH_2PO_4)	1.1 mM
Sodium chloride (NaCl)	120 mM

Table 2. Composition of Krebs-Henseleit buffer (Serag-Wiessner; Naila, Germany) used in the isolated perfused and ventilated mouse lung setup

2.2 ml of sodium bicarbonate 8.4% (NaHCO3; Serag-Wiessner; Naila, Germany) was added to the perfusion buffer to adjust pH at 7.1-7.2.

Substance and equipment	Company
Aqua distillate	B. Braun Melsungen AG; Melsungen, Germany
Blood analyzer ABL 330	Radiometer; Copenhagen, Denmark
Dimethylsulfoxide (DMSO)	Life Technologies; Carlsbad, USA
Ethanol absolute (formula: C_2H_5OH)	Sigma-Aldrich; St. Louis, USA
Heparin	Roche; Basel, Switzerland
Hydrogen peroxide (H_2O_2)	Sigma-Aldrich; St. Louis, USA
Ketamine 10%	Bela-pharm GmbH & Co. KG; Vechta, Germany
Krebs-Henseleit buffer	Serag-Wiessner; Naila, Germany
MitoTempo (2,2,6,6-tetramethyl-4-[5-(Triphenylphosphonio) pentoxy] piper-	Sigma-Aldrich; St. Louis, USA

idin-1-oxy bromide)	
Normoxic gas (21% O_2, 5% CO_2, rest N_2) Hypoxic gas (1% O_2, 5% CO_2, rest N_2)	Ludwigshafen, Germany
n-Propyl gallate (n-PG)	Sigma-Aldrich; St. Louis, USA
Peristaltic pump Reglo Digital MS-4/8	Cole-Parmer GmbH; Ismatec, Wertheim,
Potassium chloride (KCl)	Merck; Darmstadt, Germany
Potassium cyanide (KCN)	Sigma-Aldrich; St. Louis, USA
Pressure sensor	B. Braun Melsungen AG; Melsungen, Germany
Refrigeration/Heating Circulator, F32-MC	Julabo Labortechnik GmbH; Seelbach, Germany
Research Grade Isometric Force Transducer	Harvard Apparatus; Holliston, USA
S3QEL2 (1-[3, 4-Dimethylphenyl]-N, N-dipropyl-1H-pyrazolo [3, 4-d] pyrimidin 4-amine)	Sigma-Aldrich; St. Louis, USA
SKQ1	Sigma-Aldrich; St. Louis, USA
Sodium bicarbonate ($NaHCO_3$) 1 M 8.4%	Serag-Wiessner; Naila, Germany
Thromboxane analogon (U46619)	Sigma-Aldrich; St. Louis, USA
Transducer- amplifier module, Type 705/1, in Plugsys Type 601	Hugo Sachs Elektronik; March-Hugstetten, Germany
Triphenylphosphonium chloride (TPP)	Sigma-Aldrich; St. Louis, USA
Ventilator, minivent Type 845	Hugo Sachs Elektronik-Harvard Apparatus GmbH; March-Hugstetten, Germany
Xylazine 2%	Serumwerk Bernburg AG; Bernburg, Germany

Table 3. Substances and equipment used for the isolated perfused and ventilated mouse lung setup

2.1.2. Isolation of pulmonary arterial smooth muscle cell (PASMC)

Substance and equipment	Company
Agarose (low melting temperature)	Sigma-Aldrich; St. Louis, USA
Collagenase	Sigma-Aldrich; Steinheim, Germany
Fetal bovine serum (FBS)	Sigma-Aldrich; St. Louis, USA
Iron III oxide (Fe_3O_4)	Sigma-Aldrich; St. Louis, USA
Laboratory incubator	Thermo Fisher Scientific; Waltham, USA
Medium 199 (M199)	Thermofisher; Life technologies limited, UK
Penicillin-Streptomycin antibiotic (P/S)	Sigma-Aldrich; St. Louis, USA
Phosphate-buffered saline (PBS)	Pan-Biotech GmbH; Aidenbach, Germany
Smooth muscle cell (SMC) growth medium	PromoCell GmbH; Heidelberg, Germany

Table 4. Substances and equipment used for PASMC isolation

2.1.3. Mitochondrial membrane potential (MMP) measurement

Substance and equipment	Company
A closed/open heated chamber	PeCon; Mannheim, Germany
Fluorescence microscope	IX70; Olympus; Hamburg, Germany
JC1 (5,5′,6,6’-Tetrachloro-1,1′,3,3′-tetraethylimidacarbocyanine Iodide)	Invitrogen; Carlsbad, USA
Polychrome II monochromatic and IMAGO CCD camera	Till Photonics; Munich, Germany

Table 5. Substances and equipment used for MMP measurement

Substance	Concentration (mM)
Calcium chloride ($CaCl_2$)	1.8
Glucose	10
Magnesium chloride ($MgCl_2$)	1.05
Potassium chloride (KCl)	5.4

Sodium bicarbonate ($NaHCO_3$)	22
Sodium chloride (NaCl)	126.7
Sodium dihydrogen phosphate (NaH_2PO_4)	0.42

Table 6. Chemical composition of normal Tyrode's solution

2.1.4. Patch-clamp recording of cellular membrane potential

Substance	**Company**	**Concentration (mM)**
Calcium chloride ($CaCl_2$)	Carl Roth; Karlsruhe, Germany	1.8
Glucose	Carl Roth; Karlsruhe, Germany	10
Magnesium chloride ($MgCl_2$)	Carl Roth; Karlsruhe, Germany	1.05
Potassium chloride (KCl)	Carl Roth; Karlsruhe, Germany	5.4
Sodium bicarbonate ($NaHCO_3$)	Carl Roth; Karlsruhe, Germany	22
Sodium chloride (NaCl)	Sigma-Aldrich; St. Louis, USA	126.7
Sodium dihydrogen phosphate (NaH_2PO_4),	Merck Millipore; Darmstadt, Germany	0.42

Table 7. Composition of the extracellular-analogous solution
The pH was adjusted to 7.4.

Substance	**Company**	**Concentration (mM)**
4-(2-hydroxyethyl)-1-piperazineethanesulfonic acid (HEPES)	Carl Roth; Karlsruhe, Germany	10
Adenosine 5′-triphosphate magnesium salt (ATP)	Sigma-Aldrich; St. Louis, USA	4

Ethylene glycol-bis (2-aminoethylether)-N, N, N′, N′-tetraacetic acid (EGTA)	Sigma-Aldrich; St. Louis, USA	10
L-Aspartic acid potassium salt (L-aspartate)	Sigma-Aldrich; St. Louis, USA	105
Magnesium chloride ($MgCl_2$)	Carl Roth; Karlsruhe, Germany	1
Potassium chloride (KCl)	Carl Roth; Karlsruhe, Germany	25
Sodium chloride (NaCl)	Sigma-Aldrich; St. Louis, USA	4

Table 8. Composition of the intracellular-analogous solution
The pH was adjusted to 7.2 by titration with 1 M potassium hydroxide (KOH).

Equipment	**Company**
Borosilicate glass capillary tubes	Sutter Instruments; Novato, California, USA
Culture dishes	Greiner Bio-One; Frickenhausen, Germany
DMZ universal electrode puller	Zeitz; Martinsried, Germany
EPC10 USB single amplifier	HEKA Elektronik GmbH; Lambrecht, Germany
IGOR Pro software	Wavemetrics; Lake Oswego, USA
Optical needle-type FireSting O_2 sensor	PyroScience; Aachen, Germany
Patch-clamp master software	HEKA Elektronik GmbH; Lambrecht Germany
Solution heater	Warner Instruments; Hamden, USA

Table 9. Equipment used for patch-clamp measurement

2.1.5. RNA extraction and quantitative reverse transcription PCR (qRT-PCR)

Step		Temperature	Time
1	Denaturing	94°C	3 minutes
2	Denaturing	94°C	20 sec
3	Annealing	64°C	30 sec
4	Elongation	72°C	35 sec
5	Denaturing	94°C	20 sec
6	Annealing	64°C	30 sec
7	Elongation	72°C	35sec
8	Elongation	72°C	2 minutes

Table 10. The cycling conditions for cDNA

Step		Temperature	Time	Cycle
1	Initial denaturing	95°C	1 minute	1
2	Denaturing	95°C	10 seconds	30-40
3	Annealing/Extention	60°C	30 seconds	

Table 11. The cycling conditions for qRT-PCR

Substance and equipment	Company
iScript kit	Bio-Rad;Hercules, USA
Master mix, iTaq Universal SYBR® Green supermix	Bio-Rad; Hercules, USA
Mx3000P PCR system	Agilent Technologies; Santa Clara, USA
RNeasy mini kit	Qiagen; Hilden, Germany

Table 12. Substances and equipment used for qRT-PCR measurement

2.1.6. DNA extraction and standard PCR

Primer name	Forward sequence	Reverse sequence
***Aox*^{Rosa26} heterozygote (genotyping)**	GACCTCCATCGCGCACTCCG	CTCCGAGGCGGATCACAAGC
B2M (qRT-PCR)	TTCTTTCTGGCATAAATTG	AGCCCAAGACCGTCTACTGG
***Cox4i2* knockout (genotyping)**	CTAAACTGTTCACATCTTACCC AGTAGCTTGAC	AATTCTATCAGGACATAGCGT TGGCTACC

Cre transgenic (genotyping)	ATTTGCCTGCATTACCGGTC	ATCAACGTTTTGTTTTCGGA
Exon 3 of *Ucp2* (qRT-PCR)	TGGTTTCAAGGCCACAGATG	GACCTTGGCGGTATCCAGAG
Exon 4 of *Ucp2* (qRT-PCR)	GTGGCGTTCTGGGTACCATC	GACGGAGGCAAAGCTCATCT
PBGD (qRT-PCR)	GGGAACCAGCTCTCTGAGGA	GAATTCCTGCAGCTCATCCA
***Ucp2*$^{flox/flox}$ (genotyping)**	ACCAGGGCTGTCTCCAAGCAGG	1) AGAGCTGTTCGAACAC CAGGCCA 2) TAGAGGAGGGTGGTGT TCCAGCTC

Table 13. Primer sequences for PCR

2.1.7. Western blot analysis

Substance and equipment	**Company**
Antibody anti-AOX	21st Century Biochemicals; Marlborough, USA
Antibody anti-HIF-1α	Cayman Chemical; Ann Arbor, USA
Antibody anti-β-actin	Abcam; Cambridge, UK
Enhanced chemiluminescence (ECL) detection reagent	GE Healthcare Life Sciences; Little Chalfont, UK
Homogenizer	PeqLab; Erlangen, Germany
Microplate reader	Tecan Infinite M200; Grödig, Austria
Phenylmethane sulfonyl fluoride (PMSF)	Sigma-Aldrich; St. Louis, USA
Pierce detergent compatible Bradford assay kit	Bio-Rad Laboratories; Munich, Germany
Plate reader	BioTek Instruments GmbH; Lucerne, Switzerland
Polyvinylidene difluoride (PVDF) membrane	Pall Corporation; Dreieich, Germany
Sodium dodecyl sulfate-polyacrylamide gel electrophoresis (SDS-PAGE)	Bio-Rad Laboratories; Munich, Germany

Table 14. Substances and equipment used for western blot measurement

2.1.8. Cellular $O_2^{\bullet}$ release by electron spin resonance (ESR) spectroscopy

Substance and equipment	Company
Electron spin resonance (ESR) spectroscopy	Bruker Biospin GmbH; Rheinstetten, Germany
MS 100 spectrometer	Magnettech; Berlin, Germany
Polyethylene-glycol conjugated superoxide dismutase (pSOD)	Sigma-Aldrich; St. Louis, USA
Spin probe 1-hydroxy-3-methoxycarbonyl-2,2,5,5-tetramethyl-pyrrolidine (CMH)	Alexis Corporation; San Diego, USA

Table 15. Substances and equipment used for ESR spectroscopy measurement

2.1.9. Hemodynamic measurement

Substance and equipment	Company
Biemer microvessel clamp	Aesculap; Tuttlingen, Germany
Heating pad	AD Instruments; Spechbach, Germany
Isoflurane	Air Liquid; Siegen, Germany
Power Lab data acquisition systems and Lab Chart 7 for windows software	AD Instruments; Spechbach, Germany
Rectal thermistor	AD instruments; Spechbach, Germany
Small animal ventilator, minivet type 845	Hugo Sachs Electronic; March-Hugstetten, Germany

Table 16. Substances and equipment used for hemodynamic measurement

2.1.10. Pulmonary arterial remodeling and immunohistochemistry assessment

Substance and equipment	Company
Alternative oxidase antibody	21st Century Biochemicals; Marlborough, USA
Antibody anti-von Willebrand factor	Dako; Hamburg, Germany
Antibody anti-α-smooth muscle actin	Sigma-Aldrich; St. Louis, USA

Bovine serum albumin (BSA)	Serva Electrophoresis GmbH; Heidelberg, Germany
Cooling plate, EG 1150C	Leica Biosystems; Nussloch, Germany
Coverslip 24 x 36 mm and and microscope slide	R. Langenbrinck; Emmendingen, Germany
Digital camera	Leica Microsystems; Nussloch, Germany
Ethanol 70%, 96%, 99.6% denatured with methyl-ethyl ketone	Fischer; Saarbrücken, Germany
Heating chambers (37 and 59°C)	Memmert GmbH; Schwabach, Germany
Horseradish peroxidase (HRP) polymer kit	Zytomed system GmbH; Berlin, Germany
Hydrogen peroxide (H_2O_2)	Sigma-Aldrich; Steinheim, Germany
Isopropanol 99.8%	Sigma-Aldrich; Steinheim, Germany
Light microscope	Leica Microsystems; Wetzlar, Germany
Microtome	Leica Microsystems; Nussloch, Germany
Microtome blade S35	A. Hartenstein GmbH; Wuerzburg, Germany
NovaRED substrate kit	Linaris Biologische Produkte GmbH; Dossenheim, Germany
Paraffin elongation bath and paraffin embedding station	Leica Microsystems; Nussloch, Germany
Paraffin tissue embedding medium	Sigma Aldrich; Steinheim, Germany
Phosphate-buffered saline (PBS)	Pan-Biotech GmbH; Aidenbach, Germany
Proteinase K	Dako North America; Carpenteria, USA
Rodent Block M	Biocare Medical; CLSI, Wayne, USA
Xylol	Carl Roth GmbH; Karlsruhe, Germany

Table 17. Substances and equipment used for histological measurements

2.2. Animals

All animal experiments were approved by the governmental committee. C57BL/6J mice (22_30 gr) were purchased from Jackson Laboratory and were used for inhibitor studies and as WT controls for *Cox4i2* deficient mouse experiments.

Global *Cox4i2* deficient mice (*Cox4i2*$^{-/-}$): The transcription unit of the *Cox4i2* gene is composed of 5 exons, located on mouse chromosome 2. Exons 1 and 3 were replaced by homologous recombination with the *Neo* cassette to create *Cox4i2* knockout mice (breeding was continued for more than 8 generations using C57BL/6J mice) as described by Hüttemann et al. from the Center for Molecular Medicine and Genetics in Detroit, United States [222]. C57BL/6J mice were used as wild-type (WT) controls.

Global *Aox* expressing mice (*Aox*^{tg}): Szibor et al. used gene targeting into the *Rosa26* locus in mouse embryonic stem cells to generate genetically modified mice expressing *Ciona intestinalis* AOX [219]. A general description and characterization of the *Aox*-expressing mouse strain was published, previously [273]. Heterozygeous mice were used for experiments, non-*Aox* expressing littermates were used as control.

SMC-specific *Ucp2* knockout mice: B6;129S-UCP2$^{tm2.1Lowl}$/J mice (shortly called *Ucp2*$^{flox/flox}$) were a kind gift from Dr. Bradford B. Lowell from Beth Israel Deaconess Medical Center, Boston, USA. The *Ucp2* gene is composed of 8 exons, among them the transcription unit is made of 2 untranslated exons followed by 6 exons encoding *Ucp2* with the initiation site of translation in exon 3. The loxP sites were integrated between the start codon sequences of the *Ucp2* gene, one upstream of exon 3, and one downstream of exon 4 [274, 275].

The *Ucp2*$^{flox/flox\ iSmaCre}$ mouse strain was created by cross pairing of B6;129S-UCP2$^{tm2.1Lowl}$/J mice with B6-Tg (Acta2-cre/ERT2)12Pcn mice which express Cre-recombinase under the promoter of Acta2. Homo/hemizygote mice for the locus Tg (Acta2-cre/ERT2)12Pcn were selected as cre positive (*Ucp2*$^{flox/flox,\ iSmaCre+}$). For translocation of Cre-recombinase to the cytosol *Ucp2*$^{flox/flox,\ iSmaCre+}$ mice were fed with 400 mg tamoxifen /kg body weight (BW) (Altromin Spezialfutter GmbH & Co. KG; Lage, Germany) for two times one week, with a tamoxifen-food free interval of 4 weeks (Figure 5). After feeding *Ucp2*$^{flox/flox,\ iSmaCre+}$ mice with tamoxifen, UCP2 will be deleted specifically in cells with activated Acta2 (shortly called SMC-specific *Ucp2* knockout mice). *Ucp2*$^{flox/flox,\ iSmaCre+}$ fed with tamoxifen-free food were used as one control group. Tamoxifen-fed Cre negative mice in which the locus

Tg(Acta2-cre/ERT2)12Pcn was missing were used as second control group (*Ucp2*$^{flox/flox,\ iSmaCre-}$) [276].

2.3. Experimental design

For all experiments, *Aox*^{tg}, *Cox4i2* knockout, SMC-specific *Ucp2* knockout and respective controls from both gender and similar age and weight were used. The experiments with SMC-specific*Ucp2* knockout and respective controls all started at day 28 after birth with feeding of tamoxifen.

For *in vivo* chronic hypoxic experiments, all mice were randomly selected and exposed to either normobaric normoxia (21% O_2, 5% CO_2, and rest N_2) or chronic hypoxia (10% O_2, 5% CO_2, and rest N_2) for 28 days. After exposure, all mice were analysed by *in vivo* haemodynamic measurements, as well as echocardiography, and one-half of their lungs was used for molecular biological analysis and the other half was used for histological analysis.

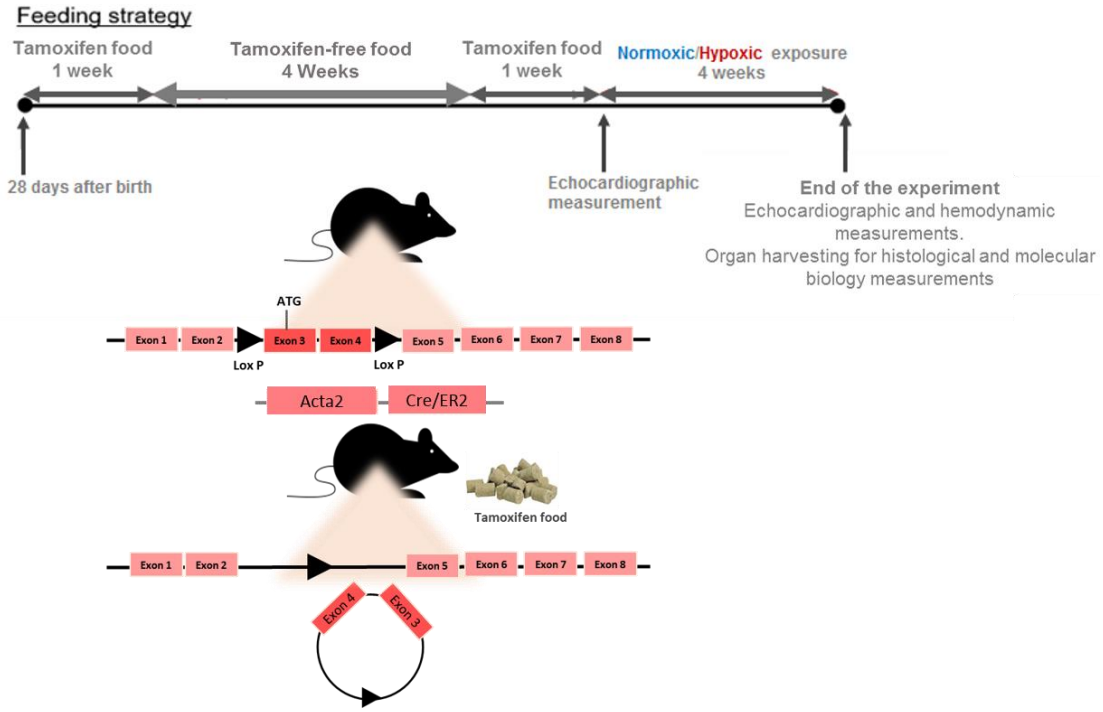

Figure 5. Experimental setup and genetic construct of UCP2

Uncoupling protein 2 (*Ucp2*)$^{flox/flox\text{-}iSmaCre+}$ mice were fed with 400 tamoxifen mg/kg body weight (BW) for two times one week to translocate Cre-recombinase to the cytosol. *Ucp2* deletion in SMC occurs by excision of the DNA sequence between 2 loxP sites containing exons 3 and 4. ATG refers to the start codon for protein translation.

2.4. Methods

2.4.1. The model of isolated perfused and ventilated mouse lungs

The isolated perfused and ventilated mouse lung system can be used to evaluate respiratory functions, such as ventilator and vascular properties. The lungs, while being removed from the body, are still an intact functional organ, and therefore can continue in their physiological context without the interference of the central nervous system and systemic circulatory factors.

Mice were deeply anesthetized with Ketamine 100 mg/kg BW (10% from Bela-pharm GmbH & Co. KG; Vechta; Company), and Xylazine 20 mg/kg BW (2%, Serumwerk Bernburg AG; Bernburg, Germany) via intraperitoneal (i.p.) injection and anticoagulated with heparin 50.000 IU/kg BW.

A central incision was made in the middle of the neck, and after that, a tracheostomy was performed. The mouse was ventilated with a gas mixture of 21% O_2, 5% CO_2, and rest N_2 through a ventilator (minivent Type 845, Hugo Sachs Elektronik; March-Hugstetten, Germany). Respiratory rate was preserved at 90 breaths/minute and with a tidal volume of 10 µl/kg (~250 ml). Positive end-expiratory pressure (PEEP), which refers to the pressure in the airway at the end of passive expiration, was set at 3 cmH_2O. PEEP is important to stabilize lung units and improve oxygenation in mouse lungs.

After opening the chest by median sternotomy, the pericardium, thymus, and fat tissue were carefully removed. Afterwards, a stainless-steel catheter was entered into the pulmonary artery through a hole in the right ventricular wall and secured with a ligature. Later, a left ventricular catheter was applied through a small incision in the left ventricular wall.

In the next step, the trachea, lungs, and heart were detached from the thoracic cage (without disturbing ventilation and perfusion) and were freely hanged from a force transducer (Research-grade Isometric Force Transducer, Harvard apparatus; Holliston, USA) to monitor lung weight. The opened lung was covered with a humid and temperature-equilibrated glass chamber and simultaneously, the temperature of the whole system was maintained at 39°C.

Subsequently, perfusion was started via a peristaltic pump (Reglo Digital MS-4/8; Cole-Parmer GmbH, Ismatec; Wertheim, Germany) at a flow rate of 0.2 ml, with sterile Krebs-Henseleit solution (see table 2) and with the total perfusate volume of 10 ml. Later, the flow rate was slowly increased from 0.2 to 2 ml/minute and after rinsing the lungs with around

20 ml buffer to wash out the blood, circulation was maintained in a closed circuit. The pulmonary arterial, left ventricular, and ventilation pressures were measured using a pressure sensor (B. Braun Melsungen AG; Melsungen, Germany). These pressures were zeroed at the height of the heart and were monitored continuously. The experiment was started after stabilizing the PAP for about 20 minutes and the basal PAP was measured. Left atrial pressure was also set at 2 mmHg (see table 3). For data recording and storage, Powerlab 8/30, Quad Bridge Amp, and LabChart (AD Instruments Pty Ltd; New South Wales, Australia) were used. In order to apply acute HOX in the mouse lung, 10-minute periods of hypoxic (1% O_2, 5 % CO_2, rest N_2) ventilation were changed with 15 minutes of NOX. HPV was determined as a mean PAP (Figure 6).

In order to determine the effect of the mitochondria-targeted 2,2,6,6-Tetramethylpiperidine-1-oxyl (Tempo) derivative (MitoTempo), S3QEL2, and SkQ1 on HPV, or the effect of MitoTempo, S3QEL2, and SkQ1 on hypoxia-independent vaso-responsiveness of the pulmonary vasculature, six repetitive hypoxic and potassium chloride (KCl) challenges in absence or presence of increasing doses of MitoTempo, S3QEL2 or SkQ1, respectively, were performed.

In order to determine the effect of triphenylphosphonium chloride (TPP) as a control solvent for MitoTempo and SKQ1, and dimethyl sulfoxide (DMSO) as a control solvent for S3QEL2 on HPV, or the effect of these control solvents on hypoxia-independent vaso-responsiveness of the pulmonary vasculature, 6 repetitive hypoxic or KCl challenges in absence or presence of increasing doses of these control solvents, respectively, were performed.

The effect on U46619 induced vasoconstriction was tested either with repetitive challenges in presence or absence of increasing doses of MitoTempo and TPP or by application of U46619 after the last repetitive hypoxic challenge in presence of the highest dose of S3QEL2, SkQ1, DMSO, or TPP. The strength of the vasoconstrictor response to hypoxia, KCl or U46619 in presence of the substances was compared to the second hypoxic or KCl/U46619 challenge, respectively. KCl or U46619 were applied as bolus infusion into the pulmonary artery during normoxic ventilation.

Figure 6. The isolated perfused and ventilated mouse lung setup

The ventilator is connected to a tracheal cannula, and the lung is ventilated with either normoxic (21% O_2, 5% CO_2, rest N_2) or hypoxic gas (1% O_2, 5% CO_2, rest N_2). Perfusion of the pulmonary vasculature is achieved using a peristaltic pump connected via tubes and a catheter to the right atrium, the perfusion medium is collected at the left ventricle. Pulmonary arterial, left ventricular, and ventilation pressures were measured by a pressure sensor.

2.4.2. Isolation of PASMC

PASMC was isolated from pulmonary precapillary arteries and cultured [99]. Briefly, the chest was opened, and the pericardium, thymus, and fat tissue were carefully removed, and then a right ventriculotomy was performed in order to insert a stainless-steel catheter into the pulmonary artery through the right ventricle. The lung was slowly washed with 3 ml phosphate-buffered saline (PBS; Pan-Biotech GmbH; Aidenbach, Germany) via a syringe (avoid air bubbles which lead to pulmonary embolism). Afterward, 3 ml warm medium 199 (M199; Thermo Fisher Scientific; Waltham, USA), containing 1% Penicillin-Streptomycin antibiotic (P/S), 5 mg/ml agarose (low melting temperature 0.5%; Sigma-Aldrich; St. Louis, USA), and 5 mg/ml Iron ш oxide (Fe3O4; Sigma-Aldrich; St. Louis, USA) were instilled carefully into the lung. Iron particles were fixed in the precapillary vessels and homogenous diffusion was controlled. Afterwards, the lung was fixed through a tracheal injection of 3 ml warm M199 containing 1% P/S, 10 mg/ml agarose low melting temperature. Subsequently, the lung was removed from the chest and was placed in a falcon containing around 2 ml ice-cold PBS and cut into pieces with scissors. This step was followed by washing 3 times with

PBS. Afterwards, tissue pieces were incubated at 37°C for 60 minutes in 10 ml M199 comprising 1% P/S, and 80 Unit/ml collagenase (Sigma-Aldrich; Steinheim, Germany) in incubator at 37°C. Next, tissues were suspended in 5 ml M199 containing 1% P/S and 10% fetal bovine serum (FBS; Sigma-Aldrich; St. Louis, USA), to stop collagenase. Afterwards, tissues were dissected intensively by moving through 15- and 18-gauge needles, accompanied by 3 times washing with this medium using a magnetic holder. Tissue pieces were suspended in SMC growth medium (Promo Cell; Heidelberg, Germany) including 1% P/S and 15% FBS, and incubated in the incubator (Thermo Fisher Scientific; Waltham, USA) at 37°C for 5-6 days. For passaging the cells, they were trypsinized at 80% confluence and seeding in new culture dishes (see table 4).

2.4.3. MMP measurement

JC1 (5, 5', 6, 6' Tetrachloro-1, 1', 3, 3'-tetraethylbenzimidazolylcarbocyanine iodide; Invitrogen; Carlsbad, USA) was used for determining MMP in a flow-through system in isolated PASMC by fluorescence microscopy. JC1 is a lipophilic cationic fluorescent dye that can enter the energized mitochondria in healthy cells and form aggregates that change the fluorescent property of JC1. At low MMP, JC1 is predominantly a monomer that exhibits green fluorescence with the emission of 530 nm, whereas, at high MMP the dye forms aggregates, called J-aggregates, and shows intense red fluorescence with the emission of 590 nm. Thus, the higher red to green fluorescence ratio indicates the higher polarization of the mitochondrial membrane. Precapillary PASMC were seeded on coverslip culture dishes and then, at the stage of passage zero were incubated in SMC growth medium (PromoCell GmbH; Heidelberg, Germany) including 50 nM of JC1 at 37°C for 20 minutes. After that, cells were transferred into a closed heated chamber (PeCon; Mannheim, Germany) which, was filled with 500 µl HEPES-Ringer buffer (HRB) (136.4 mM sodium chloride [NaCl], 5.6 mM KCl, 1 mM magnesium chloride [$MgCl_2$], 2.2 mM calcium chloride [$CaCl_2$], 10 mM 4-(2-hydroxyethyl)-1-piperazineethanesulfonic acid [HEPES], and 5 mM glucose; pH 7.4) (see table 6). Afterward, acute HOX was induced by switching from normoxic perfusion buffer (21% O_2, 5% CO_2, rest N_2) to hypoxic (1% O_2, 5% CO_2, rest N_2) buffer with a flow rate of 1 ml/minute. For control experiments, the normoxic perfusion buffer was exchanged for a second normoxic perfusion buffer. The fluorescent signal was analyzed using a polychrome II monochromatic and IMAGO CCD camera (Till Photonics; Munich,

Germany) coupled to a fluorescence microscope (IX70, Olympus; Hamburg, Germany) (Figure 7) (see table 5).

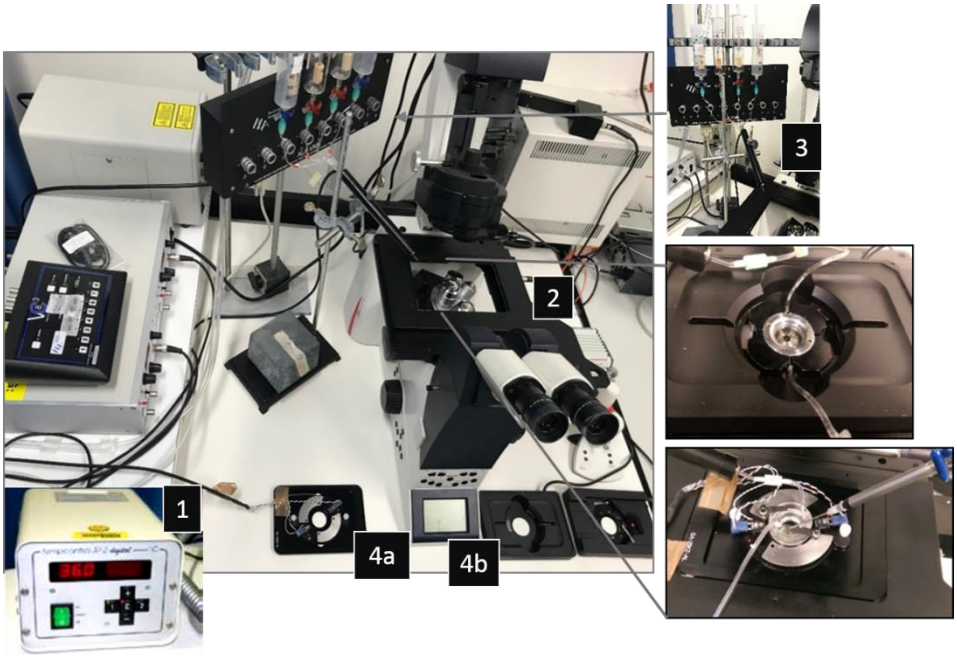

Figure 7. Setup for the measurement of MMP during normoxic and hypoxic superfusion in isolated PASMC

Acute HOX was introduced by exchanging the perfusing buffer of the closed perfusion chamber from normoxic buffer to hypoxic buffer (from 21% to 1% O_2, 5% CO_2, rest N_2). 1) The heating system for adjusting the temperature of the chamber. 2) The inverted microscope (Olympus IX70) connected to the fluorescent light source and CCD camera. 3) Heated perfusion reservoirs with buffer. 4 a) The open perfusion chambers and 4 b) Closed perfusion chambers (PeCon).

2.4.4. Patch clamp recording of cellular membrane potential

Cellular membrane potential was recorded in current-clamp mode (I = 0) in whole-cell configuration by an EPC10 USB single amplifier (HEKA Elektronik GmbH; Lambrecht Germany) which was controlled by patch software (HEKA Elektronik GmbH; Lambrecht Germany).

The setup of the measurement was placed in a Faraday cage in order to protect the measurement from electromagnetic radiation. Precapillary PASMCs (passage 0) were seeded on culture dishes (Greiner Bio-One; Frickenhausen, Germany), and during the experiments the cells were steadily perfused with an extracellular analogous bath solution (see table 7) which was pre-heated to 37 °C with an in-line solution heater (Warner Instruments; Hamden, USA) and equilibrated with a normoxic (21% O_2, 5% CO_2, rest N_2)

gas mixture. Acute HOX was induced by switching from normoxic to hypoxic bath solution (1% O_2, 5% CO_2, rest N_2), and in the vicinity of the cell, the O_2 partial pressure was measured with an optical needle-type FireSting O_2 sensor (PyroScience; Aachen, Germany). By means of a DMZ universal electrode puller (Zeitz; Martinsried, Germany), fire-polished patch pipettes with a tip resistance of 3-5 MΩ were drawn from borosilicate glass capillary tubes (Sutter Instruments; Novato, California, USA), and filled with an intracellular analog solution (adjusted to pH 7.2, by titration with 1 M potassium hydroxide [KOH]; see table 8). The data were filtered at 2.9 kHz and recorded at 50 Hz. The experimentally determined liquid potential (+12.3 mV) was electronically corrected. For analysis Fitmaster (HEKA Elektronik GmbH; Lambrecht, Germany) and IGOR Pro software (Wavemetrics; Lake Oswego, USA) were used. The stability of the membrane potential was determined for at least 1 minute before recording was started. With regard to *Aox*^{tg} and *Cox4i2* knockout experiments, 10 µM n-propyl gallate (n-PG) and 124 nmol/l H_2O_2 in the bath solution were added during the acute hypoxic exposure, respectively (see table 9). The patch clamp experiments were performed with the help of Dr. Fenja Knöpp.

2.4.5. RNA extraction and quantitative reverse transcription PCR (qRT-PCR)

The mRNA was isolated from isolated PASMCs, homogenized lung, or aorta by RNeasy mini kit (Qiagen; Hilden, Germany). 1µg mRNA was used to synthesize cDNA by iScript kit (Bio-Rad; Hercules, USA). The qRT-PCR was performed by using iTaq Universal SYBR® Green supermix (Bio-Rad; Hercules, USA) and Mx3000P PCR system (Agilent Technologies; Santa Clara, USA). The expression of targeted genes was normalized to the expression of the housekeeping genes such as porphobilinogen deaminase (PBGD) and β2 microglobulin (B2M). Primer sequences for qRT-PCR are listed below (see table 10-13)

The ΔCt values were calculated by subtracting the Ct values of the target gene from the endogenous control (ΔCt = Ct [endogenous control gene] - Ct [target gene]).

2.4.6. DNA extraction and standard PCR

DNA isolated from mouse tail was used to perform PCR. PCR was performed in 25 µL reaction mixture containing 10 mM deoxynucleoside triphosphate (dNTP), 25 mM MgCl2, 5 U/µl Taq-polymerase (Bio-Rad; Hercules, USA), and 10 µM of each primer, in a thermal cycler (Biometra; Lena, Germany). Afterwards, amplified PCR products were separated in

1% agarose gel containing 0.1% RedSafe DNA stain (Chembio Ltd; Cambridgeshire, UK). 380 bp and 250 bp bands were detected as flox and cre-recombinase insertion into the *Ucp2* mouse gene, respectively. With regard to Aox^{Rosa26} and *Cox4i2* genes, 523 bp and 1050 bp bands were identified in Aox^{tg} and *Cox4i2* knockout mice, respectively (see table 13).

2.4.7. Western blot analysis

Tissue or isolated precapillary PASMC were homogenized in lysis buffer (Cell Signalling Technology; Massachusetts, USA), containing 1mM Phenylmethane sulfonyl fluoride (PMSF) by Precelly 24 homogenizer (Peqlab; Erlangen, Germany). Tissue and cell lysates were centrifuged with a speed of 14,000 rpm at 4°C for 15 minutes. Protein concentration was measured by Bradford assay (Bio-Rad Laboratories; Munich, Germany) using a microplate reader with the 750 nm absorption (Tecan Infinite M200; Grödig, Austria). Samples containing equal amounts of protein were denatured by heating for about 10 minutes in Laemmli buffer containing β-mercaptoethanol and separated on 12% sodium dodecyl sulfate (SDS; Bio-Rad Laboratories; Munich, Germany) polyacrylamide gel at 400 mA and 150 V by electrophoresis. The separated proteins were transferred to 0.45 μm polyvinylidene difluoride (PVDF) membrane (Pall Corporation; Dreieich, Germany) in a semi-dry transfer buffer at 400 MA and 150 V. After blocking the membrane with 6% non-fat dry milk in TBS-T buffer solution (Tris buffer saline plus 0.1% Tween 20) for 1 hour, the membrane was incubated overnight at 4°C with the following primary antibodies: anti-AOX (AOX antiserum, custom-raised in rabbit, dilution 1:40000; 21st Century Biochemicals; Marlborough, MA, USA), anti-HIF-1α (dilution 1:1000, Cayman Chemical; Ann Arbor, USA), and anti-β-actin (1:50,000 dilution; Abcam). After 3 times washing with TBS-T buffer, membranes were incubated for 1 hour at room temperature with respective secondary antibody coupled to horseradish peroxidase (dilution 1:5000). After incubation, the membranes were washed 4 times with TBS-T buffer and the bands were visualized by using enhanced chemiluminescence (ECL; GE Healthcare Life Sciences; Little Chalfont, UK) (see table 14).

2.4.8. Measurement of cellular $O_2^{\bullet}$ release by electron spin resonance (ESR) spectroscopy

The ESR settings were as follows: microwave frequency 9.78 GHz, modulation frequency 100 kHz, modulation amplitude 2G, microwave power 18 mW. HOX (1% O_2, 5% CO_2, rest

N_2) and NOX (21%, 5% CO_2, rest N_2) were applied for 5 minutes by incubating the cells in a chamber. Intracellular and extracellular $O_2^{\cdot}$ levels were measured by ESR spectroscopy (Bruker Biospin GmbH; Rheinstetten, Germany) using the 0.5 mM of spin probe 1-hydroxy-3-methoxycarbonyl-2,2,5,5-tetramethyl-pyrrolidine (CMH; Alexis Corporation; San Diego, USA) and an MS 100 spectrometer (Magnettech; Berlin, Germany). The superoxide portion of ROS was determined by subtracting the ESR signal of the sample with polyethylene-glycol conjugated superoxide dismutase (pSOD; Sigma-Aldrich; St. Louis, USA) from the sample incubated for 90 minutes without 50 U/ml pSOD in ESR-Krebs-HEPES buffer (for preparation of 1 liter of the buffer: 5.786 g NaCl, 0.350 g KCl, 0.368 g $CaCl_2 \times 2\ H_2O$, 0.296 g magnesium sulfate [$MgSO_4$] × 7 H_2O, 2.1 g $NaHCO_3$, 0.142 g potassium dihydrogen phosphate [KH_2PO_4], 1.009 g D-glucose, 5.206 g Na-HEPES) with the following formula: Superoxide = CMH signal – (pSOD + CMH) signal [277] (see table 15). The ESR spectroscopy technique was done by Dr. Susan Scheibe.

2.4.9. Mouse model of chronic hypoxia-induced pulmonary hypertension

Mice were introduced to normobaric HOX (10% O_2, 5% CO_2, rest N_2) and NOX (21% O_2 5% CO_2, rest N_2) in a ventilated chamber for 28 days. The O_2 level remained constant by the autoregulatory control unit (O_2 controller, model 4010; Labotect; Gottingen, Germany). Extra humidity in the recirculating system was kept by condensation in a cooling system. CO_2 was continuously removed by soda lime. Cages were shortly opened once per day for scoring, as well as for food and water resupply (Figure 8).

Figure 8. Hypoxic and normoxic incubation chambers.

1) O_2 monitor (for normoxic [21% O_2, 5% CO_2, rest N_2] and hypoxic [1% O_2, 5% CO_2, rest N_2] gas exposure, respectively), 2a) hypoxic chamber and 2b) normoxic chambers.

2.4.10. Hemodynamic measurement

Hemodynamic parameters were evaluated in mice after 4 weeks of exposure to HOX/NOX by *in vivo* measurements. The mouse was anesthetized with 3% isoflurane in a mixture of 100% O_2 (Air Liquid; Siegen, Germany) and placed in a supine position on a heating pad (AD Instruments; Spechbach, Germany) and the body temperature was monitored continuously using a rectal thermistor (AD Instruments; Spechbach, Germany) aiming at a body temperature of 37 ± 1°C. During the cannulation procedure, the isoflurane concentration was decreased to 1.5% to maintain a proper depth of anesthesia. An incision in the anterior region of the neck was made for isolation and connection of the trachea to a small animal ventilator (minivet type 845, Hugo Sachs Electronic; March-Hugstetten, Germany). The mouse was ventilated with a frequency of 150 breaths/minute and a tidal volume of 10 µl/gr of BW. A positive-end expiratory pressure of 1 cm water column was used to avoid the collapse of the alveoli during mechanical expiration by the ventilator.

Cardiac catheterization

The connective tissue surrounding the right external jugular vein was removed and 2 ligatures with the surgeon's silk were placed at the caudal and cranial sides of the vein. In order to prevent bleeding, the cranial ligature was ligated and after that, a slight incision

was made on the vein between the ligatures. After calibration, the catheter which was preheated to 37 °C about 30 minutes before the start of the measurement (1.4F micro manometer) and soaked in physiological saline, was inserted in the caudal direction into the jugular vein. Subsequently, the catheter was quickly moved into the right atrium and then into the right ventricle, and the pressures were recorded. Power Lab data acquisition systems and Lab Chart 7 for windows software (MPVS-Ultra Single Segment Foundation System; AD Instruments; Spechbach, Germany) were used to obtain and analyze data.
Afterwards the right common carotid artery (RCA) was exposed, one suture was placed at the caudal end of the RCA, and another suture was located at the cranial part of the artery to stretch it towards the head and tail, respectively. It was important to apply a Biemer microvessel clamp (Aesculap; Tuttlingen, Germany) on the caudal part of the carotid artery to prevent bleeding and afterwards, a tiny incision was made at the cranial part of the artery. Later, the clamp was removed and a catheter was advanced into the vessel. Afterwards, the catheter was slowly advanced towards the heart and the pressures were recorded (see table 16).
RVSP, systemic arterial pressure (SAP), left ventricular systolic pressure (LVSP), and heart rate were recorded by this technique. At the end of the experiment, the mice were sacrificed and lung and heart were harvested for further examination. The hemodynamic measurements were performed by Ms. Karin Quanz.

2.4.11. Right ventricular hypertrophy assessment

To measure the fulton index the hearts were removed and right and left ventricles and septum were separated. The ratio of the weight of the right ventricule to the sum of left ventricular and septal weight (RV / [LV + S]) served as a measure for right ventricular hypertrophy.

2.4.12. Assessment of pulmonary arterial remodeling

After hemodynamic measurements, while the lungs were mechanically ventilated, the pulmonary vasculature was flushed via the pulmonary artery by the injection of 0.9% NaCl, which was drained from the incised left ventricle. This step was followed by perfusion of the pulmonary vasculature through the pulmonary artery and airways through the trachea, with a mixture of 3.5-3.7% formaldehyde (Otto Fischer GmbH; Waldkirch, Germany) with a constant pressure of 22 cmH_2O and 11 cmH_2O, respectively.

The left lung lobe was used for histological analysis and immediately after flushing was fixed in formaldehyde for 24 hours at room temperature. The left lung was embedded in paraffin blocks, and formalin-fixed paraffin-embedded (FFPE) mouse lung tissues were sectioned at 3μm thickness on a microtome. After deparaffinization and rehydration of the slides, the proteinase K (Dako North America; Carpenteria, USA) and rodent block M (Biocare Medical, CLSI; Wayne, USA) were applied to break the protein cross-links, and thus enhance the staining intensity of antibodies, and block non-specific background, respectively. Afterwards, double staining for the von Willebrand factor (with rabbit polyclonal antibody, dilution 1:1000; Dako Cytomation; Hamburg, Germany) and α-smooth muscle actin (with mouse monoclonal antibody, dilution 1:700; Sigma-Aldrich; St. Louis, USA) was performed to evaluate the muscularization of the pulmonary vessels.
To evaluate the muscularization of pulmonary vessels, all blood vessels from 20 to 150 μm diameter were counted at 40× magnification by a computer-assisted picture analysis software. The counted vessels were categorized as fully muscularized (≥ 70% of a medial layer covered by anti- α-smooth muscle actin staining), partially muscularized (> 5 - ≤ 70%), or non-muscularized vessels (≤ 5%) (see table 17).

2.4.13. Immunohistochemistry (IHC)

The FFPE mouse lung tissues were sectioned (at 3 μm thickness on microtome), and tissue slides were deparaffinized in xylol and rehydrated through a graded series of ethanol concentrations. Briefly, the epitope retrieval was performed by heating for 25 minutes in sodium citrate buffer (pH = 6.0) in a water bath at 95-100°C. Endogenous peroxidase was quenched with 3% H_2O_2 (Sigma-Aldrich; St. Louis, USA) in 15% methanol. Subsequently, proteinase K (Dako North America; Carpenteria, USA) was used for antigen retrieval and 10% bovine serum albumin (BSA) was applied to block nonspecific binding sites. After overnight incubation of tissue slides with anti-AOX antibody (primary antibody, custom-raised in rabbit, dilution 1:2000; 21st Century Biochemicals; Marlborough, USA) at 4°C, the antibody was washed out with PBS (Pan-Biotech GmbH; Aidenbach, Germany) and then incubated with a HRP polymer kit (Zytomed system GmbH; Berlin, Germany) for 30 minutes. This was followed by the NovaRED substrate kit application (Linaris Biologische Produkte GmbH; Dossenheim, Germany) and incubation at room temperature until suitable staining was developed (5-15 minutes). The sections were evaluated by light microscopy (Leica; Wetzlar, Germany) (see table 17).

2.4.14. Echocardiography (ECG) measurement

Echocardiography was performed using a commercially available Vevo® 2100 high-resolution imaging system equipped with a 40 MHz linear-array transducer (Visual Sonics; Toronto, Canada). Cardiac parameters were measured one day exposure to 28 days NOX/HOX as well as one day before the final hemodynamic measurements. The mouse was anesthetized in a transparent chamber with 3% isoflurane in O_2 (Air Liquide; Siegen, Germany) at a flow rate of 1 l/min.

Subsequently, the mouse was carefully laid in a supine position on a heating plate (AD Instruments; Spechbach, Germany) with all limbs taped to ECG electrodes for heart rate monitoring. Application of isoflurane 1.5% in O_2 was continued, in order to maintain a steady-state sedative level. The body temperature (at 37°C) was monitored constantly with a lubricated rectal thermometer, which was placed into the rectum (AD Instruments; Spechbach, Germany). During the measurement, a single channel ECG was recorded. Afterwards, the chest area was covered with bubble-free preheated ultrasound gel. Measurement of right ventricular wall thickness (RVWT) was done in the modified right parasternal long-axis view. The right ventricular internal diameter (RVID) was measured from the apical four-chamber view as the maximal transverse diameter in the middle third of the right ventricle during end-diastole. For assessment of right ventricular performance, tricuspid annular plane systolic excursion (TAPSE) was measured in the apical four-chamber view as the distance of tricuspid annular movement between end-diastole to end-systole. Pulse wave aortic flow Doppler recordings, as well as measurements of the proximal ascending aortic diameter, were used for calculation of the aortic stroke volume. Then cardiac output (CO) was calculated by multiplying the aortic stroke volume by heart rate. Aortic velocity-time integral was evaluated from the suprasternal view. The aortic diameter was measured using M-mode echocardiography at the level of the proximal ascending aorta. The whole echocardiography measurement took 25-35 minutes. The ECG measurement was done by Dr. Akylbek Sydykov.

2.5. Statistics

All experiments were performed in a blinded fashion, whenever possible. Animals were randomly assigned to a treatment. Animal numbers in the experiments may differ due to breeding reasons. The number of the animals for *in vivo* normoxic/hypoxic exposure are given in tables 18 and 19. The n-numbers for different measurement parameters may differ for technical reasons (e.g. catheters or the echocardiographic probe could not be placed appropiately).

All data are given as means ± standard error of mean (SEM). Normal distribution was tested before further statistical analysis. Statistical analysis was performed by either unpaired parametric t-test (for data with normal distribution) or paired non-parametric Mann-Whitney U test (for data with non-normal distribution) for comparison of two groups. For comparison of more than two groups two-way ANOVA was performed with either Tukey's post hoc test (comparing each group with each other group) or Sidak's test (comparing selected groups). Uncorrected Fisher's least significant difference was performed for MMP analysis. Repeated-measures one-way ANOVA with Tukey's multiple comparisons test was used for analysis of patch-clamp experiments. A p-value of less than 0.05 was considered statistically significant.

	Aox^{tg}		**WT**	
	NOX	**HOX**	**NOX**	**HOX**
***In vivo* exposure**	10	10	10	10
RVSP	9	10	10	9
LVSP	8	10	10	7
SAP	8	9	10	8
TAPSE	10	9	9	9
CO	10	10	10	10
Muscularization	4	4	5	5

Table 18. The number of the *Aox^{tg}* and WT mice for *in vivo* normoxic/hypoxic exposure

	Ucp2$^{flox/flox, iSmaCre+}$				*Ucp2*$^{flox/flox, iSmaCre-}$			
	NOX		**HOX**		**NOX**		**HOX**	
	No tamoxifen	**tamoxifen**	**No tamoxifen**	**tamoxifen**	**No tamoxifen**	**tamoxifen**	**No tamoxifen**	**tamoxifen**
***In vivo* exposure**	**12**	**13**	**8**	**12**	**9**	**12**	**8**	**8**
RVSP	10	13	8	10	9	9	5	6
LVSP	10	11	8	10	9	8	5	4
SAP	10	11	8	10	9	8	5	4
TAPSE	8	10	8	12	8	8	8	8
CI	9	10	8	12	8	8	8	8
RVWT	9	10	8	12	8	8	8	8
RVID	9	10	8	12	8	8	8	8
PAT/PET	9	10	8	12	8	8	8	8
Muscularization	5	4	5	11				

Table 19. The number of the *Ucp2*$^{flox/flox, iSmaCre+}$ and *Ucp2*$^{flox/flox, iSmaCre-}$ mice for *in vivo* normoxic/hypoxic exposure

3. Results

3.1. Effect of mitochondrial superoxide inhibitors on HPV

Ventilation of WT mouse lungs with hypoxic gas (1% O_2, 5% CO_2, rest N_2) in the isolated perfused and ventilated lung model caused an enhancement of PAP (ΔPAP) compared to normoxic values reaching a peak after approximately 5 minutes which reflects acute HPV.
The mitochondria-targeted 2,2,6,6-Tetramethylpiperidine-1-oxyl (Tempo) derivative ("MitoTempo") exhibits a superoxide dismutase property in the mitochondrial matrix and converts superoxide to hydrogen peroxide. It comprises the TPP-conjugated Tempo in which the lipophilic TPP cation enables Tempo to cross the mitochondrial membrane and accumulate in mitochondria [278, 279]. The experiments showed that MitoTempo suppressed acute HPV in isolated perfused and ventilated mouse lungs when applied in increasing concentrations (Figure 9A). In addition, TPP was applied as control and did not affect HPV. In contrast, the thromboxane mimetic U46619-induced vasoconstriction was decreased by MitoTempo compared to TPP treatment, and the vasoconstriction induced by KCl was partially inhibited at high concentrations of MitoTempo compared to TPP treatment (Figure. 9B, C). Moreover, S3QEL2 (1-[3, 4-Dimethylphenyl]-N, N-dipropyl-1H-pyrazolo [3, 4-d] pyrimidin 4-amine) which acts as a mitochondrial superoxide release inhibitor from the Q_0 site of CIII [280], inhibited HPV (Figure 10A), but not U46619- (Figure 10B) or KCl-induced vasoconstriction (Figure 10C).
Similarly, a plastoquinone derivative, SkQ1, designed as a conjugate of TPP which has a mitochondria-targeted antioxidant activity, was used. It was shown that SKQ1 could inhibit mitochondrial damage induced by the most toxic ROS such as $OH^{\bullet}$, $LO_2^{\bullet}$, and H_2O_2 [281, 282]. SkQ1 inhibited HPV, but not U46619-induced vasoconstriction. TPP as the carrier molecule was applied as control and did not affect HPV (Figure 11A, B). In these sets of experiments, MitoTempo, S3QEL2, or SkQ1 were applied in increasing concentrations in the same lung, 5 minutes before each repetitive maneuver of hypoxic ventilation or KCl/U46619 application, respectively, and compared to the respective increase of PAP in presence of the DMSO/TPP only.

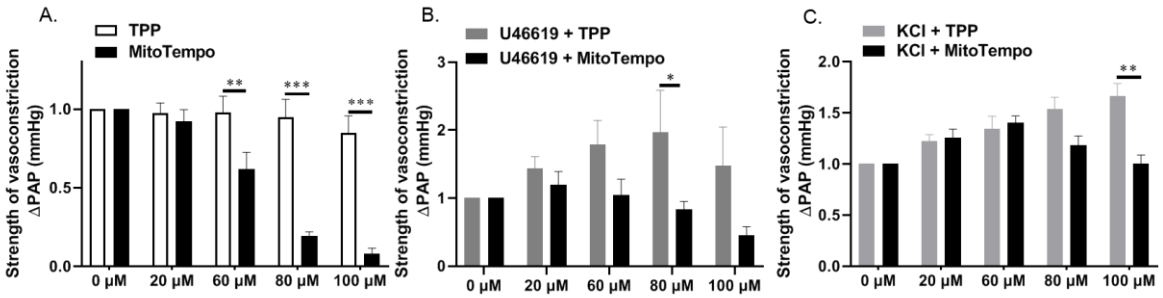

Figure 9. Effect of MitoTempo/TPP on HPV and pulmonary vasoconstriction induced by U46619 and KCl

(A), The strength of hypoxic pulmonary vasoconstriction (HPV) was determined as the increase of pulmonary arterial pressure (ΔPAP) during hypoxic (1% O_2, 5% CO_2, rest N_2) ventilation in presence of MitoTempo or triphenylphosphonium (TPP) in wild-type (WT) mouse lungs (n = 6 isolated lungs each group). (B), Pulmonary vasoconstriction induced by the thromboxane mimetic U46619 (n = 4 or 6 isolated lungs for the "TPP" or "MitoTempo" group, respectively). (C), Potassium chloride (KCl)-induced pulmonary vasoconstriction (n = 5 or 8 isolated lungs for the "TPP" or "MitoTempo" group, respectively). *p<0.05, **p<0.01, ***p<0.001, data were analyzed by two-way analysis of variance (ANOVA) with Sidak's multiple comparisons test. Data are shown as mean ± SEM.

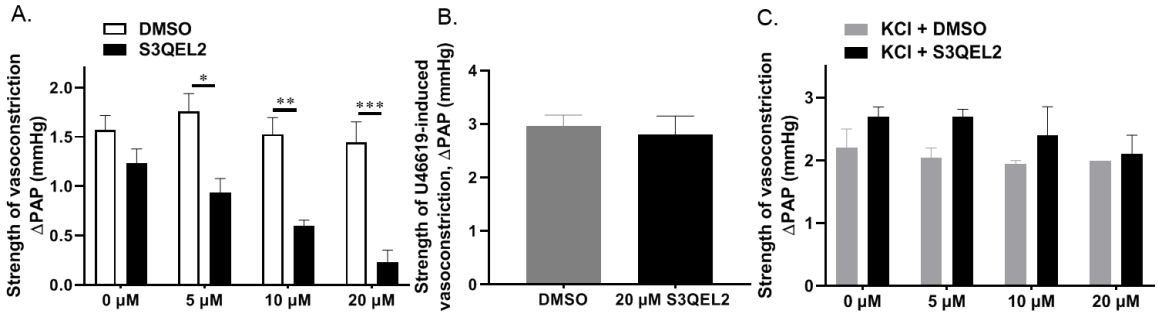

Figure 10. Effect of S3QEL2 on HPV and pulmonary vasoconstriction induced by U46619 and KCl

(A), The strength of hypoxic pulmonary vasoconstriction (HPV) was determined as the increase of pulmonary arterial pressure (ΔPAP) during hypoxic (1% O_2, 5% CO_2, rest N_2) ventilation in presence of "S3QEL2" or solvent (dimethyl sulfoxide ["DMSO"]) in wild-type (WT) mouse lungs (n = 6 isolated lungs in each group). (B), Pulmonary vasoconstriction induced by the thromboxane mimetic U46619 (n = 4 per group) in the presence or absence of 20 μM S3QEL2 OR DMSO in WT mouse lungs. (C), potassium chloride (KCl)-induced pulmonary vasoconstriction (n = 4 isolated lungs for each group). *p<0.05, **p<0.01, ***p<0.001, data were analyzed by unpaired parametric two-tailed t-test and two-way ANOVA with Sidak's multiple comparisons test. Data are shown as mean ± SEM.

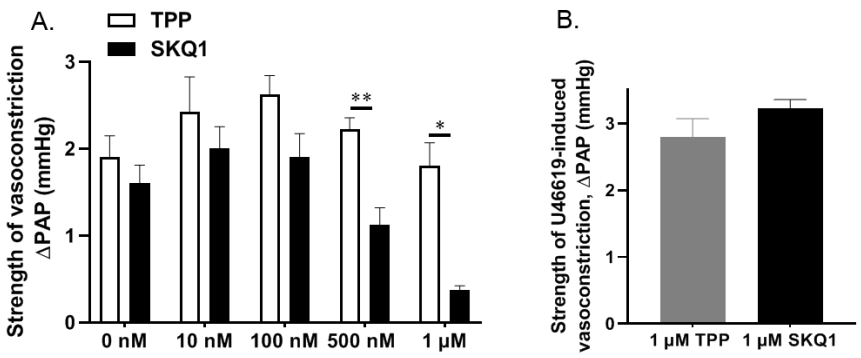

Figure 11. Effect of SKQ1/TPP on HPV and pulmonary vasoconstriction induced by U46619

(A), The strength of hypoxic pulmonary vasoconstriction (HPV) was determined as the increase of pulmonary arterial pressure (ΔPAP) during hypoxic (1% O_2, 5% CO_2, rest N_2) ventilation in presence of SKQ1 or triphenylphosphonium (TPP) in wild-type (WT) mouse lungs (n = 4 isolated lungs each group). (B), Pulmonary vasoconstriction induced by the thromboxane mimetic U46619 in the presence of 1 µM "SKQ1" or "TPP" in WT mouse lungs. *p<0.05, **p<0.01, data were analyzed by two-way ANOVA with Sidak's multiple comparisons test and unpaired parametric two-tailed t-test. Data are shown as mean ± SEM.

3.2. Effect of *Aox* expression on HPV and chronic hypoxia-induced PH

3.2.1. Protein expression of AOX in mouse lung tissue

Szibor et al. showed *Aox* gene expression in mice with the insertion of a single copy of *Ciona intestinalis* AOX into the Rosa26 locus. Highest protein expression of AOX was detected in the heart, skeletal muscle, and pancreas. Following that, we proved AOX protein expression in the pulmonary vasculature and bronchial wall of Aox^{tg} mouse lung using western blot and immunohistochemistry (Figure 12A, B).

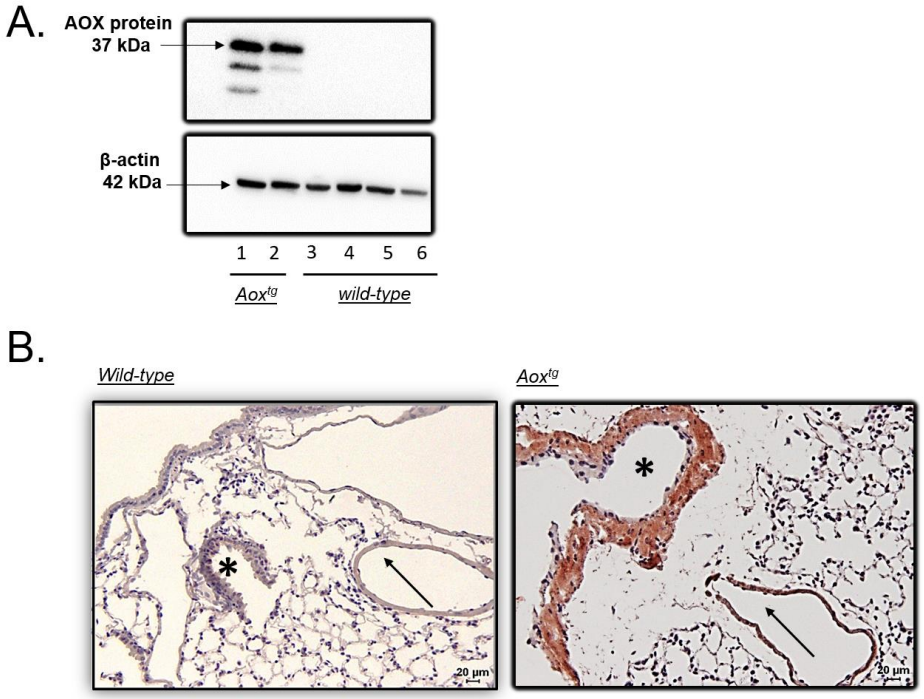

Figure 12. Expression of AOX in the lung of *Aox*^{tg} mice

(A), AOX protein expression was determined in the "wild-type" and "*Aox*^{tg}" mouse lungs by western blot (n = 3 and 4 for each *Aox*^{tg} and WT group). (B), AOX expression was determined in the "wild-type" and "*Aox*^{tg}" mouse lungs by immunostaining. Star and arrow indicate the bronchial wall and pulmonary artery, respectively.

3.2.2. Effect of *Aox* expression on HPV

HPV was quantified by repetitive ventilation of isolated WT and *Aox*^{tg} mouse lungs with hypoxic gas (1% O_2, 5% CO_2, rest N_2). HPV was absent in *Aox*^{tg} mouse lungs (Figure 13A, 1st and 2nd hypoxic challenge). Subsequently, further verification of the AOX effect on HPV was accomplished by applying n-PG, an AOX inhibitor, to the perfusate of the isolated lung system. Application of increasing concentrations of n-PG before each repetitive hypoxic maneuver (Figure 13A, 3rd to 6th hypoxic challenge) restored HPV in *Aox*^{tg} mouse lungs (Figure 13A). In contrast, the U46619-induced vasoconstriction was not different in WT and *Aox*^{tg} lungs, suggesting that the vasoreactivity of lung vessels was intact and the vessels were fully responsive in *Aox*^{tg} lungs (Figure 13B).

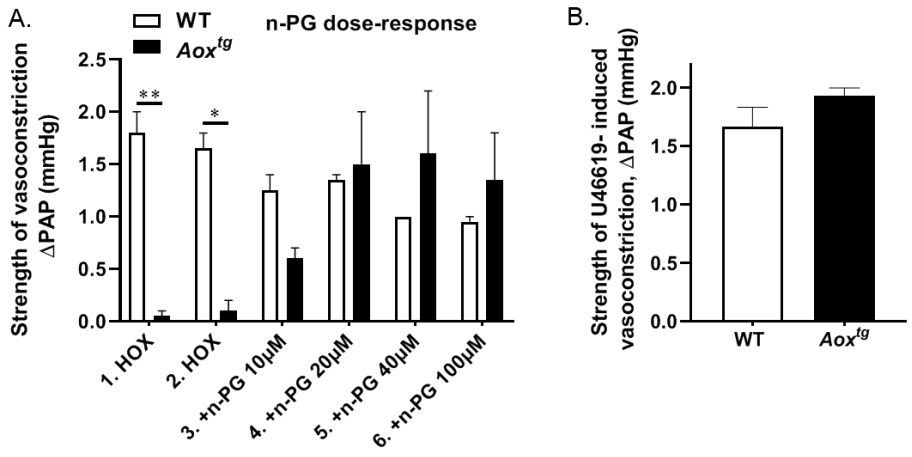

Figure 13. Effect of *Aox* mouse expression on HPV and pulmonary vasoconstriction induced by U46619

(A), The strength of hypoxic pulmonary vasoconstriction (HPV) was determined as the increase of pulmonary arterial pressure (ΔPAP) during hypoxic (1% O_2, 5% CO_2, rest N_2) ventilation in the "wild-type" and "*Aox*^{tg}" mouse lungs (n = 4 isolated lungs for each group). The first and second hypoxic (HOX) maneuver was performed in absence of the AOX inhibitor, n-propyl gallate (n-PG). Afterwards, n-PG was applied 5 minutes before the 3rd to 6th ("3., 4., 5., 6.") hypoxic ventilation. (B), Pulmonary vasoconstriction induced by the thromboxane mimetic U46619 (n = 6 isolated lungs for each group). *p<0.05, **p<0.01, for comparison between the "wild-type" and "*Aox*^{tg}" lungs. Data were analyzed by two-way ANOVA with Sidak's multiple comparisons test and unpaired parametric two-tailed t-test. Data are shown as mean ± SEM.

3.2.3. Impact of *Aox* expression on cyanide-induced vasoconstriction

Next, experiments were performed to investigate if inhibition of mitochondrial CIV with cyanide induces similar effects on PAP like hypoxic ventilation (1% O_2, 5% CO_2, rest N_2). Similar to HOX, cyanide induced pulmonary vasoconstriction in WT mouse lungs. Cyanide-induced vasoconstriction was largely diminished in *Aox*^{tg} lungs (Figure 14).

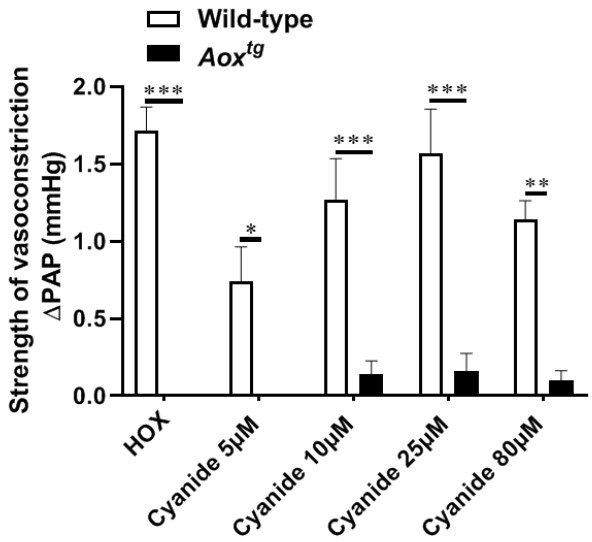

Figure 14. Cyanide-induced pulmonary vasoconstriction in WT and *Aox* expressing mouse lungs

The strength of hypoxic pulmonary vasoconstriction (HPV) was determined as the increase of pulmonary arterial pressure (ΔPAP) during hypoxic ventilation (HOX; 1% O_2, 5% CO_2, rest N_2) or in presence of cyanide (KCN) in the "wild-type" and "*Aox*^{tg}" mouse lung (n = 5 for each group). Increasing concentrations of cyanide (5, 10, 25, and 80 µM) were applied every 10 minutes. *p<0.05, **p<0.01, ***p<0.001 for comparison as indicated. Data were analyzed by two-way ANOVA with Sidak's multiple comparisons test. Data are shown as mean ± SEM.

3.2.4. Impact of *Aox* expression on cellular membrane potential

Given that cellular membrane depolarization is a crucial step in HPV, alterations of the cellular membrane potential during HOX (1% O_2, 5% CO_2, rest N_2) in WT and *Aox*^{tg} mouse PASMC were compared by patch-clamp analysis. Exposure of WT PASMC to acute HOX increased cellular membrane potential (= depolarization) (Figure 15A, C, and E). In contrast, AOX PASMC showed less depolarization in response to acute HOX, but a similar change in membrane potential (delta MP) in presence of the AOX inhibitor n-PG (Figure 15B, D, and E). In contrast, the WT cells did not show any change in membrane potential in the presence of n-PG (Figure 15A, C, and E). Patch-clamp measurements were performed by Dr. Fenja Knöpp.

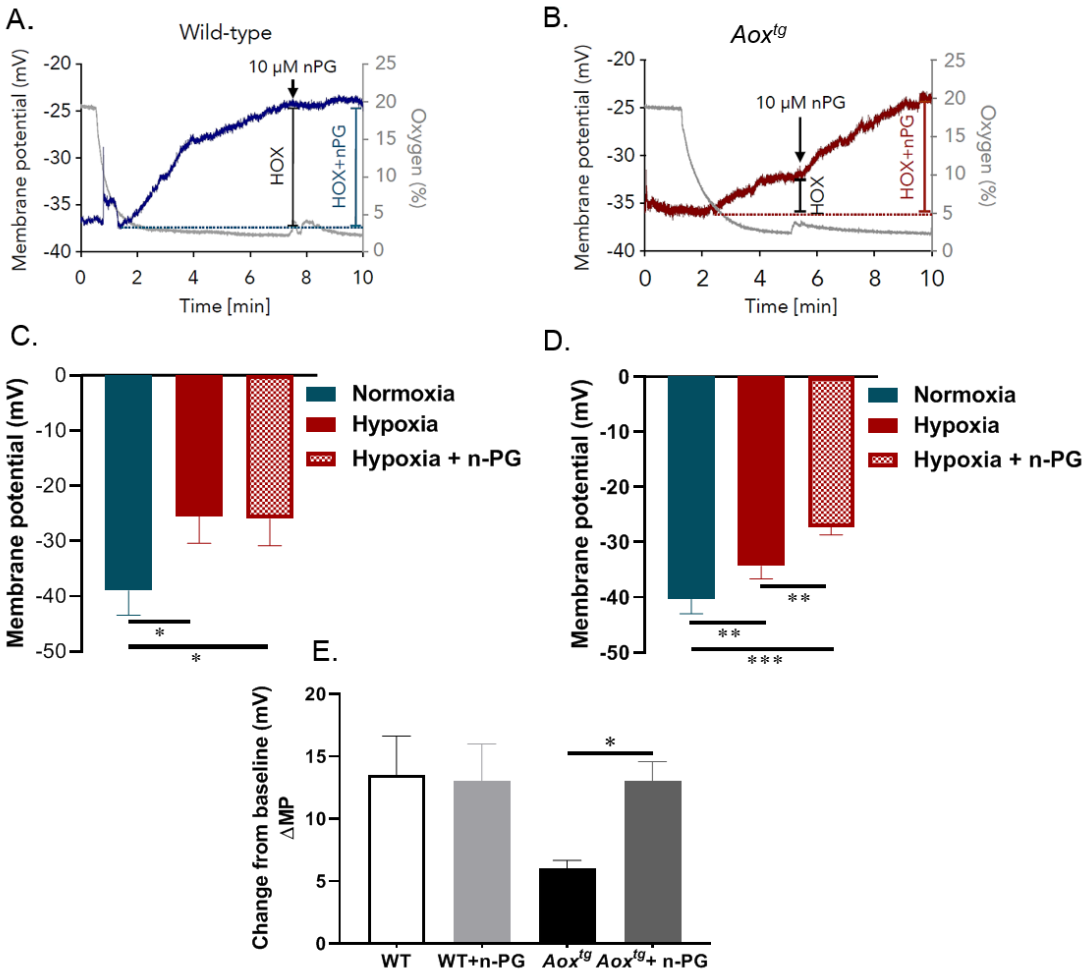

Figure 15. HOX-induced cellular membrane depolarization in WT and *Aox*^{tg} PASMC

(A, B), Representative tracings of cellular membrane potential were determined by using a whole-cell patch clamp in the absence or presence of 10 µM n-propyl gallate (n-PG) in isolated pulmonary arterial smooh muscle cell (PASMC) for the "wild-type" or "*Aox*^{tg}" mice (n = 6 experiments per group). Gray traces depict oxygen (O_2) concentration in %, blue and red traces indicate cellular membrane potential in mV. (C, D), Cellular membrane potential in the "wild-type" or "*Aox*^{tg}" mouse PASMC during "normoxia" and acute "hypoxia" or acute "hypoxia + n-PG" (10 µM). (E), Change of cellular membrane potential compared to normoxia in "WT" and "*Aox*^{tg}" PASMC in the absence and presence of 10 µM n-PG. *p<0.05, **p<0.01, ***p<0.001 for comparison as indicated. Data were analyzed by repeated-measures one-way ANOVA and Tukey's multiple comparisons test. Data are shown as mean ± SEM.

3.2.5. Effect of the baseline cellular membrane potential on AOX-induced inhibition of HPV

As cellular membrane depolarization was decreased in *Aox*^{tg} mice but not completely inhibited (Figure 15), so that potentially the threshold for activation of L-type calcium channels and subsequently hypoxic signaling could not be reached, experiments were performed to test if increasing the basal cellular membrane potential by application of KCl (during NOX; 21% O_2, 5% CO_2, rest N_2) could restore HPV in *Aox*^{tg} mice. Application of KCl after the 1st and 2nd hypoxic challenge (1% O_2, 5% CO_2, rest N_2) caused pulmonary vasoconstriction in NOX and could restore HPV in *Aox*^{tg} lungs, albeit only to a lower level than in WT lungs (Figure 16).

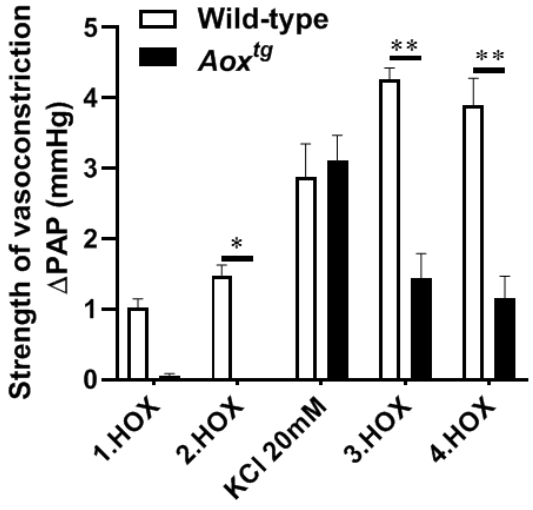

Figure 16. HPV in WT and *Aox*^{tg} mouse lungs in the presence of KCl

Pulmonary vasoconstriction in response to two maneuvers of hypoxic (1% O_2, 5% CO_2, rest N_2) ventilation (1. HOX, 2. HOX), subsequent application of potassium chloride (KCl) and afterwards two maneuvers of hypoxic ventilation in presence of KCl (3. HOX, 4. HOX) in the isolated "wild-type" and "*Aox*^{tg}" mouse lungs (n = 3 isolated lungs each group). **p<0.01, data were analyzed by two-way ANOVA with Sidak's multiple comparisons test. Data are shown as mean ± SEM.

3.2.6. Impact of *Aox* expression on cellular superoxide release

Superoxide release was determined in PASMC snap-frozen after acute hypoxic exposure (1% O_2, 5% CO_2, rest N_2, 5minutes) using ESR spectroscopy. Superoxide production was elevated in WT PASMC upon exposure to acute HOX whereas this increase was diminished in the *Aox*^{tg} PASMC (Figure 17A, B). ESR measurements were performed with help of Dr. Susan Scheibe and Alireza Saraji.

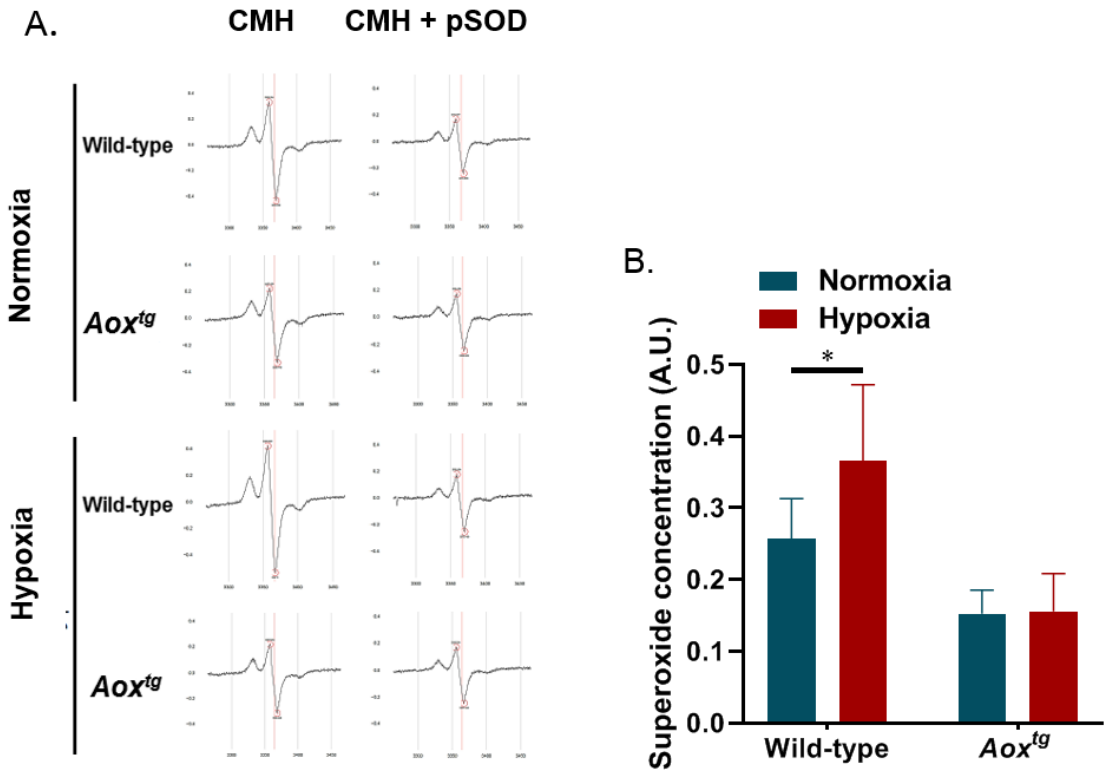

Figure 17. HOX-induced superoxide release in WT and *Aox*^{tg} PASMC

(A), Representative electron spin resonance spectroscopy (ESR) spectra from the "wild-type" and "*Aox*^{tg}" mouse pulmonary arterial smooh muscle cell (PASMC). (B), Superoxide concentration was determined by ESR in the "wild-type" and "*Aox*^{tg}" PASMC during exposure to normoxia (NOX; 21% O_2, 5% CO_2, rest N_2) and 5 minutes hypoxia (HOX; 1% O_2, 5% CO_2, rest N_2) (n = 4 experiments each group). Superoxide concentration was calculated as the portion of the 1-hydroxy-3-methoxycarbonyl-2, 2, 5, 5-tetramethylpyrrolidine (CMH) signal inhibited by a PEGylated superoxide-dismutase. AU: arbitrary units. *$p<0.05$, for comparison as indicated. Data were analyzed by two-way ANOVA with Sidak's multiple comparisons test as mean ± SEM.

3.2.7. Impact of *Aox* expression on MMP

To identify the potential mechanism underlying the increased superoxide production, we assessed the alteration of the MMP under acute HOX (1% O_2, 5% CO_2, rest N_2). MMP was increased during superfusion with the hypoxic medium in WT mouse PASMC but not in *Aox*^{tg} PASMC (Figure 18A, B).

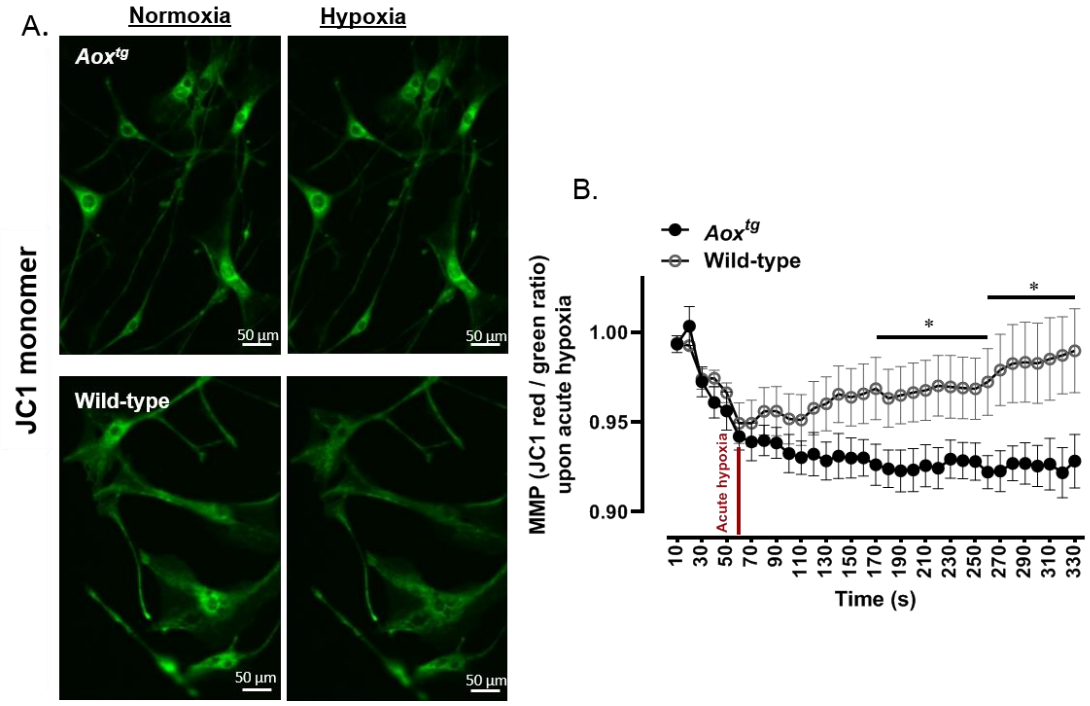

Figure 18. HOX-induced mitochondrial membrane hyperpolarization in WT and *Aox*^{tg} PASMC

(A), Representative mouse "wild-type" and "*Aox*^{tg}" pulmonary arterial smmoth muscle cell (PASMC) stained with JC1 during superfusion with hypoxic medium (1% O_2, 5% CO_2, rest N_2, 5 minutes) in culture dishes placed in closed chambers. At low mitochondrial membrane potential (MMP), JC1 is predominatly a monomer that yields green fluorescence (B), MMP was measured by JC1 as fluorescent red/green ratio in the "wild-type" and "*Aox*^{tg}" mouse PASMC during superfusion with hypoxic medium (n = 10 and n = 12 experiments,). *p<0.05, for comparison as indicated. Data were analyzed by two-way ANOVA uncorrected Fisher's least significant difference. Data are shown as mean ± SEM.

3.2.8. Effect of *Aox* expression on chronic hypoxia-induced PH in mice

To determine the effect *Aox* expression on chronic HOX-induced PH, we exposed WT and *Aox*^{tg} mice to HOX (10% O_2, 5% CO_2, rest N_2) for four weeks. Development of PH was evaluated by determination of hemodynamic, and echocardiographic parameters as well as evaluation of the level of pulmonary arterial muscularization (Figures 19_21). *Aox*^{tg} mice developed PH to a similar degree as WT mice, i.e. showed a similar increase in the muscularization of the pulmonary vasculature and RVSP (Figure 19A, B). SAP and LVSP were not changed under HOX in *Aox*^{tg} as well as WT mice (Figure 19C, D). In addition, there was a significant increase in right heart hypertrophy, characterized by fulton index (Figure 20A). Echocardiography assessment showed a decreased in TAPSE and CO in both strains in response to HOX (Figure 20B-C). Accordingly, increased HIF-1α expression was detected in both, PASMC of WT and *Aox*^{tg} mice after hypoxic exposure for three days (1% O_2, 5% CO_2, rest N_2) (Figure 21A, B) indicating that, at least under these conditions, mitochondrial ROS is not a relevant trigger for HOX-induced HIF-1α stabilization. Hemodynamic measurements were performed by Karin Quanz, echocardiographic measurements by Dr. Akylbek Sydykov. The HIF-1α protein expression was performed with the help of Dr. Oleg Pak.

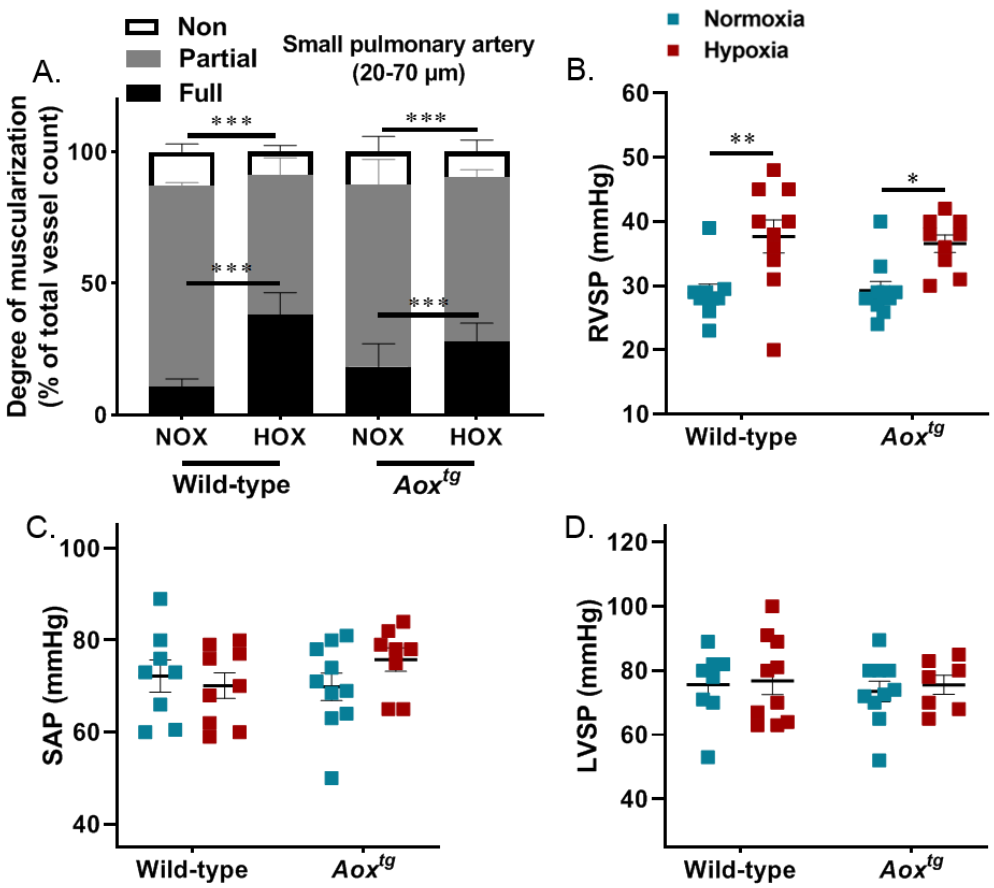

Figure 19. Hemodynamic parameters and pulmonary vascular remodeling in WT and *Aox*^{tg} mice after exposure to chronic HOX

(A), Vascular remodeling was quantified as the degree of muscularization of small pulmonary arterial vessels (20-70 µm diameter; n = 4 for normoxia [NOX] and 4 hypoxia [HOX] for the "*Aox*^{tg}" group and 5 NOX and 5 HOX for the "wild-type" group) and (B-D), Hemodynamic parameters including right ventricular systolic pressure (RVSP; n = 9 NOX and 10 HOX for the "*Aox*^{tg}" group and 10 NOX and 9 HOX for the "wild-type" group), systemic arterial pressure (SAP; n = 8 NOX and 9 HOX for the "*Aox*^{tg}" group and 10 NOX and 8 HOX for the "wild-type" group), and left ventricular systolic pressure (LVSP; n = 8 NOX and 10 HOX for the "*Aox*^{tg}" group and 10 NOX and 7 HOX for the "wild-type" group) were measured after exposure to NOX (21% O_2, 5% CO_2, rest N_2)/chronic HOX (10% O_2, 5% CO_2, rest N_2) for 28 days. Vessels were categorized as non-muscularized (non), partially muscularized (partial), or fully muscularized (full) after immunostaining against α-smooth muscle actin for the detection of the media and von-Willebrand for discrimination of endothelium. *p<0.05, **p<0.01, ***p<0.001, for comparison as indicated. Data were analyzed by two-way ANOVA with Tukey's multiple comparisons test. Data are shown as mean ± SEM.

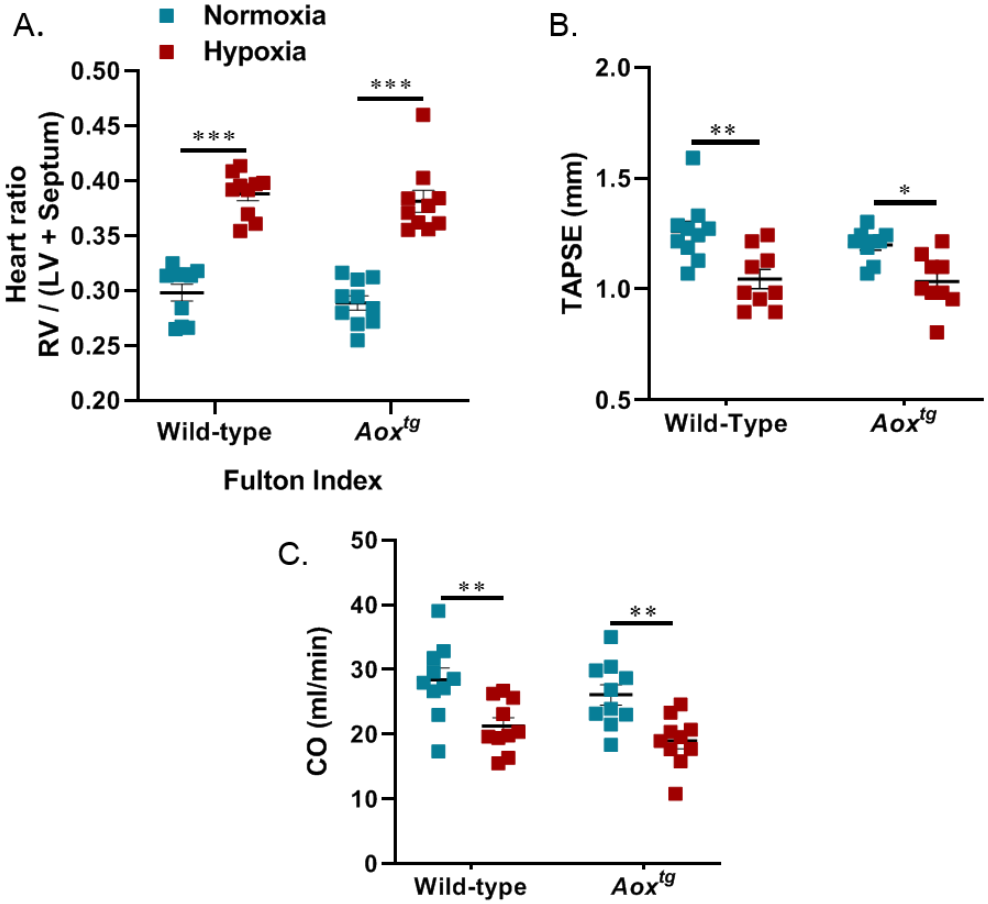

Figure 20. Cardiac parameters of WT and *Aox*^{tg} mice after exposure to chronic HOX

(A), Fulton index to determine right heart hypertrophy (n = 10 normoxia [NOX] and 10 hypoxia [HOX] for the "*Aox*^{tg}" group and 10 NOX and 10 HOX for the "wild-type" group), (B), Tricuspid annular plane systolic excursion (TAPSE; n = 10 NOX and 9 HOX for the "*Aox*^{tg}" group, and 9 NOX and 9 HOX for the "wild-type" group) and (C) cardiac output (CO; n = 10 NOX and 10 HOX for the "*Aox*^{tg}" group and 10 NOX and 10 HOX for the "wild-type" group) was quantified by echocardiography after exposure to NOX (21% O_2, 5% CO_2, rest N_2)/chronic HOX (10% O_2, 5% CO_2, rest N_2) for 28 days. *p<0.05, **p<0.01, ***p<0.001 NOX versus HOX. Data were analyzed by two-way ANOVA with Tukey's multiple comparisons test. Data are shown as mean ± SEM.

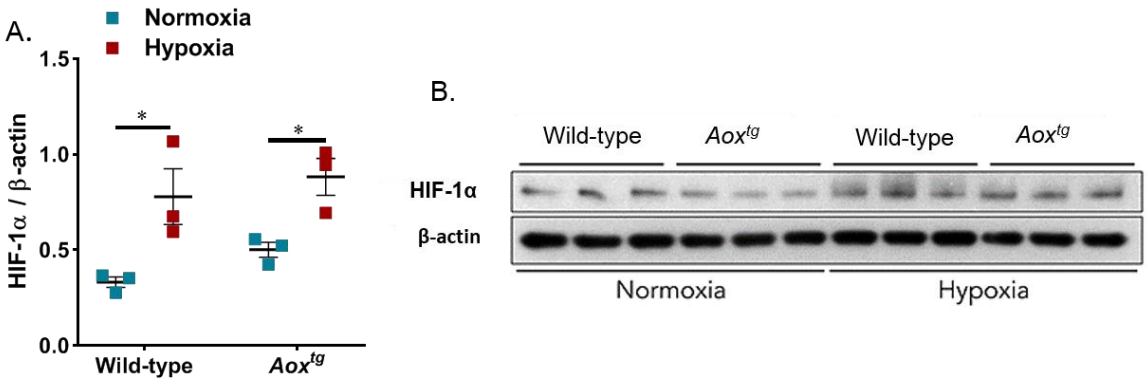

Figure 21. Changes of HIF-1α expression of WT and *Aox*^{tg} mouse PASMC after exposure to chronic HOX

(A, B), HIF-1α expression was determined by western blot analysis in the "wild-type" and *Aox*^{tg} transgenic ("*Aox*^{tg}") mouse pulmonary arterial smooth muscle cell (PASMC) under normoxic (21% O_2, 5% CO_2, rest N_2) and hypoxic (1% O_2, 5% CO_2, rest N_2) conditions (36 hours; n = 3 experiments). (A), Quantification of HIF-1α protein expression (values were normalized to β-actin expression) and (B), Representative western blot of the "wild-type" and "*Aox*^{tg}" mouse PASMC for HIF-1α expression. *$p<0.05$, for comparison as indicated. Data were analyzed by two-way ANOVA with Sidak's multiple comparisons test. Data are shown as mean ± SEM.

3.3. The role of COX4i2 in HPV

3.3.1. Effect of *Cox4i2* deficiency on HPV

In contrast to WT mice, isolated lungs of *Cox4i2* knockout mice did not display pulmonary vasoconstriction in response to acute HOX (1% O_2, 5% CO_2, rest N_2, 10 minutes). However, HOX-independent vasoconstriction induced by the application of KCl was not affected by *Cox4i2* knockout, indicating that the contractile apparatus of the lung vasculature was intact in *Cox4i2* knockout lungs (Figure 22A). Similar to the effect of KCl on the restoration of HPV in Aox^{tg} mice, acute HPV was restored in *Cox4i2* knockout mice in the presence of KCl (Figure 22B).

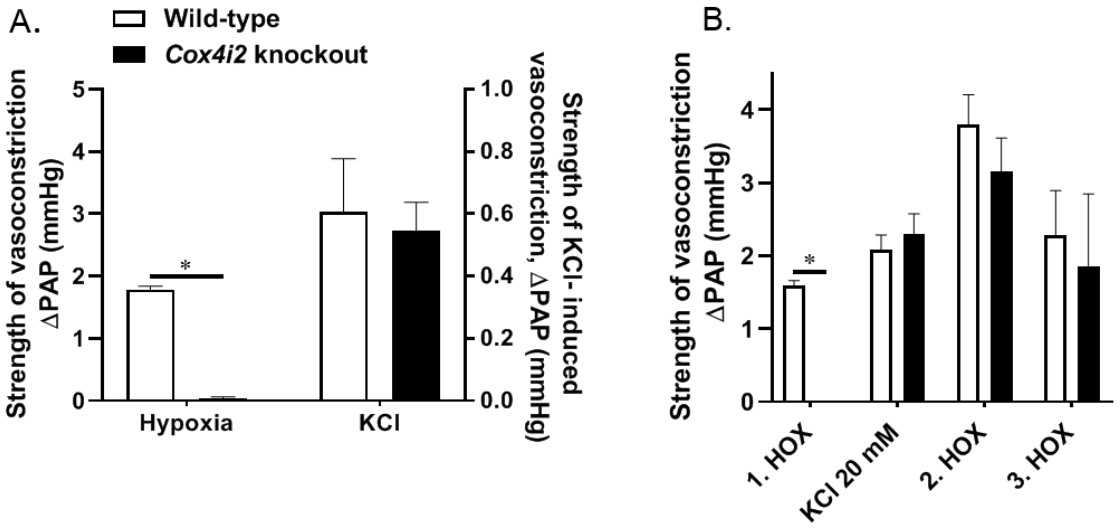

Figure 22. Acute HPV in isolated lungs of WT and *Cox4i2* knockout mice

(A), The increase of the pulmonary arterial pressure (ΔPAP) was determined in response to hypoxic ventilation (1% O_2, 5% CO_2, rest N_2) or application of 20 mM potassium chloride (KCl) in the perfusate (n = 5 isolated lungs each group). (B), Pulmonary vasoconstriction in response to hypoxic ventilation (1. HOX), subsequent application of KCl (20 mM) and afterwards two maneuvers of hypoxic ventilation in presence of KCl (2. HOX, 3. HOX) in the isolated "wild-type" and "*Cox4i2* knockout" mouse lungs (n = 3 isolated lungs for each group). *p<0.05, for comparison as indicated. Data were analyzed by two-way ANOVA with Sidak's multiple comparisons test. Data are shown as mean ± SEM.

3.3.2. Effect of *Cox4i2* deficiency on cellular membrane polarization

Similar to *Aox*^{tg} PASMC, HOX-induced cellular membrane depolarization was blunted in *Cox4i2* knockout PASMC. The application of H_2O_2, could further enhance the cellular membrane potential in *Cox4i2* knockout PASMC to the level reached in WT PASMC under acute HOX (Figure 23A-D). Patch-clamp measurements were performed by Dr. Fenja Knöpp.

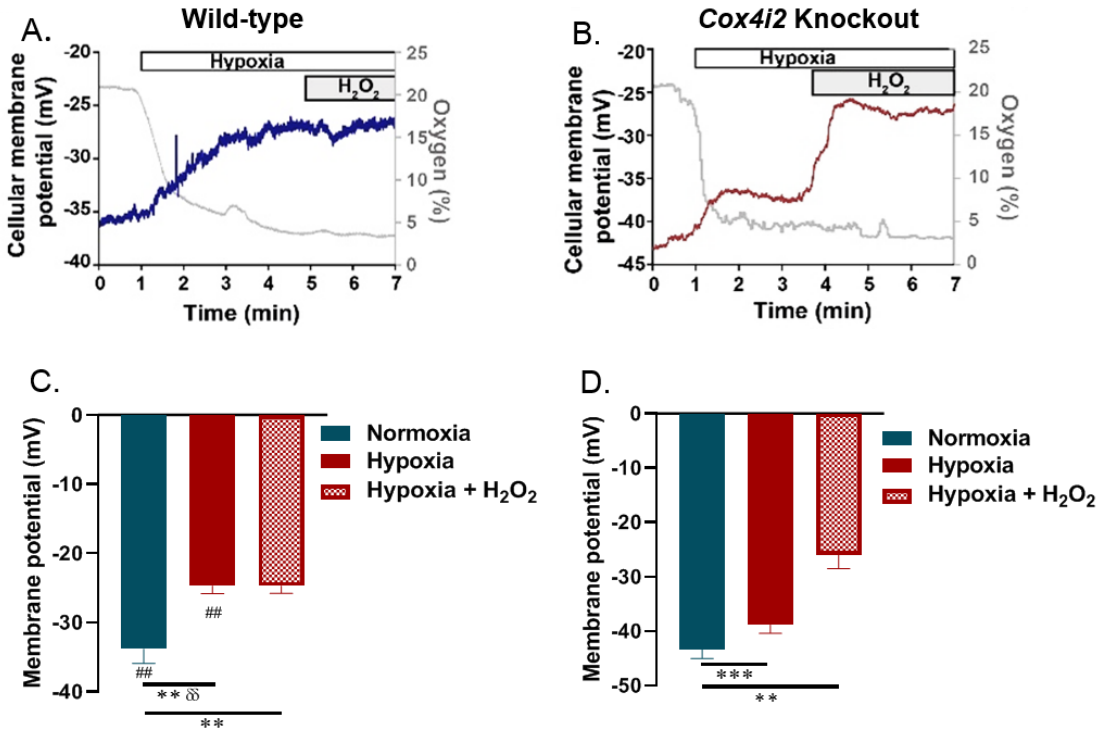

Figure 23. Acute HOX-induced cellular membrane depolarization in WT and *Cox4i2* knockout PASMC

(A, B), Representative tracings of cellular membrane potential determined by using whole-cell patch-clamp in absence or presence of 124 nM hydrogen peroxide (H_2O_2) in pulmonary arterial smooh muscle cell (PASMC; n = 7 or 6 experiments for the "wild-type" or "*Cox4i2* knockout" mice each group, respectively). Gray traces depict oxygen (O_2) concentration in %, blue and red traces indicate cellular membrane potential in mV. (C, D), Cellular membrane potential in the "wild-type" or "*Cox4i2* knockout" PASMC during normoxia (NOX) and acute hypoxia (HOX) or acute HOX plus hydrogen peroxide (H_2O_2). **p<0.01, ***p<0.001 compared to respective NOX group, ##p<0.01, compared to WT, and §§p<0.01, comparing the differences between normoxic and hypoxic measurements between the "wild-type" or "*Cox4i2* knockout" group. Data were analyzed by repeated-measures one-way ANOVA with Tukey's multiple comparisons test. Data are shown as mean ± SEM.

3.3.3. Impact of *Cox4i2* deficiency on superoxide release upon hypoxia in PASMC

Superoxide concentration increased in hypoxic WT PASMC, whereas this increase was absent in *Cox4i2* knockout PASMC (Figure 24A, B) ESR measurements were performed with the help of Dr. Susan Scheibe.

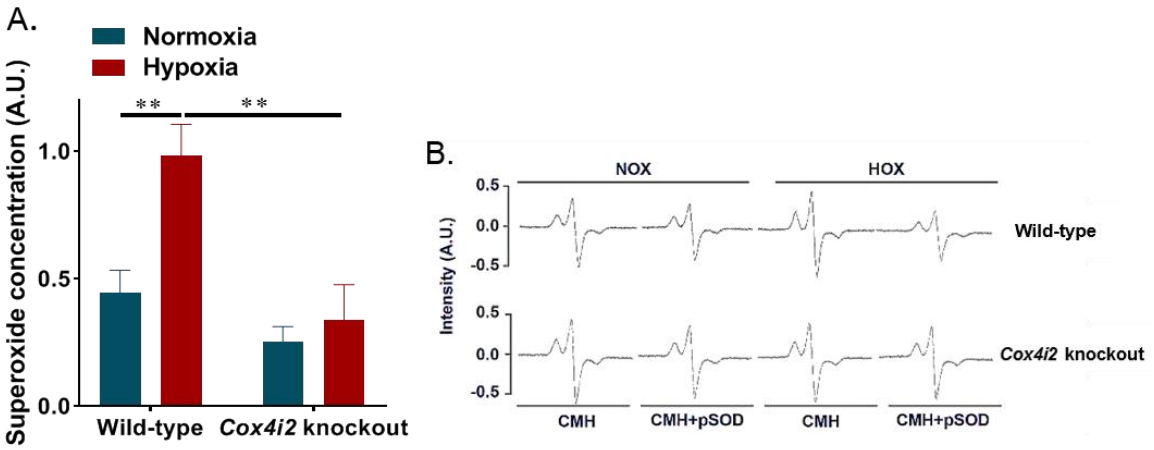

Figure 24. HOX-induced superoxide production in *Cox4i2* knockout PASMC

(A), Superoxide concentration was determined by electron spin resonance (ESR) spectroscopy in pulmonary arterial smooh muscle cell (PASMC) isolated from the "wild-type" (n = 7 experiments) or "*Cox4i2* knockout" mice (n = 8 experiments) during exposure to normoxia (NOX; 21% O_2, 5% CO_2, rest N_2) and 5 minutes hypoxia (HOX; 1% O_2, 5% CO_2, rest N_2). (B), Representative ESR spectra of PASMC from the "wild-type" and or "*Cox4i2* knockout" mice. Superoxide concentration was calculated as the portion of the 1-hydroxy-3-methoxycarbonyl-2, 2, 5, 5-tetramethylpyrrolidine (CMH) signal inhibited by a PEGylated superoxide-dismutase. AU: arbitrary units. **p<0.01, for comparison as indicated. Data were analyzed by two-way ANOVA with Sidak's multiple comparisons test. Data are shown as mean ± SEM.

3.3.4. Impact of *Cox4i2* deficiency on MMP

Perfusion of WT PASMC with hypoxic medium (1% O_2, 5% CO_2, rest N_2) caused mitochondrial membrane hyperpolarization, which was absent in *Cox4i2* knockout PASMC (Figures 25).

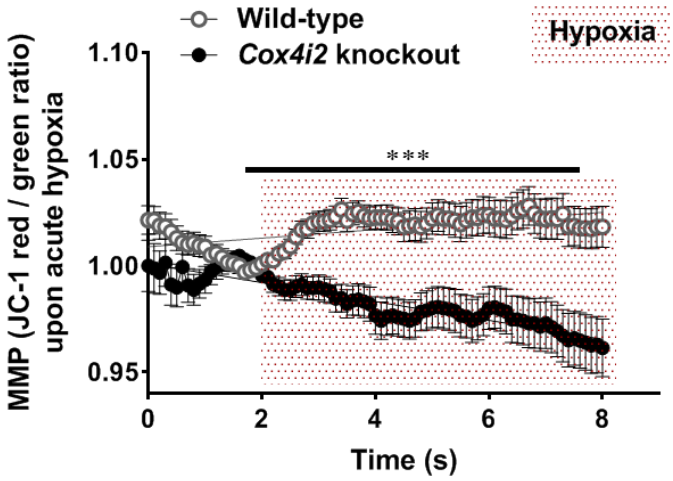

Figure 25. MMP in *Cox4i2* knockout PASMC during acute HOX

Mitochondrial membrane potential (MMP) was determined as fluorescence intensity of red/green ratio of JC1 staining in pulmonary arterial smooh muscle cell (PASMC) of the "wild-type" and or "*Cox4i2* knockout" mice during normoxic (21% O_2, 5% CO_2, rest N_2) superfusion and after switching to hypoxia (HOX; 1% O_2, 5% CO_2, rest N_2) (n = 180/207 cells for hypoxia: wild-type/*Cox4i2* knockout and n = 107/95 cells for normoxia [NOX]: wild-type/*Cox4i2* knockout), from at least three individual PASMC isolations). ***p<0.001 for comparison as indicated. Data were analyzed by a paired nonparametric two-tailed Mann-Whitney U test. Data are shown as mean ± SEM.

3.4. Effect of SMC-specific *Ucp2* deficiency on chronic hypoxia-induced PH

3.4.1. *Ucp2* mRNA expression in tamoxifen-treated PASMC

To further investigate the cell type-specific role of mitochondrial ROS in the development of PH, the model of *Ucp2* knockout in SMC was used. In previous studies, it was shown that the global absence of *Ucp2* caused an increase in MMP and ROS in isolated PASMC and was associated with increased proliferation of PASMC and *in vivo* development of PH (181). Thus, now the *in vivo* relevance of *Ucp2* knockout specifically in PASMC was tested. First, sufficient knockdown in this model was tested in isolated PASMC of $Ucp2^{flox/flox,\ iSmaCre+}$ mice treated *in vitro* with 1 µM tamoxifen for 72 hours, and the knockdown of *Ucp2* in these cells was confirmed by PCR (Figure 26A, B).

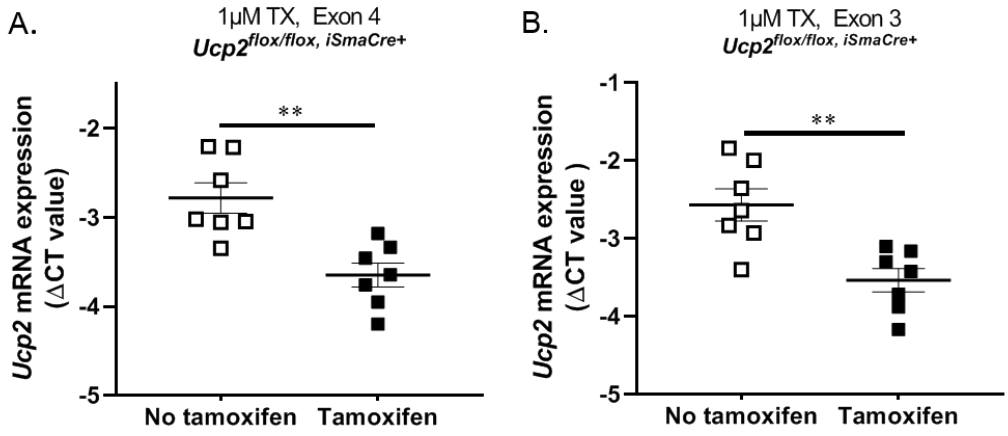

Figure 26. *Ucp2* mRNA expression in $Ucp2^{flox/flox,\ iSmaCre+}$ mice PASMC after tamoxifen treatment

(A, B), Uncoupling protein 2 (*Ucp2*) mRNA expression in pulmonary arterial smooh muscle cell (PASMC) for the "no tamoxifen" and "tamoxifen" group (1 µM tamoxifen for 72 hours) was determined by qRT-PCR (n = 7 each group). Values were compared to the expression of the house-keeping gene, porphobilinogen deaminase (PBGD). **p<0.01, for comparison as indicated. Data were analyzed by unpaired parametric two-tailed t-test. Data are shown as as mean ± SEM. Primers for Exon 3 and exon 4 of *Ucp2* gene were used. Tamoxifen: TX.

3.4.2. *Ucp2* mRNA expression in PASMC of tamoxifen-treated mice

Next *in vivo* knockdown of *Ucp2* was tested in *Ucp2*$^{flox/flox,\ iSmaCre+}$ mice treated with 400 mg tamoxifen/kg BW for two weeks with a 4-week interval of tamoxifen-free food (see methods section). Tamoxifen-fed *Ucp2*$^{flox/flox,\ iSmaCr-}$ mice were used as control. The level of *Ucp2* expression in PASMC was checked 4 weeks after end of feeding by RT-qPCR. There were no differences in *Ucp2* expression in *Ucp2*$^{flox/flox,\ iSmaCr-}$ mice (Figure 27A, C). The expression of *Ucp2* was reduced in PASMC of tamoxifen-treated *Ucp2*$^{flox/flox,\ iSmaCre+}$ compared to the non-tamoxifen group (Figure 27B, D).

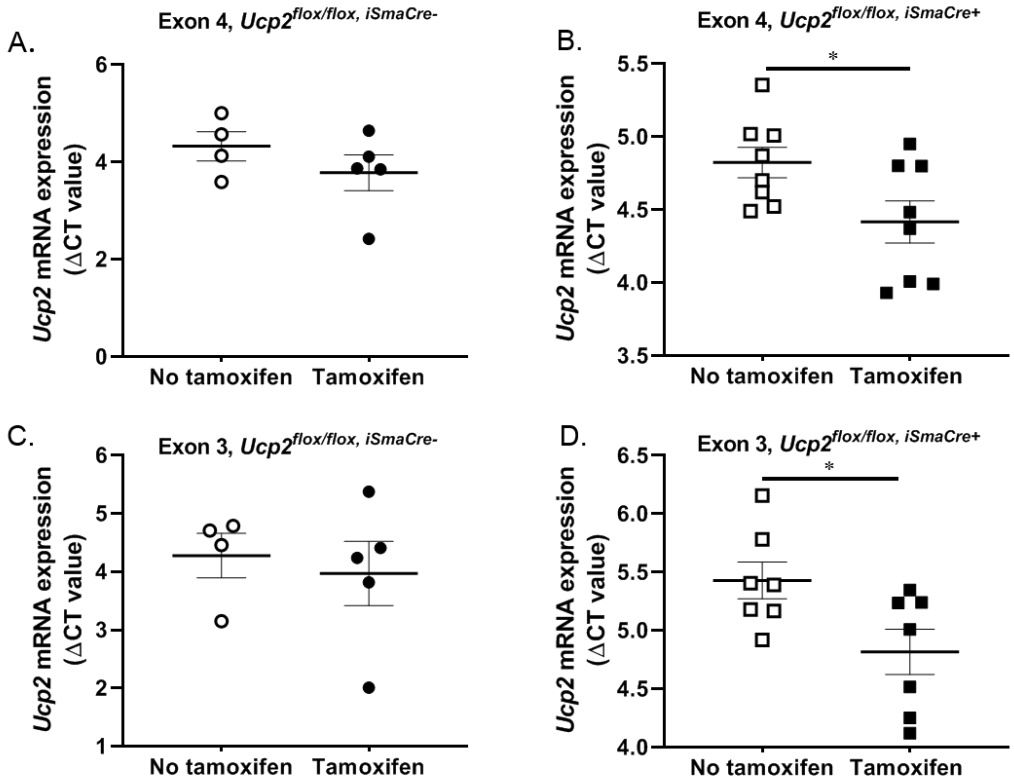

Figure 27. *Ucp2* mRNA expression in PASMC of tamoxifen-treated *Ucp2*$^{flox/flox,\ iSmaCre+}$ and *Ucp2*$^{flox/flox,\ iSmaCre-}$ mice

(A-D), Uncoupling protein 2 (*Ucp2*) mRNA expression in pulmonary arterial smooh muscle cell (PASMC) of *Ucp2*$^{flox/flox,\ iSmaCre+}$ and *Ucp2*$^{flox/flox,\ iSmaCre-}$ mice was determined by qRT-PCR after treatment with 400 mg tamoxifen/kg body weight (BW) for a total of 2 weeks (n = 4 for the "no tamoxifen" group and n=5 for the "tamoxifen" group for *Ucp2*$^{flox/flox,\ iSmaCre-}$ mice, and n = 7 for the "no tamoxifen" group and n=7 for the "tamoxifen" group for *Ucp2*$^{flox/flox,\ iSmaCre+}$ mice). Values were compared to the expression of porphobilinogen deaminase (PBGD). *p<0.05, for comparison as indicated. Data were analyzed by unpaired parametric two-tailed t-test test. Data are shown as mean ± SEM. Primers for Exon 3 and exon 4 of *Ucp2* gene were used. Tamoxifen: TX.

3.4.3. Body weight (BW) changes in *Ucp2*$^{flox/flox,\ iSmaCre}$ mice

Tamoxifen treatment did not significantly affect BW in *Ucp2*$^{flox/flox,\ iSmaCre+}$ mice compared to *Ucp2*$^{flox/flox,\ iSmaCre-}$ (Figure 28 A, B).

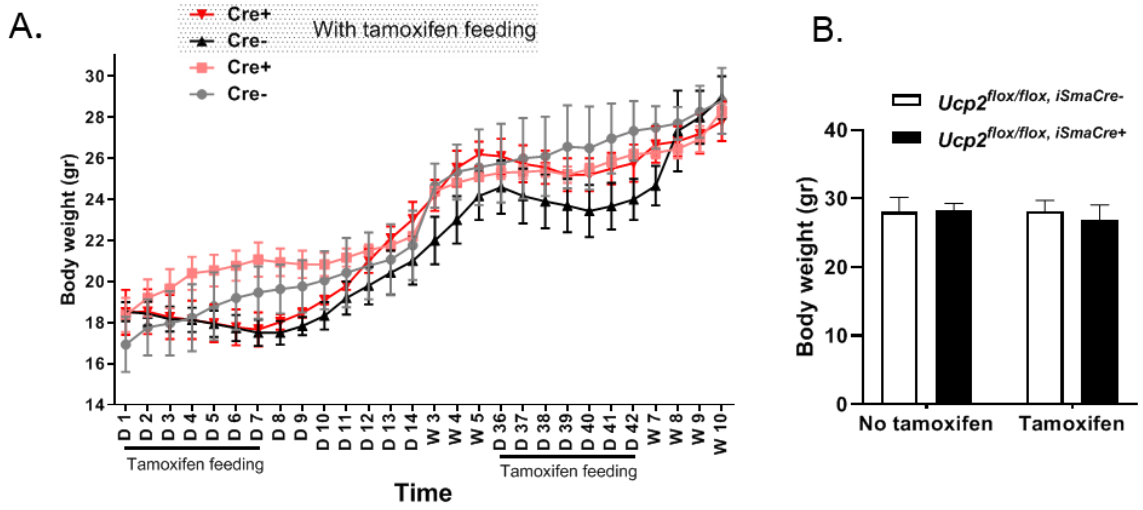

Figure 28. Change in BW in *Ucp2*$^{flox/flox,\ iSmaCre+}$ and *Ucp2*$^{flox/flox,\ iSmaCre-}$ mice during treatment with and without tamoxifen

(A), The course of the body weight (BW) from the first day of tamoxifen feeding (400 mg tamoxifen/kg BW for two times one week; n = 5 each group). B), The BW at the last day of the feeding procedure in the *Ucp2*$^{flox/flox,\ iSmaCre+}$ and *Ucp2*$^{flox/flox,\ iSmaCre-}$ mice. Data were analyzed by two-way ANOVA with Tukey's multiple comparisons test. Data are shown as mean ± SEM. Week: W, Day: D.

3.4.4. Hemodynamic and right heart hypertrophy parameter changes in *Ucp2$^{flox/flox, iSmaCre}$* mice

Under normoxic conditions there was a significant increase in right heart hypertrophy, characterized by fulton index, in *Ucp2$^{flox/flox, iSmaCre+}$* mice treated with tamoxifen compared to mice without induction of knockout (Figure 29A, I). Moreover, HOX induced a significant increase of the fulton index in both genotypes to a similar degree (Figure 29A). However, tamoxifen-treatment attenuated the HOX-induced right heart hypertrophy in *Ucp2$^{flox/flox, iSmaCre-}$* mice (Figure 29E). 2-way ANOVA analysis revealed a significant difference of the RVSP comparing the genotypes and hypoxic treatment (Figure 29B), albeit post-hoc analysis did only show significant difference between NOX and HOX in the non-tamoxifen treated *Ucp2$^{flox/flox, iSmaCre-}$* mice (Figure 29 F). There was no significant difference comparing directly *Ucp2$^{flox/flox, iSmaCre-}$ and Ucp2$^{flox/flox, iSmaCre+}$* with and without tamoxifen-treatment after normoxic exposure (Figure 29 J).

SAP and LVSP were not changed in tamoxifen-fed or non-fed *Ucp2$^{flox/flox, iSmaCre+/-}$* mice (Figure 29C, D, G, H, K, and L); however, both parameters decreased after exposure to chronic HOX in these mice (Figure 29 C, D, G, and H). Hemodynamic measurements were performed by Karin Quanz.

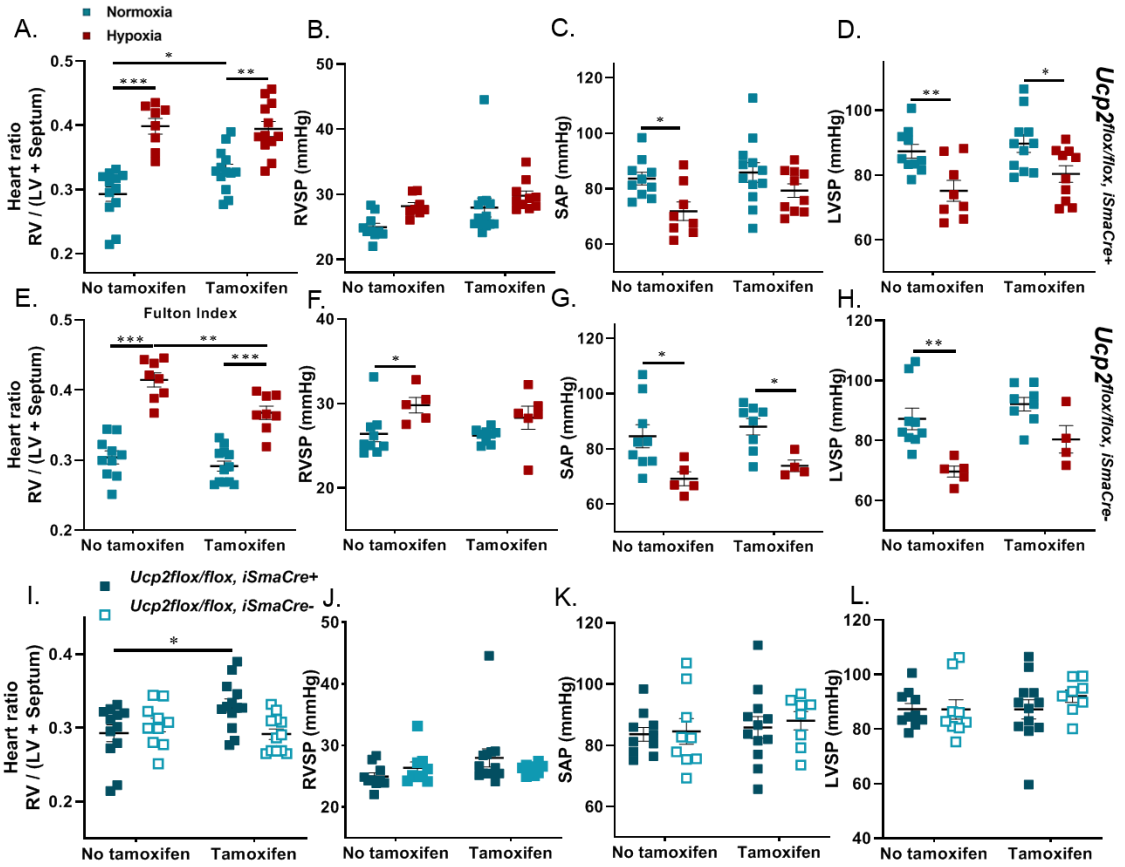

Figure 29. Change in hemodynamic and right heart hypertrophy parameters in *Ucp2*$^{flox/flox,\ iSmaCre+}$ and *Ucp2*$^{flox/flox,\ iSmaCre-}$ mice with or without tamoxifen treatment after chronic hypoxic or normoxic exposure

(A, E), Fulton index to determine right heart hypertrophy in tamoxifen-treated and non-treated *Ucp2*$^{flox/flox,\ iSmaCre+}$ and *Ucp2*$^{flox/flox,\ iSmaCre-}$ mice after exposure to normoxia (NOX; 21% O_2, 5% CO_2, rest N_2) / chronic hypoxia (HOX; 10% O_2, 5% CO_2, rest N_2), for 28 days; n = 12/13 for the "no tamoxifen" group and n=8/12 for the "tamoxifen" group, subjected to NOX and HOX, respectively in *Ucp2*$^{flox/flox,\ iSmaCre+}$ mice, and n = 8/12 for the "no tamoxifen" group and 8/8 for the "tamoxifen" group, subjected to NOX and HOX, respectively in *Ucp2*$^{flox/flox,\ iSmaCre-}$ mice. Hemodynamic parameters including (B, F), RVSP, (C, G), SAP, and (D, H), LVSP were measured after exposure to NOX or chronic HOX in tamoxifen-treated and non-treated *Ucp2*$^{flox/flox,\ iSmaCre+}$ and *Ucp2*$^{flox/flox,\ iSmaCre-}$ mice (n = 10/11 for the "no tamoxifen" group and 8/10 for the "tamoxifen" group, subjected to NOX and HOX, respectively in *Ucp2*$^{flox/flox,\ iSmaCre+}$ mice and n = 8/8 for the "no tamoxifen" group and 5/4 for the "tamoxifen" group, subjected to NOX and HOX, respectively in *Ucp2*$^{flox/flox,\ iSmaCre-}$ mice). (I-L), Fulton index, RVSP, SAP, LVSP in tamoxifen-treated and non-treated *Ucp2*$^{flox/flox,\ iSmaCre+}$ and *Ucp2*$^{flox/flox,\ iSmaCre-}$ mice during NOX. *p<0.05, **p<0.01, ***p<0.001 for comparison as indicated. Data were analyzed by two-way ANOVA with Tukey's multiple comparisons test. Data are shown as mean ± SEM. Two-way analysis showed significant differences of RVSP comparing genotype (with or without tamoxifen) and treatment (NOX/HOX) in *Ucp2*$^{flox/flox,\ iSmaCre+}$ mice.

3.4.5. Morphological heart changes in *Ucp2*$^{flox/flox,\ iSmaCre}$ mice

Echocardiographic measurements illustrated no significant difference of RVID in tamoxifen-treated *Ucp2*$^{flox/flox,\ iSmaCre+}$ mice compared to mice without induction of knockout under NOX (Figure 30E). HOX induced a significant increase in RVID in mice without induction of knockout; however, RVID was decreased in SMC-specific *Ucp2* knockout mice compared to non-tamoxifen treated *Ucp2*$^{flox/flox,\ iSmaCre+}$ mice under HOX (Figure 30A, C). RVWT showed no significant difference between the strains or treatment with HOX (Figure 30B, D, and F).

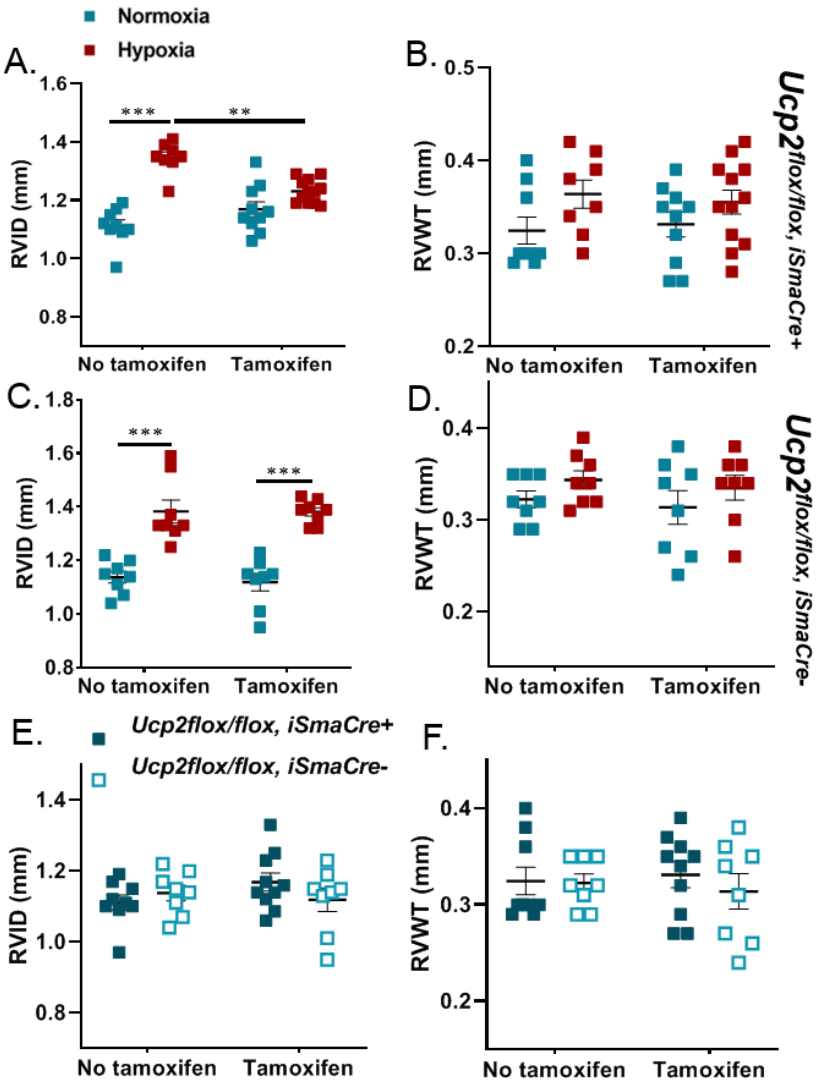

Figure 30. Morphological changes in in *Ucp2*$^{flox/flox,\ iSmaCre+}$ and *Ucp2*$^{flox/flox,\ iSmaCre-}$ mice with or without tamoxifen treatment after chronic hypoxic or normoxic exposure

(A, C), Echocardiographic measurement of the right ventricular internal diameter (RVID), and (B, D), right ventricular wall thickness (RVWT) in tamoxifen-treated and non-treated *Ucp2*$^{flox/flox,\ iSmaCre+}$ and *Ucp2*$^{flox/flox,\ iSmaCre-}$ mice after exposure to normoxia (NOX; 21% O_2, 5% CO_2, rest N_2)/chronic hypoxia (HOX; 10% O_2, 5% CO_2, rest N_2) for 28 days; n = 9/10 for the "no tamoxifen" group and 8/12 for the "tamoxifen" group, subjected to NOX and HOX, respectively in *Ucp2*$^{flox/flox,\ iSmaCre+}$ and n = 8/8 for the "no tamoxifen" group and 8/8 for the "tamoxifen" group, subjected to NOX and HOX, respectively in *Ucp2*$^{flox/flox,\ iSmaCre-}$ mice. (E, F), RVID and RVWT in tamoxifen-treated and non-treated *Ucp2*$^{flox/flox,\ iSmaCre+}$ and *Ucp2*$^{flox/flox,\ iSmaCre-}$ mice during NOX. **p<0.01, ***p<0.001, for comparison as indicated. Data were analyzed by two-way ANOVA with Tukey's multiple comparisons test. Data are shown as mean ± SEM.

3.4.6. Heart function changes in *Ucp2*$^{flox/flox,\ iSmaCre}$ mice

Under NOX, tamoxifen treatment did not change the level of TAPSE as marker for right heart function (Figure 31A, D, and G). However, TAPSE was decreased after hypoxic exposure, albeit to a lower degree in tamoxifen-treated *Ucp2*$^{flox/flox,\ iSmaCre+}$ mice compared to non-tamoxifen treated *Ucp2*$^{flox/flox,\ iSmaCre+}$ mice (Figure 31A). CI as a marker for global heart function was attenuated in SMC-specific *Ucp2* knockout mice as well as mice without induction of the knockout in HOX (Figure 31B, E).

Under normoxic conditions, there was a significant decrease in the ratio of pulmonary artery acceleration time to ejection time (PAT/PET), another parameter indicating increased PVR, in tamoxifen-treated *Ucp2*$^{flox/flox,\ iSmaCre+}$ mice compared to mice without induction of knockout (Figure 31C, I). After hypoxic exposure PAT/PET decreased in non-tamoxifen treated *Ucp2*$^{flox/flox,\ iSmaCre+}$ mice, as marker of PH (Figure 31C). The hypoxic and normoxic responses were not affected in *Ucp2*$^{flox/flox,\ iSmaCre-}$ mice by treatment with tamoxifen (Figure 31D, E, and F). Echocardiography measurements were performed by Dr. Akylbek Sydykov.

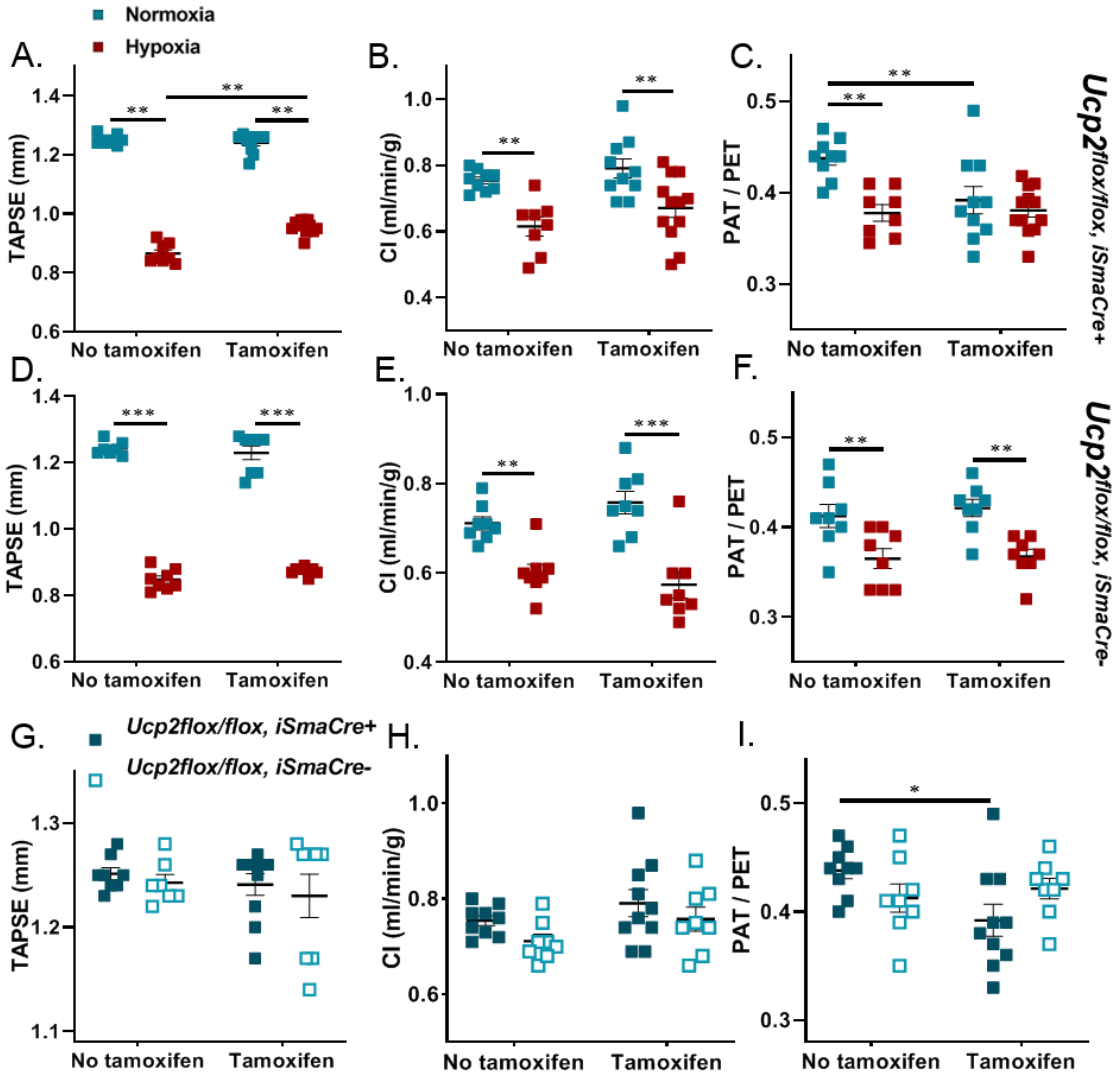

Figure 31. Heart function changes in *Ucp2*$^{flox/flox,\ iSmaCre+}$ and *Ucp2*$^{flox/flox,\ iSmaCre-}$ mice with or without tamoxifen treatment after chronic hypoxic or normoxic exposure

(A, D), Echocardiographic measurement of tricuspid annular plane systolic excursion (TAPSE), (B, E), cardiac index (CI), and (C, F), the ratio of pulmonary artery acceleration time to ejection time (PAT/PET) in tamoxifen-treated and non-treated *Ucp2*$^{flox/flox,\ iSmaCre+}$ and *Ucp2*$^{flox/flox,\ iSmaCre-}$ mice after exposure to normoxia (NOX; 21% O_2, 5% CO_2, rest N_2)/chronic hypoxia (HOX; 10% O_2, 5% CO_2, rest N_2) for 28 days; n = 8/10 for the "no tamoxifen" group and 8/12 for the "tamoxifen" group, subjected to NOX and HOX, respectively in *Ucp2*$^{flox/flox,\ iSmaCre+}$ and n = 8/8 for the "no tamoxifen" group and 8/8 for the "tamoxifen" group, subjected to NOX and HOX, respectively in *Ucp2*$^{flox/flox,\ iSmaCre-}$ mice. (G-I), TAPSE, CI, and PAT/PET in tamoxifen-treated and non-treated *Ucp2*$^{flox/flox,\ iSmaCre+}$ and *Ucp2*$^{flox/flox,\ iSmaCre-}$ mice during NOX. *p<0.05, **p<0.01, ***p<0.001 for comparison as indicated. Data were analyzed by two-way ANOVA with Tukey's multiple comparisons test. Data are shown as mean ± SEM.

3.4.7. Pulmonary vascular remodeling in *Ucp2*$^{flox/flox,\ iSmaCre}$ mice

Pulmonary vascular remodeling was increased after hypoxic exposure in *Ucp2*$^{flox/flox,\ iSmaCre+}$ mice with and without tamoxifen treatment, characterized by a higher portion of fully muscularized vessels and less non-muscularized vessels after hypoxic exposure (Figure 32A). However, there was no difference in the level of muscularization between SMC-specific *Ucp2* knockout and mice without induction of knockout in NOX (Figure 32A, B).

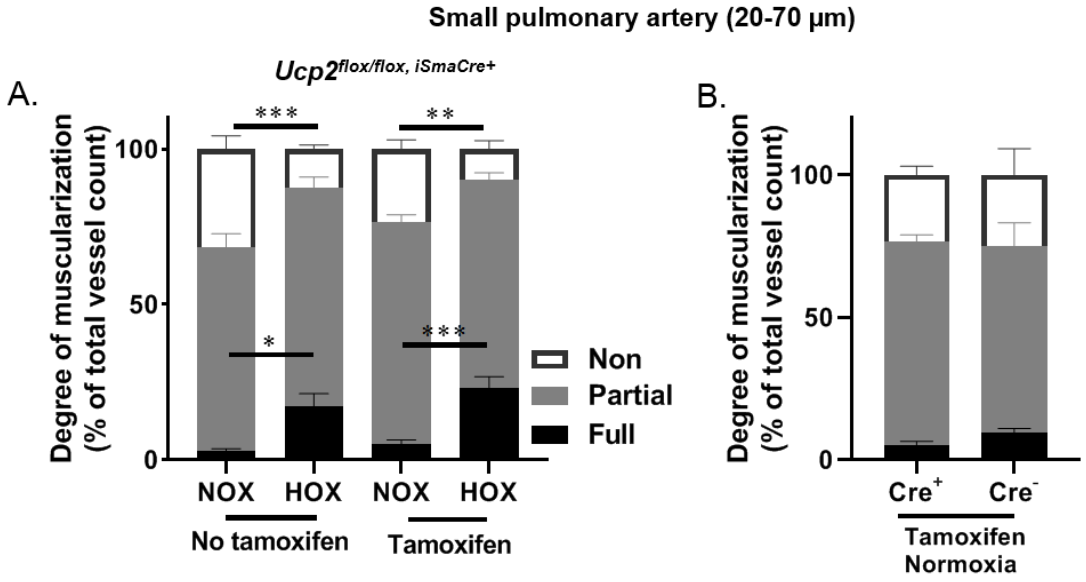

Figure 32. Pulmonary vascular remodeling in tamoxifen-treated *Ucp2*$^{flox/flox,\ iSmaCre}$ mice after exposure to NOX and chronic HOX

(A, B), Histological analysis of the pulmonary vasculature in tamoxifen-treated and non-treated *Ucp2*$^{flox/flox,\ iSmaCre+}$ mice after exposure to normoxia (NOX; 21% O_2, 5% CO_2, rest N_2)/chronic hypoxia (HOX; 10% O_2, 5% CO_2, rest N_2) for 28 days; n = 6/5 for the "no tamoxifen" group and 11/6 for the "tamoxifen" group, subjected to NOX and HOX, respectively in *Ucp2*$^{flox/flox,\ iSmaCre+}$ and n = 3 for the "tamoxifen" group, subjected to NOX in *Ucp2*$^{flox/flox,\ iSmaCre-}$. The portion of non-muscularized (none), partially muscularized (partially), and fully muscularized (fully) vessels were analyzed as percentage of the total vessel count, for vessels with an outer diameter of 20–70 µM. *p<0.05, **p<0.01, ***p<0.001 for comparison as indicated. Data were analyzed by two-way ANOVA with Tukey's multiple comparisons test as mean ± SEM.

4. Discussion

4.1. Mitochondrial ROS in acute O_2 sensing and signaling of the pulmonary vasculature

Numerous mechanisms are activated by HOX to adapt cells to low O_2 availability. HIF stabilization and signaling plays a prominent role in chronic HOX. However, the exact mechanisms underlying sensing of acute HOX and the role of factors regulating HIF signaling are still under debate. Alveolar HOX can be sensed by mitochondria located in PASMC, but the molecular mechanisms underlying O_2 sensing are still not elucidated [283]. Low alveolar O_2 tension results in the acute physiologic response of pulmonary vasoconstriction, called HPV. However, chronic exposure leads to pathological pulmonary vascular remodeling. For both responses, a contribution of mitochondrial ROS release, $[Ca^{2+}]_i$, and inhibition of K^+ channels has been suggested [284-286].

However, the exact role of ROS (originating from C I and/or III of the METC) in triggering HPV and the development of PH is still controversial [287-290]. In very early studies, Schumacker et al. showed that exposing a human cell line (hepatoma Hep3B) to low O_2 levels leads to higher ROS levels, but this reaction was absent in cells depleted of mitochondrial DNA (ρ0 cells), suggesting a crucial role of mitochondria for the generation of ROS in response to low PO_2 [98, 291].

The crucial role of ROS for HPV and PH has been demonstrated in several studies, which led to two different hypotheses: 1. The redox hypothesis suggests that decreased ROS in acute HOX leads to HPV and PH, and, 2. the ROS hypothesis suggests increased ROS as a trigger for HPV and PH [235]. In support of the first hypothesis, Archer et al. showed lower ROS levels in isolated rat lungs exposed to HOX [95, 292]. However, further studies with other methods of measuring ROS demonstrated that ROS were increased in acute HOX in mouse PASMC [293, 294]. Furthermore, Weissmann et al. found an increase in intravascular superoxide concentration of isolated mouse and rabbit lungs during acute hypoxic ventilation [295]. In addition, because the increase in ROS production induced by HOX was abrogated by the downregulation of the RISP of CIII, it has been suggested that ROS release from mitochondrial CIII could be the essential step in hypoxic signaling [296, 297].

The results from the present study support the hypothesis of increased ROS originating from complex III as a trigger for HPV by showing that inhibition of mitochondrial ROS and

bypassing complex III in the *Aox*^{tg} mouse model inhibited the HOX-induced increase in superoxide release and HPV. However, chronic HOX-induced PH was not affected in *Aox*^{tg} mice, challenging the role of mitochondrial ROS in chronic HOX-induced PH.

4.2. Effect of mitochondrial ROS inhibitors on HPV

A variety of inhibitors specific for mitochondrial ROS release were used in the present study, such as the mitochondria-targeted, superoxide dismutase mimetic MitoTempo, the more general antioxidant SKQ1, and S3QEL2, which inhibits ROS release from CIII [298]. All of these substances suppressed HPV in isolated, perfused, and ventilated mouse lungs without affecting the normoxic tone. HOX-independent vasoconstrictive stimuli (U46619 and KCl) were only affected by MitoTempo, however, especially KCl only at higher concentrations than they inhibited HPV. Altogether, these investigations confirmed the essential role of ROS from mitochondria and particularly CIII for hypoxic signaling in the pulmonary vasculature [299]. These investigations thus support the previous studies showing an increase in ROS release during acute HOX. Discrepant findings on HOX-induced ROS release in the past may be related to the limitations of techniques for ROS measurements, which include ESR spectroscopy, the cytochrome c reduction assay, detection of products of superoxide by high-performance liquid chromatography [300], and ROS-sensitive fluorescent dyes [301]. Primarily fluorescent dyes have been used in the past and are limited by false augmentation of the fluorescence intensity [302].

Previous studies on the effect of antioxidants on the pulmonary vasculature during HOX showed inhibition of HPV by an extracellular O_2 scavenger in isolated, perfused, and ventilated rabbit lungs [101]. Furthermore, overexpression of GP_X and catalase, which act as an antioxidant to convert H_2O_2 to water, could also decrease HOX-induced $[Ca^{2+}]i$ levels [303]. Another study supported the importance of mitochondrial superoxide by showing decreased HOX-induced ROS signaling in the presence of SOD2, which is located in the mitochondrial matrix [97]. However, most previous experiments were limited by the fact that the antioxidants either did not specifically target mitochondria and/or did not specifically inhibit superoxide release. The present study overcame these limitations by using mitochondria-targeted antioxidants or superoxide mimetics and the small molecule S3QEL2, which was shown to specifically inhibit superoxide release from CIII of the METC.

Based on these findings of ROS inhibitors in HPV, the genetically modified mouse models were used to gain deeper insight into the mechanism of acute HOX-induced superoxide release. First, the study used a mouse model to bypass electron flow at CIII when the METC is blocked distal to the Q cycle. The role of HOX-induced inhibition of the METC for superoxide release could be elucidated in this model. Second, the study used a mouse model with a lung-specific isoform of COX4 with hitherto unknown function but a potential regulatory role for ROS.

4.3. The effect of *Aox* expression on the acute hypoxic response of the pulmonary vasculature

AOX, an inner mitochondrial membrane protein, does not exist in mammals and can prevent the consequences of mitochondrial chain inhibition distal of CI/II. AOX protects the mitochondrial function in plants exposed to high ATP levels during daylight when the METC is inhibited [304, 305]. This protein can be expressed safely in mice [204, 218] and provides a bypass in the METC to transfer electrons from the highly reduced Q pool [207, 306] to O_2. The activity of AOX is high in the presence of a highly reduced Q pool in the METC [306] and, thus, may be activated in HOX. Furthermore, there is evidence that AOX plays a role in lowering mitochondrial membrane potential and superoxide production. Against the background of the importance of CIII for hypoxic signaling in PASMC [307], it was hypothesized that expression of *Aox* in mice, thereby bypassing CIII, might lower the HOX-induced superoxide release and hypoxic signaling.

The present study showed that bypassing CIII during acute HOX by *Aox* expression inhibited HPV and HOX-induced responses in PASMC but not the HOX-independent vasoconstriction induced by U46619. Importantly, inhibition of AOX by n-PG restored HPV in Aox^{tg} mouse lungs. Moreover, the study showed that *Aox* expression inhibited cyanide induced pulmonary vasoconstriction, suggesting that peripheral pharmacological inhibition of CIV partially mimics HOX-induced effects. Thus, electron accumulation and superoxide release at CIII may underlie HPV. With regard to cyanide, it was previously shown that mice expressing *Aox* were resistant to the poisoning effects of systemic administration of potassium cyanide [308]. These findings prove that the METC is essential for O_2 sensing in PASMC and suggest that inhibition of CIV can be the primary step in acute hypoxic

signaling in the lung, resulting in HPV. Previously, it has been suggested that CIV may act as a primary O_2 sensor in HPV. However, the high O_2 affinity of CIV made it unlikely to act as an O_2 sensor in mild HOX that triggers HPV [309]. Nevertheless, Sommer et al. have shown previously that the METC of PASMC is mildly inhibited at O_2 concentrations sufficient to induce hypoxic responses in PASMC [309]. Inhibition of CIV may cause electron accumulation and increased reduction of the Q pool, which, in turn, triggers ROS production from CIII, inhibition of potassium channels, cellular membrane depolarization, and an increase in cytosolic calcium [44, 310]. In *Aox*^{tg} mice, increased reduction of the Q pool could cause its activation and subsequent bypassing of CIII, thus preventing ROS release from CIII.

In support of this hypothesis, ESR measurements showed that AOX in PASMC was able to prevent the HOX-induced superoxide release. In accordance with our study, *Aox* expression was shown to inhibit ROS production in the mouse brain [311]. Similarly, AOX has previously been shown to decrease mitochondrial ROS production under various conditions in plants [204, 308]. For instance, AOX has been found to provide resistance to oxidative stress in fungi [312], as well as pro-oxidant-, antimycin A-, and cold-induced ROS production in plants [207, 313-316]. In addition, our data are in line with the previous investigation, showing that *Aox* suppression in tobacco cells led to an increase in ROS production, whereas *Aox* overexpression in these cells could suppress the increase [317]. Moreover, another study illustrated that AOX suppression could enhance the H_2O_2 level in plant mitochondria [316].

Our previous data with S3QEL, a ROS inhibitor, suggest that ROS originate from CIII. However, the AOX results show that ROS from CI might also play a role, as AOX activation will inhibit electron accumulation at CI and CII. In this regard, a decrease in ROS production from CI via an increase in the activity of AOX was shown [318]. However, although it has been suggested that HPV is triggered by decreased ROS release from CI, there are no reports showing that increased ROS release from CI may cause HPV, thus it seems more likely that AOX works via ROS inhibition at CIII than at CI.

In addition to increasing the reduction of the Q pool, HOX may also promote ROS release by causing mitochondrial hyperpolarization. In this regard, the previous investigations and the current study detected mitochondrial hyperpolarization as a response to acute HOX in PASMC by JC1 measurement [319, 320]. Currently, the mechanism by which HOX causes hyperpolarization despite inhibition of CIV remains unclear. It was shown previously that

inhibition of COX by nitric oxide also could result in concomitant mitochondrial hyperpolarization [321].

One must consider the possible limitations of JC1. Numerous investigations have shown that MMP can be measured using different fluorescent membrane-permeable cationic dyes such as Rhod123, tetramethylrho-daminemethyl ester (TMRM), tetramethylrho-damineethyl ester (TMRE), DiOC6 (3,3´-dihexyloxacarbocyanine iodide), and JC1. However, the most commonly used fluorescent dyes are JC1 and TMRM [322]. JC1 is a ratiometric probe that is used as an indicator for MMP by measuring the ratio of the green/red (530/590 nm) emission. Despite the reliability of JC1 for assessing MMP in intact cells [323], including cardiomyocytes [324] and spermatozoa [325], it has been shown to be harmful to mitochondria in high concentration [326]. Nevertheless, we found that *Aox* overexpression inhibits not only ROS release but also hypoxia-induced mitochondrial hyperpolarization. This effect can be expected, as AOX enables the bypassing of CIII and CIV, which are the main proton-pumping complexes [215, 218, 273].

In contrast to our findings, another study showed mitochondrial membrane depolarization and an increase in ROS release during low cellular O_2 levels in human PASMC [191]. However, it is generally accepted that mitochondrial hyperpolarization promotes ROS release [104]. In this regard, studies on isolated mitochondria demonstrated that increased MMP is associated with increased ROS levels [327]. Furthermore, Chandel et al. illustrated that the genetic reconstitution of the MMP in mitochondrial DNA-depleted cells was important for the restoration of ROS increase during the hypoxic response [328]. Besides ROS, AOX may also inhibit a HOX-induced accumulation of NADH. In this regard, a decrease of cellular redox state, and, therefore, the increase of NADH/NAD, was suggested to inhibit K_V channels and contribute to HPV [329]. The data of the present study cannot exclude that this mechanism also contributes to the effects of *Aox* expression on HPV; however, the results on ROS inhibition demonstrate that ROS are essential for HPV, even if the NADH/NAD ratio contributes to acute hypoxic signaling.

In summary, these data represented the first clear-cut demonstration that the inhibition of CIV is the primary step in acute hypoxic signaling in the lung, resulting in HPV, and that increased ROS release from mitochondria may act as a mediator.

With regard to downstream signaling, we observed an attenuation but not a complete inhibition of HOX-induced cellular membrane depolarization in *Aox*-overexpressing cells compared to WT PASMC mouse. As cellular membrane depolarization is a critical step for activation of L-type calcium channels and the subsequent intracellular calcium increase that

triggers HPV, the cellular membrane depolarization in *Aox*-overexpressing cells may not reach the level needed to activate L-type calcium channels (the threshold for activation of voltage-dependent calcium channels is at a membrane potential between –30 and –20 mV in mouse PASMC [330]. We thus tested the hypothesis that shifting cellular membrane potential to more depolarized levels by application of KCl would restore HPV.

Indeed, application of KCl to isolated *Aox*-overexpressing lungs restored HPV, which indicates that 1) mitochondria lie upstream of potassium channel inhibition in HPV and 2) other O_2 sensors, intact in *Aox*-overexpressing cells, contribute to HOX-induced cellular membrane depolarization. The mechanism behind the partial depolarization in Aox^{tg} PASMC remains to be identified. Other O_2-sensitive components in PASMC have been suggested, including HOX-sensitive potassium channels, ROS alteration by NADPH oxidases, and the cellular redox state [104, 331].

In summary, these results show the relevance of mitochondria and mitochondrial ROS for acute O_2 sensing.

4.4. The effect of *Aox* expression on the chronic hypoxic response of the pulmonary vasculature

The acute and chronic responses of the pulmonary vasculature to HOX have been assumed to involve similar primary mechanisms and to share regulatory components. However, in the present investigations, the development of chronic HOX-induced PH was not different in WT and *Aox*-overexpressing mice determined by RVSP, right heart remodeling, and pulmonary vascular remodeling. These data support the hypothesis that the signaling pathways underlying acute and chronic hypoxic responses are different in the pulmonary vasculature and that mitochondrial ROS may not affect chronic HOX-induced PH. In accordance with these results, the application of MitoQ, a mitochondria-targeted antioxidant, in a previous study inhibited acute but not chronic hypoxic signaling [332]. Moreover, ROS were decreased in PASMC in chronic, as opposed to acute HOX [332, 333].

In this regard, both an increase and a decrease of mitochondrial ROS in chronic HOX, affecting PASMC proliferation and pulmonary vascular remodeling, have been suggested [332].

Some reports suggest that mitochondrial ROS may stabilize HIF-1α during chronic HOX [334, 335], whilst others found no such effect [336]. The fact that AOX did not inhibit

chronic HOX-induced PH, nor interfere with HOX-induced stabilization of HIF-1α [337], may help to resolve these discordant findings, recasting the acute and chronic effects of HOX in lungs as two fundamentally different processes. For example, non-mitochondrial ROS sources, such as NADPH oxidases, may be of greater importance in the pulmonary vasculature under chronic hypoxic conditions.

In summary, these data indicate that respiratory inhibition (especially inhibition of CIV) is an upstream event in HPV signaling and substantiate that mitochondrial superoxide derived from CIII is essential for acute HPV. Next, the underlying mechanism of HOX-induced ROS release was investigated. To this end, *Cox4i2*-deficient mice were used because 1) *Cox4i2* is highly expressed in the mammalian lung [227], 2) *Cox4i2* expression is highly induced by HOX [230], and 3) COX4i2 had been described as regulating mitochondrial ROS release in astrocytes [269, 270].

4.5. Mitochondrial COX4i2 is essential for ac ute pulmonary O_2 sensing

The COX is a multiprotein complex and the terminal METC enzyme. It is composed of 3 mitochondrial DNA-encoded catalytic subunits (COX1, 2, and 3) and 10 regulatory subunits encoded by the nuclear DNA [338]. This enzyme catalyzes the transfer of electrons from cytochrome c to O_2. During that process, four protons are translocated across the mitochondrial membrane to generate the mitochondrial membrane potential for ATP synthesis.

Subunit 4 of COX plays an important role in COX assembly [339] and acts as a sensor to adjust COX activity to cellular energy demand by suppression of COX activity at high ATP levels [223, 224]. COX4 exists in two isoforms, but the functional differences of these isoforms are unclear. Hüttemann et al. showed that COX4i2 is preferentially expressed in SMC of the lung and, to a lesser degree, also in the fetal lung [233, 340]. Furthermore, *Cox4i2* is highly expressed in the placenta [341] which is another organ that shows hypoxic vasoconstriction. It was previously suggested that the expression of *Cox4i2* is upregulated and that of *Cox4i1* downregulated during chronic HOX [230]. Furthermore, the absence of COX4i2 decreased the activity of COX and ATP levels in the lung [342].

The present study now shows that *Cox4i2* deficiency results in the absence of HPV and the HOX-induced increase of superoxide. These investigations, for the first time, provide insight into the physiological function of COX4i2 in the pulmonary vasculature and show that

COX4i2 acts as a crucial component in the O_2 sensing process of the pulmonary vasculature. The genetic deficiency of *Cox4i2* also resulted in the attenuation of HOX-induced cellular membrane depolarization in PASMC. Similar to *Aox*^{tg} PASMC, however, cellular membrane depolarization was not completely abolished. In parallel to the *Aox*^{tg} mouse model, HPV could be restored in *Cox4i2* knockout mouse lungs by pre-conditioning with KCl, thereby replacing the mitochondrial portion of HOX-induced cellular membrane depolarization.

Moreover, we found that knockout of *Cox4i2* inhibited the HOX-induced increase of cellular ROS in mouse PASMC, supporting the previous findings that mitochondrial ROS act as a mediator for acute hypoxic responses in PASMC. Previous investigations also showed that *Cox4i2* knockout inhibits ROS release in astrocytes [270]. Furthermore, these experiments showed, like the AOX model, that acute HOX caused mitochondrial hyperpolarization, which was abolished in *Cox4i2* knockout PASMC. An increase in MMP promoted ROS production at CI and III [309]; thus, the lack of mitochondrial hyperpolarization in *Cox4i2* knockout PASMC may contribute to the lack of HOX-induced ROS release in *Cox4i2* knockout PASMC.

Mitochondrial ROS may interact with different ion channels of the cellular membrane to cause HOX-induced cellular membrane depolarization. HOX-induced cellular membrane depolarization in WT PASMC is sufficient to cause an influx of calcium into the cytoplasm through entry via Ca^{2+} channels, which can cause an increase in $[Ca^{2+}]i$ and subsequently HPV [309, 343]. Cogolludo et al. supported the role of ROS in this pathway by showing that potassium channel inhibition increased the tension in rat pulmonary arteries following H_2O_2 application [344]. In addition, cellular H_2O_2 can influence the hypoxic response of the K_V channels in mouse glomus and rat adrenomedullary chromaffin cells at high concentrations [345, 346]. The data of the present study support these findings, as HOX-induced cellular membrane depolarization was reduced in *Cox4i2* knockout mice, and the application of H_2O_2 could restore depolarization to levels that are sufficient to activate L-type calcium channels and increase cytosolic calcium. The importance of mitochondrial ROS from CIII for cellular membrane depolarization was confirmed by the application of S3QEL2, which inhibits mitochondrial ROS release from CIII and inhibits the HOX-induced cellular membrane depolarization [299].

In contrast, some studies showed that superoxide inhibited K_V channel activity could be rescued by treatment with SOD and catalase in rat vascular SMC [347]. Further investigations showed inhibition of K_V channels by antioxidants [348, 349]. In particular the redox hypoxthesis suggest that K_V channel inhibition is caused by decreased H_2O_2 and

increased level of reducing equivalents [350]. Thus, further studies are necessary to understand the exact role of K_V channels and its inhibition by ROS and the cellular redox state.

In summary, these experiments show that COX4i2 is a prerequisite for acute O_2 sensing of the pulmonary vasculature and essential for the HOX-induced superoxide release, which contributes to sufficient cellular membrane depolarization, leading to calcium entry into the cell and HPV.

As shown a) in the present study in the *Aox*^{tg} mouse model, b) in the present and previous studies in *Cox4i2* knockout mice, and c) in a previous study applying the mitochondrial ROS inhibitor MitoQ, mitochondrial ROS are essential for acute HPV but not chronic HOX-induced pulmonary vascular remodeling [332]. Therefore, the further experiments of this thesis focused on the role of mitochondrial ROS in non-HOX-induced pulmonary vascular remodeling and alternative mechanisms in pulmonary vascular remodeling.

4.6. The SMC-specific effect of *Ucp2* knockout on pulmonary vascular remodeling

UCPs are mitochondrial transporters assumed to regulate proton conductance under specific conditions, however this function has been challenged for UCP2. Several investigations have shown that coenzyme Q, fatty acids, glucose, retinoic acid, and superoxide can regulate *Ucp2* expression and function [254, 351, 352].

UCP2 is ubiquitously expressed in most cell types of several tissues, and currently, the molecular mechanism and physiological function of this mitochondrial protein is under debate. Several studies focused on the role of UCP2 in the regulation of cellular energy supply and ROS, as changes in the proton conductance would affect both parameters. Investigations on rat cardiomyocytes showed that the ATP production was decreased in response to *Ucp2* upregulation induced by HOX-reoxygenation [353]. In sepsis, knockdown of *Ucp2* in astrocytes increased ROS levels but recovered ATP production [354]. Overexpression of *Ucp2* in rat neuronal cells both prevented high ROS levels and increased neuronal cell survival [355]. Accordingly, ROS levels declined in correlation with *Ucp2* upregulation in *Toxoplasma gondii* infection-activated macrophages [356]. Moreover, it was reported that increased expression of *Ucp2* could decrease the harmful effect of a high-salt diet on vascular damage by decreasing the level of ROS production [357]. Additionally, mitochondrial ROS-induced cardiac muscle cell death was prevented by increased

expression of *Ucp2* [358]. In line with this, UCP2 was shown to exert a regulatory function on pancreatic cells by decreasing the cellular ROS [254, 359]. These results support the concept that UCP2 protects cells from oxidative damage by controlling ROS release and balancing the cellular energy supply, although it remains unclear if this is achieved via regulation of proton conductance or shuttling of mitochondrial substrates (e.g. pyruvate) [360] which also may affect ROS release and the MMP via changes in respiration.

Regarding PH, previous investigations showed that *Ucp2* deficient mice exhibited pulmonary vascular remodeling due to the proliferation of PASMC under baseline conditions by increased MMP and ROS release [272]. Another study proposed that *Ucp2* knockout-induced PH was related to the ability of UCP2 to enhance mitochondrial calcium entry and thereby mitochondrial respiration [361]. Interestingly, endothelial, cell-specific *Ucp2* knockout also displayed PH in a model of intermittent HOX [362]. Endothelial cells are most important in PH development; however, the exact contribution of endothelial cells vs PASMC for triggering PH is unknown. Therefore, the present study investigated the specific contribution of UCP2 in PASMC for the development of pulmonary vascular remodeling and PH. To this end, PH and RV remodeling under baseline normoxic and chronic hypoxic conditions was investigated in mice with specific, conditional knockout of *Ucp2* in SMC.

In this study, we used the CreERT2 transgenic mouse line which expresses Cre-recombinase fused to a mutated estrogen receptor under the Acta2 promoter. [363]. This line was crossed with a floxed UCP2 mouse line to induce cell-type specific, conditional knockout of *Ucp2*.

During normoxic baseline conditions, SMC-specific *Ucp2* knockout mice showed a significant decrease of PAT/PET as an echocardiographic marker for increased PVR [364]. Furthermore, fulton index was slightly increased in tamoxifen-treated $Ucp2^{flox/flox,\ iSmaCre+}$ mice compared to non-tamoxifen-treated $Ucp2^{flox/flox,\ iSmaCre+}$ mice. Most importantly, these parameters were also changed in tamoxifen-treated $Ucp2^{flox/flox,\ iSmaCre+}$ mice compared to $Ucp2^{flox/flox,\ iSmaCre-}$ mice under baseline conditions, suggesting that the effect was not due to tamoxifen feeding. Moreover, RVSP as a marker for PH was also increased in SMC-specific *Ucp2* knockout mice. These results altogether indicate an increase in PVR by *Ucp2* knockout in SMCs. However, no significant differences could be fdetected in RVWT, TAPSE or CI between tamoxifen-treated and non-treated mice or $Ucp2^{flox/flox,\ iSmaCre+}$ and $Ucp2^{flox/flox,\ iSmaCre-}$ mice in NOX. In particular, pulmonary vascular remodeling was not affected by knockdown of *Ucp2* in SMCs. One reason may be that SMC-specific *Ucp2* knockdown may affect stiffness of large pulmonary vessels or vascular pruning, which was not investigated

in this study, and thereby enhance PVR. Furthermore, a small increase in vascular wall muscularization, which may not be detected by the current histological method, could have a relevant impact on vascular resistance, which may cause changes in PAT/PET and fulton index.

With regard to the left ventricle, no differences could be detected in SAP or LVSP of SMC-specific *Ucp2* knockout mice compared to WT mice under normoxic conditions.

These data suggest that alterations in PASMC can increase right ventricular afterload, independently from other cell types. However, SMC-specific *Ucp2* knockout only showed mild alterations and no effect on pulmonary vascular remodeling, in contrast to global *Ucp2* knockout. These findings suggest that 1) other cell types interact with PASMC to induce pulmonary vascular remodeling, 2) UCP2 in non-PASMC may have a protective function with regard to pulmonary vascular remodeling, and 3) downregulation of *Ucp2* in SMC by tamoxifen treatment was possibly not achieved to a sufficient degree as compared to global constitutional knockout.

In contrast to NOX, *Ucp2* deficiency did not affect the severity of PH development after exposure to HOX. HOX may activate, in part, UCP2 dependent pathways, and thus *Ucp2*-deficiency may not have an additional effect on HOX-induced PH. Accordingly, it was shown that global *Ucp2* knockout mice have the same HOX-induced PH as WT mice [272, 365]. One common mechanism may be the downregulation of *Ucp2* in chronic HOX, as shown previously [272]. Interestingly, after hypoxic exposure RVID was less increased and TAPSE was less decreased in SMC-specific *Ucp2* knockout mice compared with mice without induction of knockout. This findings is in line with a previous study showing that a lack of *Ucp2* can protect the heart from pressure overload induced right ventricular remodeling [366]. However, it remains unclear which cell-type is responsible for this protective effect. As our mouse line expressed Cre-recombinase under the promoter of Acta2, not only SMCs but also myofibroblast/fibroblast in the heart may contribute to the effect, as Acta2 is also activated in these cell types [367].

In summary, these data support the previous findings that *Ucp2* knockout has an effect on the pulmonary vasculature and right ventricle, however, support the hypothesis that several cell-types contribute to pulmonary vascular remodeling.

5. Summary

Hypoxic pulmonary vasoconstriction (HPV) is essential to match local blood perfusion to ventilation, and thus to prevent life-threatening hypoxemia under conditions of acute alveolar hypoxia (HOX). Chronic hypoxic exposure can cause thickening of the pulmonary vascular lumen which leads to pulmonary hypertension (PH). An increase or decrease of reactive oxygen species release (ROS) from complex I (CI) and/or complex III (CIII) of the mitochondrial electron transport chain (METC) have been suggested as important mediators for the oxygen (O_2) sensing mechanism underlying both responses. This study thus used novel ROS inhibitors and genetically modified mice to investigate the effect of ROS inhibition on HPV and hypoxia-induced PH.

Mitochondrial ROS inhibitors, including MitoTempo, a mitochondria-targeted mimetic of the superoxide dismutase, SkQ1, a mitochondria-targeted antioxidant, and S3QEL, an inhibitor of superoxide release from mitochondrial CIII, inhibited HPV but only partially attenuated hypoxia-independent vasoconstriction.

Moreover, HPV was absent in mice overexpressing the alternative oxidase (*Aox*^{tg}) which is activated during inhibition of CIII or CIV of the METC and bypasses CIII thereby decreasing superoxide release. *Aox* expression in the mouse pulmonary arterial smooth muscle cell (PASMC) prevented acute HOX-induced mitochondrial hyperpolarization and superoxide release and attenuated HOX-induced cellular membrane depolarization. In contrast, chronic HOX exposure of *Aox*^{tg} and wild-type (WT) mice induced PH to a similar degree in both strains as well as stabilization of hypoxia-inducible factor-1α (HIF-1α).

Furthermore, in response to acute HOX, isolated lungs of mice with global knockout of cytochrome c oxidase complex 4 isoform 2 (*Cox4i2*), which is specifically expressed in oxygen sensing cell types and may regulate mitochondrial superoxide release, lacked HPV. *Cox4i2* deficient PASMC showed absence of the HOX-induced mitochondrial hyperpolarization and superoxide release and attenuated HOX-induced cellular membrane depolarization.

To further investigate the role of ROS for non-hypoxia induced PH development mice with SMC-specific inducible knockout of the uncoupling protein 2 (UCP2), a protein that is shown to attenuate mitochondrial ROS release, were investigated. These investigations showed that SMC-specific *Ucp2* knockout mice exhibited signs of PH in normoxic conditions, but no difference in pulmonary vascular remodeling. Interestingly, SMC-specific

Ucp2 knockout showed lower HOX-induced increase in right ventricular internal diameter (RVID) and decrease in tricuspid annular plane systolic excursion (TAPSE), although parameters characterizing HOX-induced PH were not different.

Taken together, the data presented in this work suggest that ROS release (most probably from mitochondrial complex III) is an upstream event in HPV signaling and COX4i2 is essential for acute hypoxic signaling in the pulmonary vasculature. The role of mitochondrial hyperpolarization needs to be further investigated. Most importantly, acute hypoxic signaling may depend on different mechanisms than chronic hypoxic signaling. Furthermore, *Ucp2* knockout specifically in smooth muscle α-actin expressing cells is sufficient to trigger pulmonary vascular alterations under normoxic conditions.

6. Zusammenfassung

Die hypoxische pulmonale Vasokonstriktion (HPV) ist essentiell, um die lokale alveoläre Perfusion an die alveoläre Ventilation anzupassen und damit eine lebensbedrohliche Hypoxämie bei einer akuten lokalen alveolären Hypoxie (HOX) zu verhindern. Chronische hypoxische Exposition kann durch Gefäßumbauprozesse zu einer Einengung des Lungengefäßlumens und damitpulmonaler Hypertonie (PH) führen. Eine Zunahme oder Abnahme der Freisetzung reaktiver Sauerstoffspezies (ROS) aus Komplex I (CI) und/oder Komplex III (CIII) der mitochondrialen Elektronentransportkette (METC) wurde als wichtiger Mediator für den Sauerstoff (O_2) -Sensor-Mechanismus, der beiden Antworten zugrunde liegt, vorgeschlagen. Diese Studie verwendete daher neuartige ROS-Inhibitoren und genetisch veränderte Mäuse, um die Wirkung der ROS-Inhibition auf die HPV und Hypoxie-induzierte PH zu untersuchen. Mitochondriale ROS-Inhibitoren, einschließlich MitoTempo, ein auf Mitochondrien gerichtetes Mimetikum der Superoxiddismutase, SkQ1, ein auf Mitochondrien gerichtetes Antioxidans, und S3QEL, ein Inhibitor der Superoxidfreisetzung aus mitochondrialem CIII, hemmten die HPV, jedoch nur teilweise die hypoxie-unabhängige Vasokonstriktion. Darüber hinaus fehlte die HPV in Mäusen, die die alternative Oxidase (*Aox*^{tg}) exprimierten, die während der Hemmung von CIII oder CIV der METC aktiviert wird und den Elektronenfluss an CIII umgehen kann, wodurch die Superoxidfreisetzung verringert werden kann. Die *Aox* Expression in glatten arteriellen Gefäßmuskelzellen der Maus (PASMC) verhinderte außerdem eine akute HOX-induzierte mitochondriale Hyperpolarisation und Superoxidfreisetzung und schwächte die HOX-induzierte Zellmembrandepolarisation ab. Im Gegensatz dazu induzierte die chronische HOX-Exposition von *Aox*^{tg} und Wild-typ (WT) Mäusen in beiden Stämmen in ähnlichem Maße eine PH sowie die Stabilisierung des Hypoxie-induzierbaren Faktors 1α (HIF-1 α). Isoliert perfundierte und ventilierte Lungen von Mäusen mit globalem Knockout für die Cytochrom c Oxidase Komplex 4 Isoform-2 (*Cox4i2*), die spezifisch in sauerstoffsensitiven Zellen exprimiert wird und möglicherweise die Superoxidfreisetzung reguliert, zeigten keine HPV. *Cox4i2*-defiziente PASMC zeigten keine HOX-induzierten mitochondriale Hyperpolarisation und Superoxidfreisetzung und eine abgeschwächte HOX-induzierte Zellmembrandepolarisation. Zur weiteren Untersuchung der Rolle der ROS by Hypoxie-unabhängiger PH wurden Mäuse mit induzierbarem SMC-spezifischen Knockout für das Entkopplungsproteins 2 (UCP2) untersucht, von dem gezeigt wurde, dass es die

mitochondriale ROS-Freisetzung abschwächt. Diese Untersuchungen ergaben, dass SMC-spezifische *Ucp2*-Knockout-Mäuse unter normoxischen Bedingungen Anzeichen von PH zeigten, jedoch keinen Unterschied beim Umbau der Lungengefäße. Interessanterweise zeigten SMC-spezifische *Ucp2*-Knockout Mäuse auch eine geringere durch Hypoxie induzierte Zunahme der rechtsventrikulären inneren Durchmessers (RVID) und eine Abnahme der rechtsventrikulären systolischen Funktion (repräsentiert durch die TAPSE), obwohl die Parameter, die Hypoxie-induzierte PH charakterisieren, nicht unterschiedlich waren. Zusammengenommen legen die in dieser Arbeit präsentierten Daten nahe, dass die ROS-Freisetzung (wahrscheinlich aus dem mitochondrialen CIII) ein vorgeschaltetes Ereignis bei der HPV-Signalübertragung ist und COX4i2 für die akute hypoxische Signalübertragung im Lungengefäßsystem essentiell ist. Die Rolle des mitochondrialen Membranpotentials muss noch weiter untersucht werden. Eine wichtige Beobachtung ist, dass die Signalübertragung von akuter Hypoxie sich von der Signalübertragung chronischer Hypoxie unterscheidet. Darüber hinaus ist ein *Ucp2*-Knockout spezifisch in α-Actin-exprimierenden Zellen der glatten Muskulatur ausreichend, um unter normoxischen Bedingungen Veränderungen der Lungengefäße auszulösen.

7. References

1. Petersson J, Glenny RW: **Gas exchange and ventilation-perfusion relationships in the lung**. *The European respiratory journal* 2014, **44**(4):1023-1041.
2. Sylvester JT, Shimoda LA, Aaronson PI, Ward JP: **Hypoxic pulmonary vasoconstriction**. *Physiological reviews* 2012, **92**(1):367-520.
3. Douglas CG, Haldane JS: **The regulation of the general circulation rate in man**. *The Journal of physiology* 1922, **56**(1-2):69-100.
4. Haldane J: **Respiration. New Haven**. In.: CT: Yale University Press; 1922.
5. Melarkode K, Nirmalan* M, Galvin I, Drummond GJBjoa: **Distribution of blood flow and ventilation in the lung: gravity is not the only factor**. 2007, **99**(2):300-301.
6. West JB: **JS Haldane and some of his contributions to physiology**. In: *Integration in Respiratory Control*. Springer; 2008: 9-15.
7. Sommer N, Strielkov I, Pak O, Weissmann N: **Oxygen sensing and signal transduction in hypoxic pulmonary vasoconstriction**. *The European respiratory journal* 2016, **47**(1):288-303.
8. Euler Uv, Liljestrand G: **Observations on the pulmonary arterial blood pressure in the cat**. *Acta physiologica Scandinavica* 1946, **12**(4):301-320.
9. Weissmann N, Akkayagil E, Quanz K, Schermuly RT, Ghofrani HA, Fink L, Hänze J, Rose F, Seeger W, Grimminger FJRp *et al*: **Basic features of hypoxic pulmonary vasoconstriction in mice**. 2004, **139**(2):191-202.
10. Weissmann N, Grimminger F, Walmrath D, Seeger WJRp: **Hypoxic vasoconstriction in buffer-perfused rabbit lungs**. 1995, **100**(2):159-169.
11. Lindgren L, MARSHALL C, Marshall BJAps: **Hypoxic pulmonary vasoconstriction in isolated rat lungs perfused with perfluorocarbon emulsion**. 1985, **123**(3):335-338.
12. Peake M, Harabin A, Brennan N, Sylvester JJJoAP: **Steady-state vascular responses to graded hypoxia in isolated lungs of five species**. 1981, **51**(5):1214-1219.
13. Motley HL, Cournand A, Werko L, Himmelstein A, Dresdale DJAJoP-LC: **The influence of short periods of induced acute anoxia upon pulmonary artery pressures in man**. 1947, **150**(2):315-320.
14. Dirken MN, Heemstra H: **Alveolar oxygen tension and lung circulation**. *Quarterly journal of experimental physiology (Cambridge, England)* 1948, **34**(3-4):193-211.
15. Motley HL, Cournand A, et al.: **The influence of short periods of induced acute anoxia upon pulmonary artery pressures in man**. *The American journal of physiology* 1947, **150**(2):315-320.
16. Lumb AB, Slinger P: **Hypoxic pulmonary vasoconstriction: physiology and anesthetic implications**. *Anesthesiology* 2015, **122**(4):932-946.
17. Hedenstierna G, Rothen HU: **Respiratory function during anesthesia: effects on gas exchange**. *Comprehensive Physiology* 2012, **2**(1):69-96.
18. Naeije R, Brimioulle S: **Physiology in medicine: importance of hypoxic pulmonary vasoconstriction in maintaining arterial oxygenation during acute respiratory failure**. *Critical Care* 2001, **5**(2):67-71.
19. Daoud FS, Reeves JT, Schaefer JW: **Failure of hypoxic pulmonary vasoconstriction in patients with liver cirrhosis**. *The Journal of clinical investigation* 1972, **51**(5):1076-1080.

20. Carter EP, Hartsfield CL, Miyazono M, Jakkula M, Morris KG, Jr., McMurtry IF: **Regulation of heme oxygenase-1 by nitric oxide during hepatopulmonary syndrome**. *American journal of physiology Lung cellular and molecular physiology* 2002, **283**(2):L346-353.
21. Ketabchi F, Egemnazarov B, Schermuly RT, Ghofrani HA, Seeger W, Grimminger F, Shid-Moosavi M, Dehghani GA, Weissmann N, Sommer N: **Effects of hypercapnia with and without acidosis on hypoxic pulmonary vasoconstriction**. *American journal of physiology Lung cellular and molecular physiology* 2009, **297**(5):L977-983.
22. Grimmer B, Kuebler WM: **The endothelium in hypoxic pulmonary vasoconstriction**. *Journal of Applied Physiology* 2017, **123**(6):1635-1646.
23. Brimioulle S, Vachiéry J-L, Brichant J-F, Delcroix M, Lejeune P, Naeije R: **Sympathetic modulation of hypoxic pulmonary vasoconstriction in intact dogs**. *Cardiovascular research* 1997, **34**(2):384-392.
24. Deem S, Berg JT, Kerr ME, Swenson ER: **Effects of the RBC membrane and increased perfusate viscosity on hypoxic pulmonary vasoconstriction**. *Journal of applied physiology (Bethesda, Md : 1985)* 2000, **88**(5):1520-1528.
25. Benumof JL, Wahrenbrock EA: **Dependency of hypoxic pulmonary vasoconstriction on temperature**. *Journal of applied physiology: respiratory, environmental and exercise physiology* 1977, **42**(1):56-58.
26. Lahm T, Crisostomo PR, Markel TA, Wang M, Wang Y, Weil B, Meldrum DR: **Exogenous estrogen rapidly attenuates pulmonary artery vasoreactivity and acute hypoxic pulmonary vasoconstriction**. *Shock (Augusta, Ga)* 2008, **30**(6):660-667.
27. Weir EK, López-Barneo J, Buckler KJ, Archer SL: **Acute oxygen-sensing mechanisms**. *New England Journal of Medicine* 2005, **353**(19):2042-2055.
28. Sylvester J, Shimoda LA, Aaronson PI, Ward JP: **Hypoxic pulmonary vasoconstriction**. *Physiological reviews* 2012, **92**(1):367-520.
29. Paddenberg R, König P, Faulhammer P, Goldenberg A, Pfeil U, Kummer W: **Hypoxic vasoconstriction of partial muscular intra-acinar pulmonary arteries in murine precision cut lung slices**. *Respiratory research* 2006, **7**(1):1-17.
30. Weissmann N, Grimminger F, Walmrath D, Seeger W: **Hypoxic vasoconstriction in buffer-perfused rabbit lungs**. *Respiration physiology* 1995, **100**(2):159-169.
31. Staub NC: **Site of hypoxic pulmonary vasoconstriction**. *Chest* 1985, **88**(4 Suppl):240s-245s.
32. al-Tinawi A, Krenz GS, Rickaby DA, Linehan JH, Dawson CA: **Influence of hypoxia and serotonin on small pulmonary vessels**. *Journal of applied physiology (Bethesda, Md : 1985)* 1994, **76**(1):56-64.
33. Murray TR, Chen L, Marshall BE, Macarak EJ: **Hypoxic contraction of cultured pulmonary vascular smooth muscle cells**. *Am J Respir Cell Mol Biol* 1990, **3**(5):457-465.
34. Madden JA, Vadula MS, Kurup VP: **Effects of hypoxia and other vasoactive agents on pulmonary and cerebral artery smooth muscle cells**. *American Journal of Physiology-Lung Cellular and Molecular Physiology* 1992, **263**(3):L384-L393.
35. Sham JS, Crenshaw BR, Jr., Deng LH, Shimoda LA, Sylvester JT: **Effects of hypoxia in porcine pulmonary arterial myocytes: roles of K(V) channel and endothelin-1**. *American journal of physiology Lung cellular and molecular physiology* 2000, **279**(2):L262-272.

36. Brimioulle S, Vachiery JL, Brichant JF, Delcroix M, Lejeune P, Naeije R: **Sympathetic modulation of hypoxic pulmonary vasoconstriction in intact dogs**. *Cardiovascular research* 1997, **34**(2):384-392.
37. van Heerden PV, Cameron PD, Karanovic A, Goodman MA: **Orthodeoxia--an uncommon presentation following bilateral thoracic sympathectomy**. *Anaesthesia and intensive care* 2003, **31**(5):581-583.
38. Frostell C, Fratacci M, Wain J, Jones R, Zapol W: **Inhaled nitric oxide. A selective pulmonary vasodilator reversing hypoxic pulmonary vasoconstriction**. *Circulation* 1991, **83**(6):2038-2047.
39. Bernal PJ, Leelavanichkul K, Bauer E, Cao R, Wilson A, Wasserloos KJ, Watkins SC, Pitt BR, St. Croix CM: **Nitric oxide–mediated zinc release contributes to hypoxic regulation of pulmonary vascular tone**. *Circulation research* 2008, **102**(12):1575-1583.
40. Weissmann N, Winterhalder S, Nollen M, Voswinckel R, Quanz K, Ghofrani HA, Schermuly RT, Seeger W, Grimminger F: **NO and reactive oxygen species are involved in biphasic hypoxic vasoconstriction of isolated rabbit lungs**. *American Journal of Physiology-Lung Cellular and Molecular Physiology* 2001, **280**(4):L638-L645.
41. Wang L, Yin J, Nickles HT, Ranke H, Tabuchi A, Hoffmann J, Tabeling C, Barbosa-Sicard E, Chanson M, Kwak BR: **Hypoxic pulmonary vasoconstriction requires connexin 40–mediated endothelial signal conduction**. *The Journal of clinical investigation* 2012, **122**(11):4218-4230.
42. Dunham-Snary KJ, Wu D, Sykes EA, Thakrar A, Parlow LR, Mewburn JD, Parlow JL, Archer SL: **Hypoxic pulmonary vasoconstriction: from molecular mechanisms to medicine**. *Chest* 2017, **151**(1):181-192.
43. Talbot NP, Balanos GM, Dorrington KL, Robbins PA: **Two temporal components within the human pulmonary vascular response to∼ 2 h of isocapnic hypoxia**. *Journal of applied physiology* 2005, **98**(3):1125-1139.
44. Sommer N, Pak O, Schörner S, Derfuss T, Krug A, Gnaiger E, Ghofrani H, Schermuly R, Huckstorf C, Seeger W: **Mitochondrial cytochrome redox states and respiration in acute pulmonary oxygen sensing**. *European Respiratory Journal* 2010, **36**(5):1056-1066.
45. Bindslev L, Jolin A, Hedenstierna G, Baehrendtz S, Santesson J: **Hypoxic Pulmonary Vasoconstriction in the Human LungEffect of Repeated Hypoxic Challenges during Anesthesia**. *Anesthesiology: The Journal of the American Society of Anesthesiologists* 1985, **62**(5):621-625.
46. Carlsson ÅJ, Bindslev L, Santesson J, Gottlieb I, Hedenstierna G: **Hypoxic pulmonary vasoconstriction in the human lung: the effect of prolonged unilateral hypoxic challenge during anaesthesia**. *Acta anaesthesiologica scandinavica* 1985, **29**(3):346-351.
47. Motley HL, Cournand A, Werko L, Himmelstein A, Dresdale D: **The influence of short periods of induced acute anoxia upon pulmonary artery pressures in man**. *American Journal of Physiology-Legacy Content* 1947, **150**(2):315-320.
48. Weissmann N, Akkayagil E, Quanz K, Schermuly RT, Ghofrani HA, Fink L, Hanze J, Rose F, Seeger W, Grimminger F: **Basic features of hypoxic pulmonary vasoconstriction in mice**. *Respiratory physiology & neurobiology* 2004, **139**(2):191-202.
49. Kang TM, Park MK, Uhm D-Y: **Characterization of hypoxia-induced [Ca^{2+}] i rise in rabbit pulmonary arterial smooth muscle cells**. *Life sciences* 2002, **70**(19):2321-2333.

50. Wiener CM, Sylvester J: **Effects of glucose on hypoxic vasoconstriction in isolated ferret lungs**. *Journal of Applied Physiology* 1991, **70**(1):439-446.
51. Muñoz-Sánchez J, Chánez-Cárdenas ME: **A review on hemeoxygenase-2: focus on cellular protection and oxygen response**. *Oxidative medicine and cellular longevity* 2014, **2014**.
52. Bevilacqua E, Gomes SZ, Lorenzon AR, Hoshida MS, Amarante-Paffaro AM: **NADPH oxidase as an important source of reactive oxygen species at the mouse maternal–fetal interface: putative biological roles**. *Reproductive biomedicine online* 2012, **25**(1):31-43.
53. Collin F: **Chemical basis of reactive oxygen species reactivity and involvement in neurodegenerative diseases**. *International journal of molecular sciences* 2019, **20**(10):2407.
54. Hernández-Reséndiz S, Buelna-Chontal M, Correa F, Zazueta C: **Oxidative stress and mitochondrial dysfunction in cardiovascular diseases**. *Oxidative Stress and Diseases* 2012:157.
55. Yang S, Ma H-W, Yu L, Yu C-A: **On the Mechanism of Quinol Oxidation at the QP Site in the Cytochrome bc1 Complex STUDIED USING MUTANTS LACKING CYTOCHROME bL OR bH**. *Journal of Biological Chemistry* 2008, **283**(42):28767-28776.
56. Skulachev VP: **Uncoupling: new approaches to an old problem of bioenergetics**. *Biochimica et biophysica acta* 1998, **1363**(2):100-124.
57. Chance B, Williams GJJoBC: **Respiratory enzymes in oxidative phosphorylation III. The steady state**. 1955, **217**(1):409-428.
58. Halliwell B, Gutteridge JM: **Role of free radicals and catalytic metal ions in human disease: an overview**. *Methods in enzymology* 1990, **186**:1-85.
59. Cadenas E, Davies KJ: **Mitochondrial free radical generation, oxidative stress, and aging**. *Free radical biology and medicine* 2000, **29**(3-4):222-230.
60. Lenaz G: **The mitochondrial production of reactive oxygen species: mechanisms and implications in human pathology**. *IUBMB life* 2001, **52**(3- 5):159-164.
61. Starkov AA, Fiskum G, Chinopoulos C, Lorenzo BJ, Browne SE, Patel MS, Beal MF: **Mitochondrial α-ketoglutarate dehydrogenase complex generates reactive oxygen species**. *Journal of Neuroscience* 2004, **24**(36):7779-7788.
62. Tretter L, Adam-Vizi V: **Generation of reactive oxygen species in the reaction catalyzed by α-ketoglutarate dehydrogenase**. *Journal of Neuroscience* 2004, **24**(36):7771-7778.
63. Mittal M, Roth M, Konig P, Hofmann S, Dony E, Goyal P, Selbitz AC, Schermuly RT, Ghofrani HA, Kwapiszewska G *et al*: **Hypoxia-dependent regulation of nonphagocytic NADPH oxidase subunit NOX4 in the pulmonary vasculature**. *Circulation research* 2007, **101**(3):258-267.
64. Hartney T, Birari R, Venkataraman S, Villegas L, Martinez M, Black SM, Stenmark KR, Nozik-Grayck E: **Xanthine oxidase-derived ROS upregulate Egr-1 via ERK1/2 in PA smooth muscle cells; model to test impact of extracellular ROS in chronic hypoxia**. *PloS one* 2011, **6**(11):e27531.
65. Zangar RC, Davydov DR, Verma S: **Mechanisms that regulate production of reactive oxygen species by cytochrome P450**. *Toxicology and applied pharmacology* 2004, **199**(3):316-331.
66. Cho KJ, Seo JM, Kim JH: **Bioactive lipoxygenase metabolites stimulation of NADPH oxidases and reactive oxygen species**. *Molecules and cells* 2011, **32**(1):1-5.

67. Satoh M, Fujimoto S, Haruna Y, Arakawa S, Horike H, Komai N, Sasaki T, Tsujioka K, Makino H, Kashihara N: **NAD(P)H oxidase and uncoupled nitric oxide synthase are major sources of glomerular superoxide in rats with experimental diabetic nephropathy**. *American journal of physiology Renal physiology* 2005, **288**(6):F1144-1152.
68. Choi TG, Kim SS: **Physiological Functions of Mitochondrial Reactive Oxygen Species**. In: *Free Radical Medicine and Biology*. IntechOpen; 2019.
69. Kowaltowski AJ, de Souza-Pinto NC, Castilho RF, Vercesi AE: **Mitochondria and reactive oxygen species**. *Free Radical Biology and Medicine* 2009, **47**(4):333-343.
70. Bindoli A, Fukuto JM, Forman HJJA, signaling r: **Thiol chemistry in peroxidase catalysis and redox signaling**. 2008, **10**(9):1549-1564.
71. Day BJ: **Catalase and glutathione peroxidase mimics**. *Biochemical pharmacology* 2009, **77**(3):285-296.
72. Halliwell B: **Antioxidant defence mechanisms: From the beginning to the end (of the beginning)**. *Free Radical Research* 1999, **31**(4):261-272.
73. López-Barneo J, González-Rodríguez P, Gao L, Fernández-Agüera MC, Pardal R, Ortega-Sáenz P: **Oxygen sensing by the carotid body: mechanisms and role in adaptation to hypoxia**. *American Journal of Physiology-Cell Physiology* 2016, **310**(8):C629-C642.
74. Nurse CA, Buttigieg J, Brown S, Holloway AC: **Regulation of oxygen sensitivity in adrenal chromaffin cells**. *Annals of the New York Academy of Sciences* 2009, **1177**(1):132-139.
75. Chandel NS, Schumacker PT: **Cells depleted of mitochondrial DNA (rho0) yield insight into physiological mechanisms**. *FEBS letters* 1999, **454**(3):173-176.
76. Waypa GB, Chandel NS, Schumacker PT: **Model for hypoxic pulmonary vasoconstriction involving mitochondrial oxygen sensing**. *Circulation research* 2001, **88**(12):1259-1266.
77. Weissmann N, Voswinckel R, Tadic A, Hardebusch T, Ghofrani HA, Schermuly RT, Seeger W, Grimminger FJAjorc, biology m: **Nitric Oxide (NO)–Dependent but Not NO-Independent Guanylate Cyclase Activation Attenuates Hypoxic Vasoconstriction in Rabbit Lungs**. 2000, **23**(2):222-227.
78. Rounds S, McMurtry IFJCr: **Inhibitors of oxidative ATP production cause transient vasoconstriction and block subsequent pressor responses in rat lungs**. 1981, **48**(3):393-400.
79. Weissmann N: **Ebert N, Ahrens M, Ghofrani HA, Schermuly RT, Hanze J, Fink L, Rose F, Conzen J, Seeger W, and Grimminger F**. *Effects of mitochondrial inhibitors and uncouplers on hypoxic vasoconstriction in rabbit lungs Am J Respir Cell Mol Biol* 2003, **29**:721-732.
80. Sylvester J: **Hypoxic pulmonary vasoconstriction: a radical view**. In.: Am Heart Assoc; 2001.
81. Waypa GB, Schumacker PT: **Hypoxic pulmonary vasoconstriction: redox events in oxygen sensing**. *Journal of Applied Physiology* 2005, **98**(1):404-414.
82. Evans AM, Hardie DG, Galione A, Peers C, Kumar P, Wyatt CN: **AMP-activated protein kinase couples mitochondrial inhibition by hypoxia to cell-specific Ca^{2+} signalling mechanisms in oxygen-sensing cells**. In: *Novartis Found Symp: 2006*. Wiley Online Library: 234-252.
83. Robertson TP, Mustard KJ, Lewis TH, Clark JH, Wyatt CN, Blanco EA, Peers C, Hardie DG, Evans AM: **AMP-activated protein kinase and hypoxic pulmonary vasoconstriction**. *European journal of pharmacology* 2008, **595**(1-3):39-43.

84. Pryde KR, Hirst JJJoBC: **Superoxide Is produced by the reduced Flavin in mitochondrial complex IA single, unified mechanism that applies during both forward and reverse electron transfer**. 2011, **286**(20):18056-18065.
85. Paddenberg R, Ishaq B, Goldenberg A, Faulhammer P, Rose F, Weissmann N, Braun-Dullaeus RC, Kummer WJAJoP-LC, Physiology M: **Essential role of complex II of the respiratory chain in hypoxia-induced ROS generation in the pulmonary vasculature**. 2003, **284**(5):L710-L719.
86. Archer SL, Will JA, Weir EK: **Redox status in the control of pulmonary vascular tone**. *Herz* 1986, **11**(3):127-141.
87. Leach RM, Hill HM, Snetkov VA, Robertson TP, Ward JP: **Divergent roles of glycolysis and the mitochondrial electron transport chain in hypoxic pulmonary vasoconstriction of the rat: identity of the hypoxic sensor**. *The Journal of physiology* 2001, **536**(Pt 1):211-224.
88. Archer SL, Weir EK, Reeve HL, Michelakis E: **Molecular identification of O_2 sensors and O_2-sensitive potassium channels in the pulmonary circulation**. *Advances in experimental medicine and biology* 2000, **475**:219-240.
89. Sommer N, Strielkov I, Pak O, Weissmann N: **Oxygen sensing and signal transduction in hypoxic pulmonary vasoconstriction**. *European Respiratory Journal* 2016, **47**(1):288-303.
90. Desireddi JR, Farrow KN, Marks JD, Waypa GB, Schumacker PT: **Hypoxia increases ROS signaling and cytosolic Ca^{2+} in pulmonary artery smooth muscle cells of mouse lungs slices**. *Antioxidants & redox signaling* 2010, **12**(5):595-602.
91. Archer SL, Huang J, Henry T, Peterson D, Weir EK: **A redox-based O_2 sensor in rat pulmonary vasculature**. *Circulation research* 1993, **73**(6):1100-1112.
92. Weir EK, Archer SL: **The mechanism of acute hypoxic pulmonary vasoconstriction: the tale of two channels**. *FASEB journal : official publication of the Federation of American Societies for Experimental Biology* 1995, **9**(2):183-189.
93. Michelakis ED, Hampl V, Nsair A, Wu X, Harry G, Haromy A, Gurtu R, Archer SL: **Diversity in mitochondrial function explains differences in vascular oxygen sensing**. *Circulation research* 2002, **90**(12):1307-1315.
94. Archer SL, Nelson DP, Weir EKJJoAP: **Simultaneous measurement of O_2 radicals and pulmonary vascular reactivity in rat lung**. 1989, **67**(5):1903-1911.
95. Archer SL, Huang J, Henry T, Peterson D, Weir EKJCr: **A redox-based O_2 sensor in rat pulmonary vasculature**. 1993, **73**(6):1100-1112.
96. Michelakis ED, Hampl V, Nsair A, Wu X, Harry G, Haromy A, Gurtu R, Archer SLJCr: **Diversity in mitochondrial function explains differences in vascular oxygen sensing**. 2002, **90**(12):1307-1315.
97. Waypa GB, Guzy R, Mungai PT, Mack MM, Marks JD, Roe MW, Schumacker PTJCr: **Increases in mitochondrial reactive oxygen species trigger hypoxia-induced calcium responses in pulmonary artery smooth muscle cells**. 2006, **99**(9):970-978.
98. Waypa GB, Chandel NS, Schumacker PTJCr: **Model for hypoxic pulmonary vasoconstriction involving mitochondrial oxygen sensing**. 2001, **88**(12):1259-1266.
99. Sommer N, Pak O, Schorner S, Derfuss T, Krug A, Gnaiger E, Ghofrani HA, Schermuly RT, Huckstorf C, Seeger W *et al*: **Mitochondrial cytochrome redox states and respiration in acute pulmonary oxygen sensing**. *The European respiratory journal* 2010, **36**(5):1056-1066.

100. Smith KA, Schumacker PT: **Sensors and signals: the role of reactive oxygen species in hypoxic pulmonary vasoconstriction**. *The Journal of physiology* 2019, **597**(4):1033-1043.
101. Weissmann N, Grimminger F, Voswinckel R, Conzen Jr, Seeger WJAJoP-LC, Physiology M: **Nitro blue tetrazolium inhibits but does not mimic hypoxic vasoconstriction in isolated rabbit lungs**. 1998, **274**(5):L721-L727.
102. Waypa GB, Marks JD, Guzy R, Mungai PT, Schriewer J, Dokic D, Schumacker PTJCr: **Hypoxia triggers subcellular compartmental redox signaling in vascular smooth muscle cells**. 2010, **106**(3):526.
103. Waypa GB, Marks JD, Guzy RD, Mungai PT, Schriewer JM, Dokic D, Ball MK, Schumacker PT: **Superoxide generated at mitochondrial complex III triggers acute responses to hypoxia in the pulmonary circulation**. *American journal of respiratory and critical care medicine* 2013, **187**(4):424-432.
104. Sommer N, Strielkov I, Pak O, Weissmann NJERJ: **Oxygen sensing and signal transduction in hypoxic pulmonary vasoconstriction**. 2016, **47**(1):288-303.
105. Lin MJ, Yang XR, Cao YN, Sham JS: **Hydrogen peroxide-induced Ca^{2+} mobilization in pulmonary arterial smooth muscle cells**. *American journal of physiology Lung cellular and molecular physiology* 2007, **292**(6):L1598-1608.
106. Post JM, Hume JR, Archer SL, Weir EK: **Direct role for potassium channel inhibition in hypoxic pulmonary vasoconstriction**. *The American journal of physiology* 1992, **262**(4 Pt 1):C882-890.
107. Archer SL, Huang JM, Reeve HL, Hampl V, Tolarova S, Michelakis E, Weir EK: **Differential distribution of electrophysiologically distinct myocytes in conduit and resistance arteries determines their response to nitric oxide and hypoxia**. *Circulation research* 1996, **78**(3):431-442.
108. Archer SL, Souil E, Dinh-Xuan AT, Schremmer B, Mercier JC, El Yaagoubi A, Nguyen-Huu L, Reeve HL, Hampl V: **Molecular identification of the role of voltage-gated K+ channels, Kv1.5 and Kv2.1, in hypoxic pulmonary vasoconstriction and control of resting membrane potential in rat pulmonary artery myocytes**. *The Journal of clinical investigation* 1998, **101**(11):2319-2330.
109. Waypa GB, Guzy R, Mungai PT, Mack MM, Marks JD, Roe MW, Schumacker PT: **Increases in mitochondrial reactive oxygen species trigger hypoxia-induced calcium responses in pulmonary artery smooth muscle cells**. *Circulation research* 2006, **99**(9):970-978.
110. Weigand L, Foxson J, Wang J, Shimoda LA, Sylvester JT: **Inhibition of hypoxic pulmonary vasoconstriction by antagonists of store-operated Ca^{2+} and nonselective cation channels**. *American journal of physiology Lung cellular and molecular physiology* 2005, **289**(1):L5-l13.
111. Wang J, Shimoda LA, Weigand L, Wang W, Sun D, Sylvester JT: **Acute hypoxia increases intracellular [Ca^{2+}] in pulmonary arterial smooth muscle by enhancing capacitative Ca^{2+} entry**. *American journal of physiology Lung cellular and molecular physiology* 2005, **288**(6):L1059-1069.
112. Ohe M, Ogata M, Shirato K, Takishima T: **Effects of verapamil and BAY K 8644 on the hypoxic contraction of the isolated human pulmonary artery**. *The Tohoku journal of experimental medicine* 1989, **157**(1):81-82.
113. Tucker A, McMurtry IF, Grover RF, Reeves JT: **Attenuation of hypoxic pulmonary vasoconstriction by verapamil in intact dogs**. *Proceedings of the Society for Experimental Biology and Medicine Society for Experimental Biology and Medicine (New York, NY)* 1976, **151**(3):611-614.

114. Patel AJ, Lazdunski M, Honore E: **Kv2.1/Kv9.3, a novel ATP-dependent delayed-rectifier K+ channel in oxygen-sensitive pulmonary artery myocytes**. *The EMBO journal* 1997, **16**(22):6615-6625.
115. Archer SL, Souil E, Dinh-Xuan AT, Schremmer B, Mercier J-C, El Yaagoubi A, Nguyen-Huu L, Reeve HL, Hampl V: **Molecular identification of the role of voltage-gated K+ channels, Kv1. 5 and Kv2. 1, in hypoxic pulmonary vasoconstriction and control of resting membrane potential in rat pulmonary artery myocytes**. *The Journal of clinical investigation* 1998, **101**(11):2319-2330.
116. Wang J, Juhaszova M, Rubin LJ, Yuan X-J: **Hypoxia inhibits gene expression of voltage-gated K+ channel alpha subunits in pulmonary artery smooth muscle cells**. *The Journal of clinical investigation* 1997, **100**(9):2347-2353.
117. Simonneau G, Montani D, Celermajer DS, Denton CP, Gatzoulis MA, Krowka M, Williams PG, Souza R: **Haemodynamic definitions and updated clinical classification of pulmonary hypertension**. *European Respiratory Journal* 2019, **53**(1).
118. Simonneau G, Gatzoulis MA, Adatia I, Celermajer D, Denton C, Ghofrani A, Sanchez MAG, Kumar RK, Landzberg M, Machado RF: **Updated clinical classification of pulmonary hypertension**. *Journal of the American College of Cardiology* 2013, **62**(25 Supplement):D34-D41.
119. Frost A, Badesch D, Gibbs JSR, Gopalan D, Khanna D, Manes A, Oudiz R, Satoh T, Torres F, Torbicki AJERJ: **Diagnosis of pulmonary hypertension**. 2019, **53**(1):1801904.
120. Shimoda LA, Laurie SS: **Vascular remodeling in pulmonary hypertension**. *J Mol Med (Berl)* 2013, **91**(3):297-309.
121. Machado RD, Pauciulo MW, Thomson JR, Lane KB, Morgan NV, Wheeler L, Phillips JA, 3rd, Newman J, Williams D, Galie N *et al*: **BMPR2 haploinsufficiency as the inherited molecular mechanism for primary pulmonary hypertension**. *American journal of human genetics* 2001, **68**(1):92-102.
122. Deng Z, Morse JH, Slager SL, Cuervo N, Moore KJ, Venetos G, Kalachikov S, Cayanis E, Fischer SG, Barst RJ *et al*: **Familial primary pulmonary hypertension (gene PPH1) is caused by mutations in the bone morphogenetic protein receptor-II gene**. *American journal of human genetics* 2000, **67**(3):737-744.
123. Roberts KE, McElroy JJ, Wong WP, Yen E, Widlitz A, Barst RJ, Knowles JA, Morse JH: **BMPR2 mutations in pulmonary arterial hypertension with congenital heart disease**. *The European respiratory journal* 2004, **24**(3):371-374.
124. Christman BW, McPherson CD, Newman JH, King GA, Bernard GR, Groves BM, Loyd JE: **An imbalance between the excretion of thromboxane and prostacyclin metabolites in pulmonary hypertension**. *The New England journal of medicine* 1992, **327**(2):70-75.
125. Giaid A, Saleh D: **Reduced expression of endothelial nitric oxide synthase in the lungs of patients with pulmonary hypertension**. *The New England journal of medicine* 1995, **333**(4):214-221.
126. Stewart DJ, Levy RD, Cernacek P, Langleben D: **Increased plasma endothelin-1 in pulmonary hypertension: marker or mediator of disease?** *Annals of internal medicine* 1991, **114**(6):464-469.
127. Schermuly RT, Dony E, Ghofrani HA, Pullamsetti S, Savai R, Roth M, Sydykov A, Lai YJ, Weissmann N, Seeger W *et al*: **Reversal of experimental pulmonary hypertension by PDGF inhibition**. *The Journal of clinical investigation* 2005, **115**(10):2811-2821.

128. Hecker M, Zaslona Z, Kwapiszewska G, Niess G, Zakrzewicz A, Hergenreider E, Wilhelm J, Marsh LM, Sedding D, Klepetko W *et al*: **Dysregulation of the IL-13 receptor system: a novel pathomechanism in pulmonary arterial hypertension**. *American journal of respiratory and critical care medicine* 2010, **182**(6):805-818.
129. Humbert M, Monti G, Brenot F, Sitbon O, Portier A, Grangeot-Keros L, Duroux P, Galanaud P, Simonneau G, Emilie D: **Increased interleukin-1 and interleukin-6 serum concentrations in severe primary pulmonary hypertension**. *American journal of respiratory and critical care medicine* 1995, **151**(5):1628-1631.
130. Bonnet S, Michelakis ED, Porter CJ, Andrade-Navarro MA, Thébaud B, Bonnet S, Haromy A, Harry G, Moudgil R, McMurtry MS: **An abnormal mitochondrial–hypoxia inducible factor-1α–Kv channel pathway disrupts oxygen sensing and triggers pulmonary arterial hypertension in fawn hooded rats: similarities to human pulmonary arterial hypertension**. *Circulation* 2006, **113**(22):2630-2641.
131. Piao L, Sidhu VK, Fang Y-H, Ryan JJ, Parikh KS, Hong Z, Toth PT, Morrow E, Kutty S, Lopaschuk GD: **FOXO1-mediated upregulation of pyruvate dehydrogenase kinase-4 (PDK4) decreases glucose oxidation and impairs right ventricular function in pulmonary hypertension: therapeutic benefits of dichloroacetate**. *Journal of molecular medicine* 2013, **91**(3):333-346.
132. Yu Y, Keller SH, Remillard CV, Safrina O, Nicholson A, Zhang SL, Jiang W, Vangala N, Landsberg JW, Wang J-Y: **A functional single-nucleotide polymorphism in the TRPC6 gene promoter associated with idiopathic pulmonary arterial hypertension**. *Circulation* 2009, **119**(17):2313-2322.
133. Hansmann G, Zamanian RT: **PPARγ activation: a potential treatment for pulmonary hypertension**. *Science translational medicine* 2009, **1**(12):12ps14-12ps14.
134. Morrell NW, Adnot S, Archer SL, Dupuis J, Jones PL, MacLean MR, McMurtry IF, Stenmark KR, Thistlethwaite PA, Weissmann N: **Cellular and molecular basis of pulmonary arterial hypertension**. *Journal of the American College of Cardiology* 2009, **54**(1 Supplement):S20-S31.
135. Simonneau G, Montani D, Celermajer DS, Denton CP, Gatzoulis MA, Krowka M, Williams PG, Souza RJERJ: **Haemodynamic definitions and updated clinical classification of pulmonary hypertension**. 2019, **53**(1):1801913.
136. Penaloza D, Arias-Stella J: **The heart and pulmonary circulation at high altitudes: healthy highlanders and chronic mountain sickness**. *Circulation* 2007, **115**(9):1132-1146.
137. Stenmark KR, McMurtry IF: **Vascular remodeling versus vasoconstriction in chronic hypoxic pulmonary hypertension: a time for reappraisal?** *Circulation research* 2005, **97**(2):95-98.
138. Stenmark KR, Fagan KA, Frid MG: **Hypoxia-induced pulmonary vascular remodeling: cellular and molecular mechanisms**. *Circulation research* 2006, **99**(7):675-691.
139. Durmowicz AG, Stenmark KRJPR: **Mechanisms of structural remodeling in chronic pulmonary hypertension**. 1999, **20**(11):e91-e102.
140. Pak O, Aldashev A, Welsh D, Peacock AJERJ: **The effects of hypoxia on the cells of the pulmonary vasculature**. 2007, **30**(2):364-372.
141. Zhong H, De Marzo AM, Laughner E, Lim M, Hilton DA, Zagzag D, Buechler P, Isaacs WB, Semenza GL, Simons JWJCr: **Overexpression of hypoxia-inducible factor 1α in common human cancers and their metastases**. 1999, **59**(22):5830-5835.

142. Stolze IP, Tian Y-M, Appelhoff RJ, Turley H, Wykoff CC, Gleadle JM, Ratcliffe PJJJoBC: **Genetic analysis of the role of the asparaginyl hydroxylase factor inhibiting hypoxia-inducible factor (HIF) in regulating HIF transcriptional target genes**. 2004, **279**(41):42719-42725.
143. Semenza GL: **Hypoxia-inducible factors in physiology and medicine**. *Cell* 2012, **148**(3):399-408.
144. Bruick RK, McKnight SL: **A conserved family of prolyl-4-hydroxylases that modify HIF**. *Science (New York, NY)* 2001, **294**(5545):1337-1340.
145. Epstein AC, Gleadle JM, McNeill LA, Hewitson KS, O'Rourke J, Mole DR, Mukherji M, Metzen E, Wilson MI, Dhanda A *et al*: **C. elegans EGL-9 and mammalian homologs define a family of dioxygenases that regulate HIF by prolyl hydroxylation**. *Cell* 2001, **107**(1):43-54.
146. Ivan M, Kondo K, Yang H, Kim W, Valiando J, Ohh M, Salic A, Asara JM, Lane WS, Kaelin WG, Jr.: **HIFalpha targeted for VHL-mediated destruction by proline hydroxylation: implications for O_2 sensing**. *Science (New York, NY)* 2001, **292**(5516):464-468.
147. Huang LE, Gu J, Schau M, Bunn HF: **Regulation of hypoxia-inducible factor 1α is mediated by an O_2-dependent degradation domain via the ubiquitin-proteasome pathway**. *Proceedings of the National Academy of Sciences* 1998, **95**(14):7987-7992.
148. Carroll VA, Ashcroft MJErimm: **Targeting the molecular basis for tumour hypoxia**. 2005, **7**(6):1-16.
149. Shimoda LA, Semenza GLJAjor, medicine cc: **HIF and the lung: role of hypoxia-inducible factors in pulmonary development and disease**. 2011, **183**(2):152-156.
150. Carmeliet P, Dor Y, Herbert J-M, Fukumura D, Brusselmans K, Dewerchin M, Neeman M, Bono F, Abramovitch R, Maxwell P: **Role of HIF-1α in hypoxia-mediated apoptosis, cell proliferation and tumour angiogenesis**. *Nature* 1998, **394**(6692):485.
151. Iyer NV, Kotch LE, Agani F, Leung SW, Laughner E, Wenger RH, Gassmann M, Gearhart JD, Lawler AM, Aimee YY: **Cellular and developmental control of O_2 homeostasis by hypoxia-inducible factor 1α**. *Genes & development* 1998, **12**(2):149-162.
152. Gleadle JM, Ratcliffe PJ: **Induction of hypoxia-inducible factor-1, erythropoietin, vascular endothelial growth factor, and glucose transporter-1 by hypoxia: evidence against a regulatory role for Src kinase**. *Blood* 1997, **89**(2):503-509.
153. Yu AY, Frid MG, Shimoda LA, Wiener CM, Stenmark K, Semenza GLJAJoP-LC, Physiology M: **Temporal, spatial, and oxygen-regulated expression of hypoxia-inducible factor-1 in the lung**. 1998, **275**(4):L818-L826.
154. Wiener CM, Booth G, Semenza GLJB, communications br: **In vivoexpression of mRNAs encoding hypoxia-inducible factor 1**. 1996, **225**(2):485-488.
155. Jain S, Maltepe E, Lu MM, Simon C, Bradfield CAJMod: **Expression of ARNT, ARNT2, HIF1α, HIF2α and Ah receptor mRNAs in the developing mouse**. 1998, **73**(1):117-123.
156. Semenza GL: **Regulation of mammalian O_2 homeostasis by hypoxia-inducible factor 1**. *Annual review of cell and developmental biology* 1999, **15**:551-578.
157. Huang LE, Arany Z, Livingston DM, Bunn HF: **Activation of hypoxia-inducible transcription factor depends primarily upon redox-sensitive stabilization of its α subunit**. *Journal of Biological Chemistry* 1996, **271**(50):32253-32259.

158. Holmquist L, Jögi A, Påhlman S: **Phenotypic persistence after reoxygenation of hypoxic neuroblastoma cells**. *International journal of cancer* 2005, **116**(2):218-225.
159. Li L, Madu CO, Lu A, Lu YJTobj: **HIF-1α promotes a hypoxia-independent cell migration**. 2010, **3**:8.
160. Shimoda LA, Manalo DJ, Sham JS, Semenza GL, Sylvester J: **Partial HIF-1α deficiency impairs pulmonary arterial myocyte electrophysiological responses to hypoxia**. *American Journal of Physiology-Lung Cellular and Molecular Physiology* 2001, **281**(1):L202-L208.
161. Ball MK, Waypa GB, Mungai PT, Nielsen JM, Czech L, Dudley VJ, Beussink L, Dettman RW, Berkelhamer SK, Steinhorn RH *et al*: **Regulation of hypoxia-induced pulmonary hypertension by vascular smooth muscle hypoxia-inducible factor-1α**. *American journal of respiratory and critical care medicine* 2014, **189**(3):314-324.
162. Ball MK, Waypa GB, Mungai PT, Nielsen JM, Czech L, Dudley VJ, Beussink L, Dettman RW, Berkelhamer SK, Steinhorn RH: **Regulation of hypoxia-induced pulmonary hypertension by vascular smooth muscle hypoxia-inducible factor-1α**. *American journal of respiratory and critical care medicine* 2014, **189**(3):314-324.
163. Li Y, Shi B, Huang L, Wang X, Yu X, Guo B, Ren W: **Suppression of the expression of hypoxia-inducible factor-1α by RNA interference alleviates hypoxia-induced pulmonary hypertension in adult rats**. *International journal of molecular medicine* 2016, **38**(6):1786-1794.
164. Aimee YY, Shimoda LA, Iyer NV, Huso DL, Sun X, McWilliams R, Beaty T, Sham JS, Wiener CM, Sylvester J: **Impaired physiological responses to chronic hypoxia in mice partially deficient for hypoxia-inducible factor 1α**. *The Journal of clinical investigation* 1999, **103**(5):691-696.
165. Bonnet S, Archer SL, Allalunis-Turner J, Haromy A, Beaulieu C, Thompson R, Lee CT, Lopaschuk GD, Puttagunta L, Bonnet S: **A mitochondria-K+ channel axis is suppressed in cancer and its normalization promotes apoptosis and inhibits cancer growth**. *Cancer cell* 2007, **11**(1):37-51.
166. Archer SL: **Pyruvate kinase and Warburg metabolism in pulmonary arterial hypertension: uncoupled glycolysis and the cancer-like phenotype of pulmonary arterial hypertension**. In.: Am Heart Assoc; 2017.
167. Michelakis ED, McMurtry MS, Wu X-C, Dyck JR, Moudgil R, Hopkins TA, Lopaschuk GD, Puttagunta L, Waite R, Archer SLJC: **Dichloroacetate, a metabolic modulator, prevents and reverses chronic hypoxic pulmonary hypertension in rats: role of increased expression and activity of voltage-gated potassium channels**. 2002, **105**(2):244-250.
168. McMurtry MS, Bonnet S, Wu X, Dyck JR, Haromy A, Hashimoto K, Michelakis EDJCr: **Dichloroacetate prevents and reverses pulmonary hypertension by inducing pulmonary artery smooth muscle cell apoptosis**. 2004, **95**(8):830-840.
169. Michelakis ED, Gurtu V, Webster L, Barnes G, Watson G, Howard L, Cupitt J, Paterson I, Thompson RB, Chow KJSTM: **Inhibition of pyruvate dehydrogenase kinase improves pulmonary arterial hypertension in genetically susceptible patients**. 2017, **9**(413):eaao4583.
170. Bonnet S, Michelakis ED, Porter CJ, Andrade-Navarro MA, Thébaud B, Bonnet S, Haromy A, Harry G, Moudgil R, McMurtry MS: **An abnormal mitochondrial-hypoxia inducible factor-1a-Kv channel pathway disrupts oxygen sensing and**

triggers pulmonary arterial hypertension in fawn hooded rats: similarities to human pulmonary arterial hypertension. *Circulation* 2006, **113**(22):2630-2641.

171. Sutendra G, Bonnet S, Rochefort G, Haromy A, Folmes KD, Lopaschuk GD, Dyck JR, Michelakis ED: **Fatty acid oxidation and malonyl-CoA decarboxylase in the vascular remodeling of pulmonary hypertension**. *Science translational medicine* 2010, **2**(44):44ra58-44ra58.
172. Wu W, Platoshyn O, Firth AL, Yuan JX-J: **Hypoxia divergently regulates production of reactive oxygen species in human pulmonary and coronary artery smooth muscle cells**. *American Journal of Physiology-Lung Cellular and Molecular Physiology* 2007, **293**(4):L952-L959.
173. Wu W, Platoshyn O, Firth AL, Yuan JX-JJAJoP-LC, Physiology M: **Hypoxia divergently regulates production of reactive oxygen species in human pulmonary and coronary artery smooth muscle cells**. 2007, **293**(4):L952-L959.
174. Dupuy F, Tabariès S, Andrzejewski S, Dong Z, Blagih J, Annis MG, Omeroglu A, Gao D, Leung S, Amir E: **PDK1-dependent metabolic reprogramming dictates metastatic potential in breast cancer**. *Cell metabolism* 2015, **22**(4):577-589.
175. Kim J-w, Tchernyshyov I, Semenza GL, Dang CV: **HIF-1-mediated expression of pyruvate dehydrogenase kinase: a metabolic switch required for cellular adaptation to hypoxia**. *Cell metabolism* 2006, **3**(3):177-185.
176. Hernansanz-Agustín P, Izquierdo-Álvarez A, Sánchez-Gómez FJ, Ramos E, Villa-Piña T, Lamas S, Bogdanova A, Martínez-Ruiz A: **Acute hypoxia produces a superoxide burst in cells**. *Free radical biology and medicine* 2014, **71**:146-156.
177. Guzy RD, Sharma B, Bell E, Chandel NS, Schumacker PTJM, biology c: **Loss of the SdhB, but Not the SdhA, subunit of complex II triggers reactive oxygen species-dependent hypoxia-inducible factor activation and tumorigenesis**. 2008, **28**(2):718-731.
178. Yue X, Zhao P, Wu K, Huang J, Zhang W, Wu Y, Liang X, He XJTB: **GRIM-19 inhibition induced autophagy through activation of ERK and HIF-1α not STAT3 in Hela cells**. 2016, **37**(7):9789-9796.
179. Saito Y, Ishii K-a, Aita Y, Ikeda T, Kawakami Y, Shimano H, Hara H, Takekoshi KJNr: **Loss of SDHB elevates catecholamine synthesis and secretion depending on ROS production and HIF stabilization**. 2016, **41**(4):696-706.
180. Comito G, Calvani M, Giannoni E, Bianchini F, Calorini L, Torre E, Migliore C, Giordano S, Chiarugi PJFRB, Medicine: **HIF-1α stabilization by mitochondrial ROS promotes Met-dependent invasive growth and vasculogenic mimicry in melanoma cells**. 2011, **51**(4):893-904.
181. Brunelle JK, Bell EL, Quesada NM, Vercauteren K, Tiranti V, Zeviani M, Scarpulla RC, Chandel NSJCm: **Oxygen sensing requires mitochondrial ROS but not oxidative phosphorylation**. 2005, **1**(6):409-414.
182. Guzy RD, Hoyos B, Robin E, Chen H, Liu L, Mansfield KD, Simon MC, Hammerling U, Schumacker PT: **Mitochondrial complex III is required for hypoxia-induced ROS production and cellular oxygen sensing**. *Cell metabolism* 2005, **1**(6):401-408.
183. Mansfield KD, Guzy RD, Pan Y, Young RM, Cash TP, Schumacker PT, Simon MC: **Mitochondrial dysfunction resulting from loss of cytochrome c impairs cellular oxygen sensing and hypoxic HIF-α activation**. *Cell metabolism* 2005, **1**(6):393-399.
184. Klimova T, Chandel NJCD, Differentiation: **Mitochondrial complex III regulates hypoxic activation of HIF**. 2008, **15**(4):660-666.

185. Chua YL, Dufour E, Dassa EP, Rustin P, Jacobs HT, Taylor CT, Hagen TJJoBC: **Stabilization of hypoxia-inducible factor-1α protein in hypoxia occurs independently of mitochondrial reactive oxygen species production**. 2010, **285**(41):31277-31284.
186. Vander Heiden MG, Cantley LC, Thompson CBJs: **Understanding the Warburg effect: the metabolic requirements of cell proliferation**. 2009, **324**(5930):1029-1033.
187. Paulin R, Meloche J, Jacob MH, Bisserier M, Courboulin A, Bonnet S: **Dehydroepiandrosterone inhibits the Src/STAT3 constitutive activation in pulmonary arterial hypertension**. *American Journal of Physiology-Heart and Circulatory Physiology* 2011, **301**(5):H1798-H1809.
188. Chen C, Chen C, Wang Z, Wang L, Yang L, Ding M, Ding C, Sun Y, Lin Q, Huang X: **Puerarin induces mitochondria-dependent apoptosis in hypoxic human pulmonary arterial smooth muscle cells**. *PloS one* 2012, **7**(3):e34181.
189. Ma YY, Chen HW, Tzeng CR: **Low oxygen tension increases mitochondrial membrane potential and enhances expression of antioxidant genes and implantation protein of mouse blastocyst cultured in vitro**. *Journal of ovarian research* 2017, **10**(1):47.
190. Pak O, Sommer N, Hoeres T, Bakr A, Waisbrod S, Sydykov A, Haag D, Esfandiary A, Kojonazarov B, Veit F: **Mitochondrial hyperpolarization in pulmonary vascular remodeling. Mitochondrial uncoupling protein deficiency as disease model**. *American journal of respiratory cell and molecular biology* 2013, **49**(3):358-367.
191. Hu H-l, Zhang Z-X, Chen C-S, Cai C, Zhao J-P, Wang XJAjorc, biology m: **Effects of mitochondrial potassium channel and membrane potential on hypoxic human pulmonary artery smooth muscle cells**. 2010, **42**(6):661-666.
192. Marsboom G, Toth PT, Ryan JJ, Hong Z, Wu X, Fang Y-H, Thenappan T, Piao L, Zhang HJ, Pogoriler J: **Dynamin-related protein 1–mediated mitochondrial mitotic fission permits hyperproliferation of vascular smooth muscle cells and offers a novel therapeutic target in pulmonary hypertension**. *Circulation research* 2012, **110**(11):1484-1497.
193. Parra V, Bravo-Sagua R, Norambuena-Soto I, Hernández-Fuentes CP, Gómez-Contreras AG, Verdejo HE, Mellado R, Chiong M, Lavandero S, Castro PF: **Inhibition of mitochondrial fission prevents hypoxia-induced metabolic shift and cellular proliferation of pulmonary arterial smooth muscle cells**. *Biochimica et Biophysica Acta (BBA)-Molecular Basis of Disease* 2017, **1863**(11):2891-2903.
194. Sutendra G, Dromparis P, Wright P, Bonnet S, Haromy A, Hao Z, McMurtry MS, Michalak M, Vance JE, Sessa WC: **The role of Nogo and the mitochondria–endoplasmic reticulum unit in pulmonary hypertension**. *Science translational medicine* 2011, **3**(88):88ra55-88ra55.
195. Wang J, Weigand L, Lu W, Sylvester J, L. Semenza G, Shimoda LA: **Hypoxia inducible factor 1 mediates hypoxia-induced TRPC expression and elevated intracellular Ca^{2+} in pulmonary arterial smooth muscle cells**. *Circulation research* 2006, **98**(12):1528-1537.
196. Firth AL, Won JY, Park WS: **Regulation of ca(2+) signaling in pulmonary hypertension**. *Korean J Physiol Pharmacol* 2013, **17**(1):1-8.
197. Genevois M: **Sur la fermentation et sur la respiration chez les végétaux chlorophylliens**. *Revue Generale de Botanique* 1929, **41**:252-265.
198. Huq S, Palmer J: **Isolation of a cyanide- resistant duroquinol oxidase from arum maculatum mitochondria**. *FEBS letters* 1978, **95**(2):217-220.

199. Rich PR: **Quinol oxidation in Arum maculatum mitochondria and its application to the assay, solubilisation and partial purification of the alternative oxidase**. *FEBS letters* 1978, **96**(2):252-256.
200. McDonald AE, Vanlerberghe GCJG: **Alternative oxidase and plastoquinol terminal oxidase in marine prokaryotes of the Sargasso Sea**. 2005, **349**:15-24.
201. McDonald AE, Vanlerberghe GCJCB, Genomics PPD, Proteomics: **Origins, evolutionary history, and taxonomic distribution of alternative oxidase and plastoquinol terminal oxidase**. 2006, **1**(3):357-364.
202. McDonald AE, Amirsadeghi S, Vanlerberghe GCJPmb: **Prokaryotic orthologues of mitochondrial alternative oxidase and plastid terminal oxidase**. 2003, **53**(6):865-876.
203. Moore AL, Siedow JN: **The regulation and nature of the cyanide-resistant alternative oxidase of plant mitochondria**. *Biochimica et Biophysica Acta (BBA)-Bioenergetics* 1991, **1059**(2):121-140.
204. El-Khoury R, Dufour E, Rak M, Ramanantsoa N, Grandchamp N, Csaba Z, Duvillié B, Bénit P, Gallego J, Gressens P: **Alternative oxidase expression in the mouse enables bypassing cytochrome c oxidase blockade and limits mitochondrial ROS overproduction**. *PLoS genetics* 2013, **9**(1):e1003182.
205. Minagawa N, Sakajo S, Komiyama T, Yoshimoto A: **Essential role of ferrous iron in cyanide- resistant respiration in Hansenula anomala**. *FEBS letters* 1990, **267**(1):114-116.
206. Amirsadeghi S, Robson CA, McDonald AE, Vanlerberghe GCJP, Physiology C: **Changes in plant mitochondrial electron transport alter cellular levels of reactive oxygen species and susceptibility to cell death signaling molecules**. 2006, **47**(11):1509-1519.
207. Maxwell DP, Wang Y, McIntosh LJPotNAoS: **The alternative oxidase lowers mitochondrial reactive oxygen production in plant cells**. 1999, **96**(14):8271-8276.
208. Van Aken O, Giraud E, Clifton R, Whelan JJPp: **Alternative oxidase: a target and regulator of stress responses**. 2009, **137**(4):354-361.
209. Van Der Merwe MJ, Osorio S, Moritz T, Nunes-Nesi A, Fernie ARJPp: **Decreased mitochondrial activities of malate dehydrogenase and fumarase in tomato lead to altered root growth and architecture via diverse mechanisms**. 2009, **149**(2):653-669.
210. Bendall D, Bonner WJPp: **Cyanide-insensitive respiration in plant mitochondria**. 1971, **47**(2):236-245.
211. Moore AL, Siedow JNJBeBA-B: **The regulation and nature of the cyanide-resistant alternative oxidase of plant mitochondria**. 1991, **1059**(2):121-140.
212. Maxwell DP, Wang Y, McIntosh L: **The alternative oxidase lowers mitochondrial reactive oxygen production in plant cells**. *Proceedings of the National Academy of Sciences* 1999, **96**(14):8271-8276.
213. Purvis AC: **Role of the alternative oxidase in limiting superoxide production by plant mitochondria**. *Physiologia Plantarum* 1997, **100**(1):165-170.
214. Vanlerberghe GC, Mclntosh L: **Signals regulating the expression of the nuclear gene encoding alternative oxidase of plant mitochondria**. *Plant Physiology* 1996, **111**(2):589-595.
215. Hakkaart GA, Dassa EP, Jacobs HT, Rustin P: **Allotopic expression of a mitochondrial alternative oxidase confers cyanide resistance to human cell respiration**. *EMBO reports* 2006, **7**(3):341-345.

216. Dassa EP, Dufour E, Gonçalves S, Paupe V, Hakkaart GA, Jacobs HT, Rustin P: **Expression of the alternative oxidase complements cytochrome c oxidase deficiency in human cells**. *EMBO molecular medicine* 2009, **1**(1):30-36.
217. Chua YL, Dufour E, Dassa EP, Rustin P, Jacobs HT, Taylor CT, Hagen T: **Stabilization of HIF-1α protein in hypoxia occurs independently of mitochondrial reactive oxygen species production**. *Journal of Biological Chemistry* 2010:jbc. M110. 158485.
218. Fernandez-Ayala DJ, Sanz A, Vartiainen S, Kemppainen KK, Babusiak M, Mustalahti E, Costa R, Tuomela T, Zeviani M, Chung J: **Expression of the Ciona intestinalis alternative oxidase (AOX) in Drosophila complements defects in mitochondrial oxidative phosphorylation**. *Cell metabolism* 2009, **9**(5):449-460.
219. Szibor M, Dhandapani PK, Dufour E, Holmström KM, Zhuang Y, Salwig I, Wittig I, Heidler J, Gizatullina Z, Gainutdinov TJDm *et al*: **Broad AOX expression in a genetically tractable mouse model does not disturb normal physiology**. 2017, **10**(2):163-171.
220. Tsukihara T, Aoyama H, Yamashita E, Tomizaki T, Yamaguchi H, Shinzawa-Itoh K, Nakashima R, Yaono R, Yoshikawa S: **The whole structure of the 13-subunit oxidized cytochrome c oxidase at 2.8 Å**. *Science (New York, NY)* 1996, **272**(5265):1136-1144.
221. Fukuda R, Zhang H, Kim J-w, Shimoda L, Dang CV, Semenza GL: **HIF-1 regulates cytochrome oxidase subunits to optimize efficiency of respiration in hypoxic cells**. *Cell* 2007, **129**(1):111-122.
222. Huttemann M, Lee I, Gao X, Pecina P, Pecinova A, Liu J, Aras S, Sommer N, Sanderson TH, Tost M *et al*: **Cytochrome c oxidase subunit 4 isoform 2-knockout mice show reduced enzyme activity, airway hyporeactivity, and lung pathology**. *FASEB journal : official publication of the Federation of American Societies for Experimental Biology* 2012, **26**(9):3916-3930.
223. Shteyer E, Saada A, Shaag A, Kidess R, Revel-Vilk S, Elpeleg O: **Exocrine pancreatic insufficiency, dyserythropoeitic anemia, and calvarial hyperostosis are caused by a mutation in the COX4I2 gene**. *The American Journal of Human Genetics* 2009, **84**(3):412-417.
224. Aras S, Pak O, Sommer N, Finley Jr R, Hüttemann M, Weissmann N, Grossman LI: **Oxygen-dependent expression of cytochrome c oxidase subunit 4-2 gene expression is mediated by transcription factors RBPJ, CXXC5 and CHCHD2**. *Nucleic acids research* 2013, **41**(4):2255-2266.
225. Napiwotzki J, Kadenbach BJBc: **Extramitochondrial ATP/ADP-ratios regulate cytochrome c oxidase activity via binding to the cytosolic domain of subunit IV**. 1998, **379**(3):335-340.
226. Arnold S, Kadenbach BJFl: **The intramitochondrial ATP/ADP- ratio controls cytochrome c oxidase activity allosterically**. 1999, **443**(2):105-108.
227. Hüttemann M, Kadenbach B, Grossman LIJG: **Mammalian subunit IV isoforms of cytochrome c oxidase**. 2001, **267**(1):111-123.
228. Hüttemann M, Lee I, Gao X, Pecina P, Pecinova A, Liu J, Aras S, Sommer N, Sanderson TH, Tost M: **Cytochrome c oxidase subunit 4 isoform 2- knockout mice show reduced enzyme activity, airway hyporeactivity, and lung pathology**. *The FASEB Journal* 2012, **26**(9):3916-3930.
229. Horvat S, Beyer C, Arnold S: **Effect of hypoxia on the transcription pattern of subunit isoforms and the kinetics of cytochrome c oxidase in cortical astrocytes and cerebellar neurons**. *J Neurochem* 2006, **99**(3):937-951.

230. Fukuda R, Zhang H, Kim J-w, Shimoda L, Dang CV, Semenza GLJC: **HIF-1 regulates cytochrome oxidase subunits to optimize efficiency of respiration in hypoxic cells**. 2007, **129**(1):111-122.
231. Burke PV, Raitt DC, Allen LA, Kellogg EA, Poyton ROJJoBC: **Effects of oxygen concentration on the expression of cytochrome c and cytochrome c oxidase genes in yeast**. 1997, **272**(23):14705-14712.
232. Hüttemann M, Lee I, Liu J, Grossman LI: **Transcription of mammalian cytochrome c oxidase subunit IV- 2 is controlled by a novel conserved oxygen responsive element**. *The FEBS journal* 2007, **274**(21):5737-5748.
233. Hüttemann M, Kadenbach B, Grossman LI: **Mammalian subunit IV isoforms of cytochrome c oxidase**. *Gene* 2001, **267**(1):111-123.
234. Čunátová K, Vrbacký M, Pecinová A, Houštěk J, Mráček T, Pecina P: **Cytochrome c Oxidase Subunit 4 Isoform Exchange Results in Modulation of Oxygen Affinity**. *Cells* 2020, **9**(2).
235. Bonnet S, Boucherat O: **The ROS controversy in hypoxic pulmonary hypertension revisited**. In.: Eur Respiratory Soc; 2018.
236. Michelakis ED, Thébaud B, Weir EK, Archer SL: **Hypoxic pulmonary vasoconstriction: redox regulation of O_2-sensitive K^+ channels by a mitochondrial O_2-sensor in resistance artery smooth muscle cells**. *Journal of molecular and cellular cardiology* 2004, **37**(6):1119-1136.
237. Nicholls DG, Bernson VS, Heaton GM: **The identification of the component in the inner membrane of brown adipose tissue mitochondria responsible for regulating energy dissipation**. *Experientia Supplementum* 1978, **32**:89-93.
238. Ho PW, Ho JW, Liu H-F, So DH, Tse ZH, Chan K-H, Ramsden DB, Ho S-L: **Mitochondrial neuronal uncoupling proteins: a target for potential disease-modification in Parkinson's disease**. *Transl Neurodegener* 2012, **1**(1):3-3.
239. Boss O, Samec S, Paoloni-Giacobino A, Rossier C, Dulloo A, Seydoux J, Muzzin P, Giacobino JP: **Uncoupling protein-3: a new member of the mitochondrial carrier family with tissue-specific expression**. *FEBS letters* 1997, **408**(1):39-42.
240. Pecqueur C, Alves-Guerra M-C, Gelly C, Lévi-Meyrueis C, Couplan E, Collins S, Ricquier D, Bouillaud F, Miroux B: **Uncoupling protein 2, in vivo distribution, induction upon oxidative stress, and evidence for translational regulation**. *Journal of Biological Chemistry* 2001, **276**(12):8705-8712.
241. Rousset S, Mozo J, Dujardin G, Emre Y, Masscheleyn S, Ricquier D, Cassard-Doulcier A-M: **UCP2 is a mitochondrial transporter with an unusual very short half- life**. *FEBS letters* 2007, **581**(3):479-482.
242. Pecqueur C, Couplan E, Bouillaud F, Ricquier D: **Genetic and physiological analysis of the role of uncoupling proteins in human energy homeostasis**. *Journal of Molecular Medicine* 2001, **79**(1):48-56.
243. Argiles JM, Busquets S, Lopez-Soriano FJ: **The role of uncoupling proteins in pathophysiological states**. *Biochemical and biophysical research communications* 2002, **293**(4):1145-1152.
244. Jabůrek M, Var□echa M, Gimeno RE, Dembski M, Jez□ek P, Zhang M, Burn P, Tartaglia LA, Garlid KDJJoBC: **Transport function and regulation of mitochondrial uncoupling proteins 2 and 3**. 1999, **274**(37):26003-26007.
245. Fleury CJUp-anglto, Genet hN: **Neverova M, Collins S, Raimbault S, Champigny O, Levi-Meyrueis C, Bouillaud F, Seldin MF, Surwit RS, Ricquier D, and Warden CH**. 1997, **15**:269-272.

246. Fink BD, Reszka KJ, Herlein JA, Mathahs MM, Sivitz WIJAJoP-E, Metabolism: **Respiratory uncoupling by UCP1 and UCP2 and superoxide generation in endothelial cell mitochondria**. 2005, **288**(1):E71-E79.
247. Couplan E, del Mar Gonzalez-Barroso M, Alves-Guerra MC, Ricquier D, Goubern M, Bouillaud F: **No evidence for a basal, retinoic or superoxide-induced uncoupling activity of the UCP2 present in spleen or lung mitochondria**. *Journal of Biological Chemistry* 2002.
248. Echtay KS, Roussel D, St-Pierre J, Jekabsons MB, Cadenas S, Stuart JA, Harper JA, Roebuck SJ, Morrison A, Pickering S: **Superoxide activates mitochondrial uncoupling proteins**. *Nature* 2002, **415**(6867):96.
249. Krauss S, Zhang C-Y, Lowell BB: **A significant portion of mitochondrial proton leak in intact thymocytes depends on expression of UCP2**. *Proceedings of the National Academy of Sciences* 2002, **99**(1):118-122.
250. Echtay KS, Winkler E, Frischmuth K, Klingenberg M: **Uncoupling proteins 2 and 3 are highly active H+ transporters and highly nucleotide sensitive when activated by coenzyme Q (ubiquinone)**. *Proceedings of the National Academy of Sciences* 2001, **98**(4):1416-1421.
251. Jabůrek M, Garlid KD: **Reconstitution of recombinant uncoupling proteins UCP1,-2, and-3 have similar affinities for ATP and are unaffected by coenzyme Q10**. *Journal of Biological Chemistry* 2003, **278**(28):25825-25831.
252. Krauss S, Zhang C-Y, Lowell BBJPotNAoS: **A significant portion of mitochondrial proton leak in intact thymocytes depends on expression of UCP2**. 2002, **99**(1):118-122.
253. Zhang C-Y, Baffy G, Perret P, Krauss S, Peroni O, Grujic D, Hagen T, Vidal-Puig AJ, Boss O, Kim Y-B: **Uncoupling protein-2 negatively regulates insulin secretion and is a major link between obesity, β cell dysfunction, and type 2 diabetes**. *Cell* 2001, **105**(6):745-755.
254. Krauss S, Zhang C-Y, Scorrano L, Dalgaard LT, St-Pierre J, Grey ST, Lowell BB: **Superoxide-mediated activation of uncoupling protein 2 causes pancreatic β cell dysfunction**. *The Journal of clinical investigation* 2003, **112**(12):1831-1842.
255. Echtay KS, Roussel D, St-Pierre J, Jekabsons MB, Cadenas S, Stuart JA, Harper JA, Roebuck SJ, Morrison A, Pickering S *et al*: **Superoxide activates mitochondrial uncoupling proteins**. *Nature* 2002, **415**:96.
256. Lee K-U, Lee IK, Han J, Song D-K, Kim YM, Song HS, Kim HS, Lee WJ, Koh EH, Song K-H: **Effects of recombinant adenovirus-mediated uncoupling protein 2 overexpression on endothelial function and apoptosis**. *Circulation research* 2005, **96**(11):1200-1207.
257. Lee SC, Robson-Doucette CA, Wheeler MB: **Uncoupling protein 2 regulates reactive oxygen species formation in islets and influences susceptibility to diabetogenic action of streptozotocin**. *Journal of Endocrinology* 2009, **203**(1):33-43.
258. Deng S, Yang Y, Han Y, Li X, Wang X, Li X, Zhang Z, Wang YJPo: **UCP2 inhibits ROS-mediated apoptosis in A549 under hypoxic conditions**. 2012, **7**(1):e30714.
259. Trenker M, Malli R, Fertschai I, Levak-Frank S, Graier WFJNcb: **Uncoupling proteins 2 and 3 are fundamental for mitochondrial Ca 2+ uniport**. 2007, **9**(4):445-452.
260. Madreiter-Sokolowski CT, Klec C, Parichatikanond W, Stryeck S, Gottschalk B, Pulido S, Rost R, Eroglu E, Hofmann NA, Bondarenko AI *et al*: **PRMT1-mediated methylation of MICU1 determines the UCP2/3 dependency of mitochondrial Ca^{2+} uptake in immortalized cells**. *Nature Communications* 2016, **7**:12897.

261. Pendin D, Greotti E, Pozzan TJCc: **The elusive importance of being a mitochondrial Ca^{2+} uniporter**. 2014, **55**(3):139-145.
262. Brookes PS, Parker N, Buckingham JA, Vidal-Puig A, Halestrap AP, Gunter TE, Nicholls DG, Bernardi P, Lemasters JJ, Brand MD: **UCPs--unlikely calcium porters**. *Nature cell biology* 2008, **10**(11):1235-1240.
263. Pecqueur C, Bui T, Gelly C, Hauchard J, Barbot C, Bouillaud F, Ricquier D, Miroux B, Thompson CB: **Uncoupling protein-2 controls proliferation by promoting fatty acid oxidation and limiting glycolysis-derived pyruvate utilization**. *The FASEB Journal* 2008, **22**(1):9-18.
264. Lameloise N, Muzzin P, Prentki M, Assimacopoulos-Jeannet FJD: **Uncoupling protein 2: a possible link between fatty acid excess and impaired glucose-induced insulin secretion?** 2001, **50**(4):803-809.
265. Patanè G, Anello M, Piro S, Vigneri R, Purrello F, Rabuazzo AMJD: **Role of ATP production and uncoupling protein-2 in the insulin secretory defect induced by chronic exposure to high glucose or free fatty acids and effects of peroxisome proliferator-activated receptor-γ inhibition**. 2002, **51**(9):2749-2756.
266. Vozza A, Parisi G, De Leonardis F, Lasorsa FM, Castegna A, Amorese D, Marmo R, Calcagnile VM, Palmieri L, Ricquier D: **UCP2 transports C4 metabolites out of mitochondria, regulating glucose and glutamine oxidation**. *Proceedings of the National Academy of Sciences* 2014, **111**(3):960-965.
267. Haslip M, Dostanic I, Huang Y, Zhang Y, Russell KS, Jurczak MJ, Mannam P, Giordano F, Erzurum SC, Lee PJ: **Endothelial uncoupling protein 2 regulates mitophagy and pulmonary hypertension during intermittent hypoxia**. *Arteriosclerosis, thrombosis, and vascular biology* 2015, **35**(5):1166-1178.
268. Dromparis P, Paulin R, Sutendra G, Qi AC, Bonnet S, Michelakis EDJCr: **Uncoupling protein 2 deficiency mimics the effects of hypoxia and endoplasmic reticulum stress on mitochondria and triggers pseudohypoxic pulmonary vascular remodeling and pulmonary hypertension**. 2013, **113**(2):126-136.
269. Misiak M, Singh S, Drewlo S, Beyer C, Arnold SJC, research t: **Brain region-specific vulnerability of astrocytes in response to 3-nitropropionic acid is mediated by cytochrome c oxidase isoform expression**. 2010, **341**(1):83-93.
270. Singh S, Misiak M, Beyer C, Arnold SJG: **Cytochrome c oxidase isoform IV- 2 is involved in 3- nitropropionic acid- induced toxicity in striatal astrocytes**. 2009, **57**(14):1480-1491.
271. Horsch M, Aguilar-Pimentel JA, Bönisch C, Côme C, Kolster-Fog C, Jensen KT, Lund AH, Lee I, Grossman LI, Sinkler C *et al*: **Cox4i2, Ifit2, and Prdm11 Mutant Mice: Effective Selection of Genes Predisposing to an Altered Airway Inflammatory Response from a Large Compendium of Mutant Mouse Lines**. *PloS one* 2015, **10**(8):e0134503-e0134503.
272. Pak O, Sommer N, Hoeres T, Bakr A, Waisbrod S, Sydykov A, Haag D, Esfandiary A, Kojonazarov B, Veit FJAjorc *et al*: **Mitochondrial hyperpolarization in pulmonary vascular remodeling. Mitochondrial uncoupling protein deficiency as disease model**. 2013, **49**(3):358-367.
273. El-Khoury R, Dufour E, Rak M, Ramanantsoa N, Grandchamp N, Csaba Z, Duvillie B, Benit P, Gallego J, Gressens P: **Alternative oxidase expression in the mouse enables bypassing cytochrome c oxidase blockade and limits mitochondrial ROS overproduction**. *PLoS Genet* 2013, **9**(1):e1003182.
274. Pecqueur C, Cassard-Doulcier AM, Raimbault S, Miroux B, Fleury C, Gelly C, Bouillaud F, Ricquier D: **Functional organization of the human uncoupling**

protein-2 gene, and juxtaposition to the uncoupling protein-3 gene. *Biochemical and biophysical research communications* 1999, **255**(1):40-46.

275. Ricquier D, Fleury C, Larose M, Sanchis D, Pecqueur C, Raimbault S, Gelly C, Vacher D, Cassard-Doulcier AM, Levi-Meyrueis C *et al*: **Contributions of studies on uncoupling proteins to research on metabolic diseases**. *Journal of internal medicine* 1999, **245**(6):637-642.
276. El Agha E, Al Alam D, Carraro G, MacKenzie B, Goth K, De Langhe SP, Voswinckel R, Hajihosseini MK, Rehan VK, Bellusci S: **Characterization of a novel fibroblast growth factor 10 (Fgf10) knock-in mouse line to target mesenchymal progenitors during embryonic development**. *PloS one* 2012, **7**(6):e38452.
277. Sommer N, Huttemann M, Pak O, Scheibe S, Knoepp F, Sinkler C, Malczyk M, Gierhardt M, Esfandiary A, Kraut S *et al*: **Mitochondrial Complex IV Subunit 4 Isoform 2 Is Essential for Acute Pulmonary Oxygen Sensing**. *Circulation research* 2017, **121**(4):424-438.
278. Trnka J, Blaikie FH, Logan A, Smith RA, Murphy MPJFrr: **Antioxidant properties of MitoTEMPOL and its hydroxylamine**. 2009, **43**(1):4-12.
279. Ma Y, Huang Z, Zhou Z, He X, Wang Y, Meng C, Huang G, Fang NJFRB, Medicine: **A novel antioxidant Mito-Tempol inhibits ox-LDL-induced foam cell formation through restoration of autophagy flux**. 2018, **129**:463-472.
280. Zhang Y, Bharathi SS, Beck ME, Goetzman ES: **The fatty acid oxidation enzyme long-chain acyl-CoA dehydrogenase can be a source of mitochondrial hydrogen peroxide**. *Redox biology* 2019, **26**:101253.
281. Antonenko YN, Avetisyan A, Bakeeva L, Chernyak B, Chertkov V, Domnina L, Ivanova OY, Izyumov D, Khailova L, Klishin S: **Mitochondria-targeted plastoquinone derivatives as tools to interrupt execution of the aging program. 1. Cationic plastoquinone derivatives: synthesis and in vitro studies**. *Biochemistry (Moscow)* 2008, **73**(12):1273-1287.
282. Rademann P, Weidinger A, Drechsler S, Meszaros A, Zipperle J, Jafarmadar M, Dumitrescu S, Hacobian A, Ungelenk L, Röstel F: **Mitochondria-targeted antioxidants SkQ1 and MitoTEMPO failed to exert a long-term beneficial effect in murine polymicrobial sepsis**. *Oxidative medicine and cellular longevity* 2017, **2017**.
283. Weissmann N, Sommer N, Schermuly RT, Ghofrani HA, Seeger W, Grimminger F: **Oxygen sensors in hypoxic pulmonary vasoconstriction**. *Cardiovascular Research* 2006, **71**(4):620-629.
284. Sommer N, Dietrich A, Schermuly R, Ghofrani H, Gudermann T, Schulz R, Seeger W, Grimminger F, Weissmann N: **Regulation of hypoxic pulmonary vasoconstriction: basic mechanisms**. *European Respiratory Journal* 2008, **32**(6):1639-1651.
285. Weissmann N, Zeller S, Schafer RU, Turowski C, Ay M, Quanz K, Ghofrani HA, Schermuly RT, Fink L, Seeger W: **Impact of mitochondria and NADPH oxidases on acute and sustained hypoxic pulmonary vasoconstriction**. *American journal of respiratory cell and molecular biology* 2006, **34**(4):505-513.
286. Moudgil R, Michelakis ED, Archer SL: **Hypoxic pulmonary vasoconstriction**. *Journal of applied physiology* 2005, **98**(1):390-403.
287. Waypa GB, Smith KA, Schumacker PT: **O_2 sensing, mitochondria and ROS signaling: the fog is lifting**. *Molecular aspects of medicine* 2016, **47**:76-89.

288. Yang Z, Zhuan B, Yan Y, Jiang S, Wang T: **Roles of different mitochondrial electron transport chain complexes in hypoxia- induced pulmonary vasoconstriction**. *Cell Biology International* 2016, **40**(2):188-195.
289. Song T, Zheng Y-M, Wang Y-X: **Cross talk between mitochondrial reactive oxygen species and sarcoplasmic reticulum calcium in pulmonary arterial smooth muscle cells**. In: *Pulmonary Vasculature Redox Signaling in Health and Disease.* Springer; 2017: 289-298.
290. Archer SL, Nelson DP, Weir EK: **Simultaneous measurement of O_2 radicals and pulmonary vascular reactivity in rat lung**. *Journal of Applied Physiology* 1989, **67**(5):1903-1911.
291. Chandel NS, Budinger GS, Schumacker PTJJoBC: **Molecular oxygen modulates cytochrome c oxidase function**. 1996, **271**(31):18672-18677.
292. Paky A, Michael JR, Burke-Wolin TM, Wolin MS, Gurtner GHJJoap: **Endogenous production of superoxide by rabbit lungs: effects of hypoxia or metabolic inhibitors**. 1993, **74**(6):2868-2874.
293. Rathore R, Zheng Y-M, Li X-Q, Wang Q-S, Liu Q-H, Ginnan R, Singer HA, Ho Y-S, Wang Y-XJB, communications br: **Mitochondrial ROS-PKCε signaling axis is uniquely involved in hypoxic increase in [Ca^{2+}] i in pulmonary artery smooth muscle cells**. 2006, **351**(3):784-790.
294. Rathore R, Zheng Y-M, Niu C-F, Liu Q-H, Korde A, Ho Y-S, Wang Y-XJFRB, Medicine: **Hypoxia activates NADPH oxidase to increase [ROS] i and [Ca^{2+}] i through the mitochondrial ROS-PKCε signaling axis in pulmonary artery smooth muscle cells**. 2008, **45**(9):1223-1231.
295. Weissmann N, Kuzkaya N, Fuchs B, Tiyerili V, Schäfer RU, Schütte H, Ghofrani HA, Schermuly RT, Schudt C, Sydykov AJRr: **Detection of reactive oxygen species in isolated, perfused lungs by electron spin resonance spectroscopy**. 2005, **6**(1):86.
296. Leach RM, Hill HM, Snetkov VA, Robertson TP, Ward JP: **Divergent roles of glycolysis and the mitochondrial electron transport chain in hypoxic pulmonary vasoconstriction of the rat: identity of the hypoxic sensor**. *The Journal of physiology* 2001, **536**(1):211-224.
297. Schumacker PT: **Lung cell hypoxia: role of mitochondrial reactive oxygen species signaling in triggering responses**. *Proceedings of the American Thoracic Society* 2011, **8**(6):477-484.
298. Orr AL, Vargas L, Turk CN, Baaten JE, Matzen JT, Dardov VJ, Attle SJ, Li J, Quackenbush DC, Goncalves RLJNcb: **Suppressors of superoxide production from mitochondrial complex III**. 2015, **11**(11):834.
299. Sommer N, Hüttemann M, Pak O, Scheibe S, Knoepp F, Sinkler C, Malczyk M, Gierhardt M, Esfandiary A, Kraut S: **Mitochondrial complex IV subunit 4 isoform 2 is essential for acute pulmonary oxygen sensing**. *Circulation research* 2017, **121**(4):424-438.
300. Fink B, Laude K, McCann L, Doughan A, Harrison DG, Dikalov SJAJoP-CP: **Detection of intracellular superoxide formation in endothelial cells and intact tissues using dihydroethidium and an HPLC-based assay**. 2004, **287**(4):C895-C902.
301. McBee ME, Chionh YH, Sharaf ML, Ho P, Cai MW, Dedon PCJFim: **Production of superoxide in bacteria is stress-and cell state-dependent: A gating-optimized flow cytometry method that minimizes ROS measurement artifacts with fluorescent dyes**. 2017, **8**:459.

302. Debowska K, Debski D, Hardy M, Jakubowska M, Kalyanaraman B, Marcinek A, Michalski R, Michalowski B, Ouari O, Sikora AJPR: **Toward selective detection of reactive oxygen and nitrogen species with the use of fluorogenic probes—Limitations, progress, and perspectives**. 2015, **67**(4):756-764.
303. Wang Q-S, Zheng Y-M, Dong L, Ho Y-S, Guo Z, Wang Y-XJFRB, Medicine: **Role of mitochondrial reactive oxygen species in hypoxia-dependent increase in intracellular calcium in pulmonary artery myocytes**. 2007, **42**(5):642-653.
304. Noguchi K, Yoshida KJM: **Interaction between photosynthesis and respiration in illuminated leaves**. 2008, **8**(1):87-99.
305. Rustin P, Lance CJPP: **Malate metabolism in leaf mitochondria from the crassulacean acid metabolism plant Kalanchoë blossfeldiana Poelln**. 1986, **81**(4):1039-1043.
306. Dry IB, Moore AL, Day DA, Wiskich JTJAoB, Biophysics: **Regulation of alternative pathway activity in plant mitochondria: nonlinear relationship between electron flux and the redox poise of the quinone pool**. 1989, **273**(1):148-157.
307. Schumacker PTJPotATS: **Lung cell hypoxia: role of mitochondrial reactive oxygen species signaling in triggering responses**. 2011, **8**(6):477-484.
308. Szibor M, Dhandapani PK, Dufour E, Holmström KM, Zhuang Y, Salwig I, Wittig I, Heidler J, Gizatullina Z, Gainutdinov T: **Broad AOX expression in a genetically tractable mouse model does not disturb normal physiology**. *Disease models & mechanisms* 2017, **10**(2):163-171.
309. Sommer N, Pak O, Schörner S, Derfuss T, Krug A, Gnaiger E, Ghofrani H, Schermuly R, Huckstorf C, Seeger WJERJ: **Mitochondrial cytochrome redox states and respiration in acute pulmonary oxygen sensing**. 2010, **36**(5):1056-1066.
310. Veit F, Pak O, Brandes RP, Weissmann N: **Hypoxia-dependent reactive oxygen species signaling in the pulmonary circulation: focus on ion channels**. *Antioxidants & redox signaling* 2015, **22**(6):537-552.
311. El-Khoury R, Dufour E, Rak M, Ramanantsoa N, Grandchamp N, Csaba Z, Duvillie B, Benit P, Gallego J, Gressens PJPG: **Alternative oxidase expression in the mouse enables bypassing cytochrome c oxidase blockade and limits mitochondrial ROS overproduction**. 2013, **9**(1):e1003182.
312. Lorin S, Dufour E, Boulay J, Begel O, Marsy S, Sainsard- Chanet AJMm: **Overexpression of the alternative oxidase restores senescence and fertility in a long- lived respiration- deficient mutant of Podospora anserina**. 2001, **42**(5):1259-1267.
313. Castro-Guerrero NA, Rodríguez-Zavala JS, Marín-Hernández A, Rodríguez-Enríquez S, Moreno-Sánchez RJJoB, Biomembranes: **Enhanced alternative oxidase and antioxidant enzymes under Cd 2+ stress in Euglena**. 2008, **40**(3):227-235.
314. Watanabe M, Henmi K, Ogawa Ki, Suzuki TJCB, Toxicology PPC, Pharmacology: **Cadmium-dependent generation of reactive oxygen species and mitochondrial DNA breaks in photosynthetic and non-photosynthetic strains of Euglena gracilis**. 2003, **134**(2):227-234.
315. Sugie A, Naydenov N, Mizuno N, Nakamura C, Takumi SJG, systems g: **Overexpression of wheat alternative oxidase gene Waox1a alters respiration capacity and response to reactive oxygen species under low temperature in transgenic Arabidopsis**. 2006, **81**(5):349-354.

316. Popov V, Simonian R, Skulachev V, Starkov AJFl: **Inhibition of the alternative oxidase stimulates H_2O_2 production in plant mitochondria**. 1997, **415**(1):87-90.
317. Dry IB, Moore AL, Day DA, Wiskich JT: **Regulation of alternative pathway activity in plant mitochondria: nonlinear relationship between electron flux and the redox poise of the quinone pool**. *Archives of biochemistry and biophysics* 1989, **273**(1):148-157.
318. Szibor M, Gainutdinov T, Fernandez-Vizarra E, Dufour E, Gizatullina Z, Debska-Vielhaber G, Heidler J, Wittig I, Viscomi C, Gellerich FJBeBA-B: **Bioenergetic consequences from xenotopic expression of a tunicate AOX in mouse mitochondria: switch from RET and ROS to FET**. 2020, **1861**(2):148137.
319. Salvioli S, Ardizzoni A, Franceschi C, Cossarizza A: **JC- 1, but not DiOC6 (3) or rhodamine 123, is a reliable fluorescent probe to assess ΔΨ changes in intact cells: implications for studies on mitochondrial functionality during apoptosis**. *FEBS letters* 1997, **411**(1):77-82.
320. Mathur A, Hong Y, Kemp BK, Barrientos AA, Erusalimsky JD: **Evaluation of fluorescent dyes for the detection of mitochondrial membrane potential changes in cultured cardiomyocytes**. *Cardiovascular research* 2000, **46**(1):126-138.
321. Brown GCJBeBA-B: **Regulation of mitochondrial respiration by nitric oxide inhibition of cytochrome c oxidase**. 2001, **1504**(1):46-57.
322. Perry SW, Norman JP, Barbieri J, Brown EB, Gelbard HAJB: **Mitochondrial membrane potential probes and the proton gradient: a practical usage guide**. 2011, **50**(2):98-115.
323. Salvioli S, Ardizzoni A, Franceschi C, Cossarizza AJFl: **JC-1, but not DiOC6 (3) or rhodamine 123, is a reliable fluorescent probe to assess ΔΨ changes in intact cells: implications for studies on mitochondrial functionality during apoptosis**. 1997, **411**(1):77-82.
324. Mathur A, Hong Y, Kemp BK, Barrientos AA, Erusalimsky JDJCR: **Evaluation of fluorescent dyes for the detection of mitochondrial membrane potential changes in cultured cardiomyocytes**. 2000, **46**(1):126-138.
325. Marchetti C, Jouy N, Leroy-Martin B, Defossez A, Formstecher P, Marchetti PJHr: **Comparison of four fluorochromes for the detection of the inner mitochondrial membrane potential in human spermatozoa and their correlation with sperm motility**. 2004, **19**(10):2267-2276.
326. Dedkova EN, Blatter LAJJom, cardiology c: **Measuring mitochondrial function in intact cardiac myocytes**. 2012, **52**(1):48-61.
327. Murphy MP: **How mitochondria produce reactive oxygen species**. *Biochemical journal* 2009, **417**(1):1-13.
328. Peers C, Bell EL, Chandel NSJEib: **Mitochondrial oxygen sensing: regulation of hypoxia-inducible factor by mitochondrial generated reactive oxygen species**. 2007, **43**:17-28.
329. Archer S, Will J, Weir EJH: **Redox status in the control of pulmonary vascular tone**. 1986, **11**(3):127-141.
330. Ko EA, Wan J, Yamamura A, Zimnicka AM, Yamamura H, Yoo HY, Tang H, Smith KA, Sundivakkam PC, Zeifman AJAJoP-CP: **Functional characterization of voltage-dependent Ca^{2+} channels in mouse pulmonary arterial smooth muscle cells: divergent effect of ROS**. 2013, **304**(11):C1042-C1052.
331. Jones RD, Hancock JT, Morice AHJFRB, Medicine: **NADPH oxidase: a universal oxygen sensor?** 2000, **29**(5):416-424.

332. Pak O, Scheibe S, Esfandiary A, Gierhardt M, Sydykov A, Logan A, Fysikopoulos A, Veit F, Hecker M, Kroschel FJERJ: **Impact of the mitochondria-targeted antioxidant MitoQ on hypoxia-induced pulmonary hypertension**. 2018, **51**(3).
333. Aggarwal S, Gross CM, Sharma S, Fineman JR, Black SMJCP: **Reactive oxygen species in pulmonary vascular remodeling**. 2013, **3**(3):1011-1034.
334. Mansfield KD, Guzy RD, Pan Y, Young RM, Cash TP, Schumacker PT, Simon MCJCm: **Mitochondrial dysfunction resulting from loss of cytochrome c impairs cellular oxygen sensing and hypoxic HIF-α activation**. 2005, **1**(6):393-399.
335. Guzy RD, Hoyos B, Robin E, Chen H, Liu L, Mansfield KD, Simon MC, Hammerling U, Schumacker PTJCm: **Mitochondrial complex III is required for hypoxia-induced ROS production and cellular oxygen sensing**. 2005, **1**(6):401-408.
336. Hsu C-C, Wang C-H, Wu L-C, Hsia C-Y, Chi C-W, Yin P-H, Chang C-J, Sung M-T, Wei Y-H, Lu S-HJBeBA-GS: **Mitochondrial dysfunction represses HIF-1α protein synthesis through AMPK activation in human hepatoma HepG2 cells**. 2013, **1830**(10):4743-4751.
337. Sommer N, Alebrahimdehkordi N, Pak O, Knoepp F, Strielkov I, Scheibe S, Dufour E, Andjelković A, Sydykov A, Saraji A: **Bypassing mitochondrial complex III using alternative oxidase inhibits acute pulmonary oxygen sensing**. *Science Advances* 2020, **6**(16):eaba0694.
338. Tsukihara T, Aoyama H, Yamashita E, Tomizaki T, Yamaguchi H, Shinzawa-Itoh K, Nakashima R, Yaono R, Yoshikawa SJS: **The whole structure of the 13-subunit oxidized cytochrome c oxidase at 2.8 Å**. 1996, **272**(5265):1136-1144.
339. Nijtmans LG, Taanman JW, Muijsers AO, Speijer D, Van den Bogert C: **Assembly of cytochrome-c oxidase in cultured human cells**. *European journal of biochemistry* 1998, **254**(2):389-394.
340. Aras S, Bai M, Lee I, Springett R, Hüttemann M, Grossman LI: **MNRR1 (formerly CHCHD2) is a bi-organellar regulator of mitochondrial metabolism**. *Mitochondrion* 2015, **20**:43-51.
341. Aras S, Pak O, Sommer N, Finley Jr R, Hüttemann M, Weissmann N, Grossman LIJNar: **Oxygen-dependent expression of cytochrome c oxidase subunit 4-2 gene expression is mediated by transcription factors RBPJ, CXXC5 and CHCHD2**. 2013, **41**(4):2255-2266.
342. Hüttemann M, Lee I, Gao X, Pecina P, Pecinova A, Liu J, Aras S, Sommer N, Sanderson TH, Tost M: **Cytochrome c oxidase subunit 4 isoform 2-knockout mice show reduced enzyme activity, airway hyporeactivity, and lung pathology**. *The FASEB Journal* 2012, **26**(9):3916-3930.
343. Veit F, Pak O, Brandes RP, Weissmann NJA, signaling r: **Hypoxia-dependent reactive oxygen species signaling in the pulmonary circulation: focus on ion channels**. 2015, **22**(6):537-552.
344. Cogolludo A, Frazziano G, Cobeno L, Moreno L, Lodi F, Villamor E, Tamargo J, PEREZ- VIZCAINO FJAotNYAoS: **Role of reactive oxygen species in Kv channel inhibition and vasoconstriction induced by TP receptor activation in rat pulmonary arteries**. 2006, **1091**(1):41-51.
345. Fernández-Agüera MC, Gao L, González-Rodríguez P, Pintado CO, Arias-Mayenco I, García-Flores P, García-Pergañeda A, Pascual A, Ortega-Sáenz P, López-Barneo JJCm: **Oxygen sensing by arterial chemoreceptors depends on mitochondrial complex I signaling**. 2015, **22**(5):825-837.

346. Thompson R, Buttigieg J, Zhang M, Nurse CJN: **A rotenone-sensitive site and H_2O_2 are key components of hypoxia-sensing in neonatal rat adrenomedullary chromaffin cells**. 2007, **145**(1):130-141.
347. Liu Y, Gutterman DD: **Oxidative stress and potassium channel function**. *Clinical and experimental pharmacology and physiology* 2002, **29**(4):305-311.
348. Moudgil R, Michelakis ED, Archer SL: **The role of K+ channels in determining pulmonary vascular tone, oxygen sensing, cell proliferation, and apoptosis: implications in hypoxic pulmonary vasoconstriction and pulmonary arterial hypertension**. *Microcirculation* 2006, **13**(8):615-632.
349. Olschewski A, Weir EK: **Redox regulation of ion channels in the pulmonary circulation**. *Antioxidants & redox signaling* 2015, **22**(6):465-485.
350. Reeve H, Michelakis E, Nelson D, Weir EK, Archer S: **Alterations in a redox oxygen sensing mechanism in chronic hypoxia**. *Journal of applied physiology* 2001, **90**(6):2249-2256.
351. Brand MD, Esteves TC: **Physiological functions of the mitochondrial uncoupling proteins UCP2 and UCP3**. *Cell metabolism* 2005, **2**(2):85-93.
352. Bouillaud F: **UCP2, not a physiologically relevant uncoupler but a glucose sparing switch impacting ROS production and glucose sensing**. *Biochimica et Biophysica Acta (BBA)-Bioenergetics* 2009, **1787**(5):377-383.
353. Bodyak N, Rigor DL, Chen Y-S, Han Y, Bisping E, Pu WT, Kang PMJAjop-h, physiology c: **Uncoupling protein 2 modulates cell viability in adult rat cardiomyocytes**. 2007, **293**(1):H829-H835.
354. Mattiasson G, Shamloo M, Gido G, Mathi K, Tomasevic G, Yi S, Warden CH, Castilho RF, Melcher T, Gonzalez-Zulueta M: **Uncoupling protein-2 prevents neuronal death and diminishes brain dysfunction after stroke and brain trauma**. *Nature medicine* 2003, **9**(8):1062-1068.
355. Rau TF, Lu Q, Sharma S, Sun X, Leary G, Beckman ML, Hou Y, Wainwright MS, Kavanaugh M, Poulsen DJ: **Oxygen glucose deprivation in rat hippocampal slice cultures results in alterations in carnitine homeostasis and mitochondrial dysfunction**. *PloS one* 2012, **7**(9):e40881.
356. Arsenijevic D, Onuma H, Pecqueur C, Raimbault S, Manning BS, Miroux B, Couplan E, Alves-Guerra M-C, Goubern M, Surwit R: **Disruption of the uncoupling protein-2 gene in mice reveals a role in immunity and reactive oxygen species production**. *Nature genetics* 2000, **26**(4):435-439.
357. Ma S, Ma L, Yang D, Luo Z, Hao X, Liu D, Zhu Z: **Uncoupling protein 2 ablation exacerbates high-salt intake-induced vascular dysfunction**. *American journal of hypertension* 2010, **23**(8):822-828.
358. Bo H, Jiang N, Ma G, Qu J, Zhang G, Cao D, Wen L, Liu S, Ji LL, Zhang Y: **Regulation of mitochondrial uncoupling respiration during exercise in rat heart: role of reactive oxygen species (ROS) and uncoupling protein 2**. *Free Radical Biology and Medicine* 2008, **44**(7):1373-1381.
359. Ježek P, Olejár T, Smolková K, Ježek J, Dlasková A, Plecitá-Hlavatá L, Zelenka J, Špaček T, Engstová H, Pajuelo Reguera D: **Antioxidant and regulatory role of mitochondrial uncoupling protein UCP2 in pancreatic beta-cells**. *Physiol Res* 2014, **63**(Suppl 1):S73-S91.
360. Pecqueur C, Bui T, Gelly C, Hauchard J, Barbot C, Bouillaud F, Ricquier D, Miroux B, Thompson CB: **Uncoupling protein- 2 controls proliferation by promoting fatty acid oxidation and limiting glycolysis- derived pyruvate utilization**. *The FASEB Journal* 2008, **22**(1):9-18.

361. Han J, Bae JH, Kim S-Y, Lee H-Y, Jang B-C, Lee I-K, Cho C-H, Lim J-G, Suh S-I, Kwon T-KJAJoP-E *et al*: **Taurine increases glucose sensitivity of UCP2-overexpressing β-cells by ameliorating mitochondrial metabolism**. 2004, **287**(5):E1008-E1018.
362. Haslip M, Dostanic I, Huang Y, Zhang Y, Russell KS, Jurczak MJ, Mannam P, Giordano F, Erzurum SC, Lee PJJA, thrombosis, *et al*: **Endothelial uncoupling protein 2 regulates mitophagy and pulmonary hypertension during intermittent hypoxia**. 2015, **35**(5):1166-1178.
363. Nagy A: **Cre recombinase: the universal reagent for genome tailoring**. *genesis* 2000, **26**(2):99-109.
364. Zhu Z, Godana D, Li A, Rodriguez B, Gu C, Tang H, Minshall RD, Huang W, Chen J: **Echocardiographic assessment of right ventricular function in experimental pulmonary hypertension**. *Pulmonary circulation* 2019, **9**(2):2045894019841987.
365. Dromparis P, Paulin R, Sutendra G, Qi AC, Bonnet S, Michelakis ED: **Uncoupling protein 2 deficiency mimics the effects of hypoxia and endoplasmic reticulum stress on mitochondria and triggers pseudohypoxic pulmonary vascular remodeling and pulmonary hypertension**. *Circulation research* 2013, **113**(2):126-136.
366. Esfandiary A, Kutsche HS, Schreckenberg R, Weber M, Pak O, Kojonazarov B, Sydykov A, Hirschhäuser C, Wolf A, Haag DJCr: **Protection against pressure overload-induced right heart failure by uncoupling protein 2 silencing**. 2019, **115**(7):1217-1227.
367. Chakraborty R, Saddouk FZ, Carrao AC, Krause DS, Greif DM, Martin KA: **Promoters to study vascular smooth muscle: mistaken identity?** *Arteriosclerosis, thrombosis, and vascular biology* 2019, **39**(4):603-612.

8. Acknowledgment

I would like to express my sincere gratitude and appreciation to Professor Norbert Weissmann for providing me the opportunity to do my Ph.D. study in the excellent research group and for continuous guidance and support.

I would like to express the appreciation to PD Dr. Natascha Sommer, for all scientific supervision, motivation, and support. I would never have been able to finish my dissertation without her guidance and it was a great pleasure to have her encouragement and inspiration.

I would like to thank the International Giessen Graduation center (GGL) and Molecular Biology and Medicine of the Lung (MBML) team members for their excellent programs that increase my scientific knowledge and paved my way for having a successful Ph.D. graduation.

I was privileged to have the expertise, scientific discussion, and fruitful collaboration of Dr. Oleg Pak, Dr. Fenja Knöpp, and Dr. Susan Scheibe in performing and analyzing patch-clamp and ESR spectroscopy experiments in my project. I would like to thank Dr. Akylbek Sydykov for good cooperation in doing and analyzing the echocardiographic measurements of the mice in my project. I would like to acknowledge Ms. Karin Quanz, Ms. Ingrid Breitenborn-Müller, and Ingrid Henneke for their help and it has been a great pleasure to have their extensive support and help for doing the experimental parts of the project.

My sincere thanks belong to Prof. Dr. Klaus-Dieter Schlüter from the Physiology Institute and Prof. Sybille Mazurek from the Institute for Veterinary Physiology and Biochemistry for the review of this thesis and helpful insights and comments on that. I would like to thank Dr. Simone Kraut, Dr. Monika Malczyk, Ms. Carmen Homberger, Ms. Elisabeth Kappes, and Ms. Ewa Bieniek for their great support in this project.